Optimising Supply Air Control in Combined Radiant Ceiling and AHU Systems: A Simulation-Based Approach for Operational Performance

MASTER THESIS IN BUILDING AND ARCHITECTURAL ENGINEERING

Author: **Jennifer Wong**

Student ID: 10986877
Advisor: Francesco Causone
Co-advisors: Yacine Allab, Vincent Lugherini
Academic Year: 2025/26

Abstract

A key challenge in reducing energy consumption in the building sector lies in the gap between theoretical and real-world performance. This discrepancy often arises from the complex interactions between HVAC subsystems and fragmented sizing processes—particularly in setups combining radiant ceilings with Air Handling Units (AHUs)—configurations increasingly adopted in the French tertiary building sector.

Drawing on years of professional experience, such configurations have been found to frequently result in poor coordination between subsystems and suboptimal control of supply air temperature and humidity. This is particularly critical during summer months, when the risk of condensation is high, often leading to overly conservative ventilation settings, unnecessary energy use, or conflicting control strategies. The core objective of this thesis is therefore to optimise supply air control and maximise overall system performance.

This research begins with the modelling of a standard office space conditioned by the combined system—a radiant ceiling coupled with an AHU—using a mixing ventilation strategy. A numerical model developed in DesignBuilder, based on EnergyPlus algorithms, enables dynamic simulations and a parametric analysis of supply air configurations.

System performance is assessed across three dimensions—energy consumption, condensation prevention, and thermal comfort—through performance indicators derived from model outputs and reflecting the system's operational behaviour. A ranking based on a weighted average of these indicator scores identifies the optimised yearly supply air control strategy from the combination of the best-performing seasonal configurations.

Compared with a common suboptimal control strategy, the optimised approach features lower heating and cooling supply temperatures, and lower outdoor temperature thresholds for heating and cooling activation. When AHU heat recovery is not activated, the optimised configuration achieves a modest improvement in energy efficiency. Despite a slight increase in total energy demand (+2.0%), the increase in ceiling demand share (+1.4%) results in a 2.3% decrease in primary energy consumption. Most notably, condensation prevention improves significantly, with a 98% reduction in yearly occurrences, and control coordination improves with a 56% decrease in energy wasted through simultaneous heating and cooling. Summer thermal comfort also improves with a 37% reduction in cooling discomfort over the season.

Key-words: HVAC automation, radiant ceiling, Air Handling Unit, operational energy efficiency, condensation, supply air control

Abstract in lingua italiana

Una delle principali sfide nella riduzione dei consumi energetici nel settore edilizio risiede nel divario tra prestazioni teoriche e reali, spesso dovuto alle complesse interazioni tra i sottosistemi HVAC e a processi di dimensionamento frammentati, in particolare nelle configurazioni che integrano soffitti radianti e Unità di Trattamento dell’Aria (UTA), una soluzione sempre più adottata nel terziario francese.

Sulla base di anni di esperienza professionale, è stato riscontrato che tali configurazioni risultano frequentemente in una scarsa coordinazione tra i sottosistemi e in un controllo non ottimale della temperatura e dell'umidità dell'aria di mandata. Ciò è particolarmente critico durante i mesi estivi, quando il rischio di condensazione è elevato, portando spesso a impostazioni conservative, consumi non necessari o strategie di controllo conflittuali. L'obiettivo di questa tesi è quindi ottimizzare il controllo dell'aria di mandata e massimizzare le prestazioni complessive del sistema.

La ricerca inizia con la modellazione di un ufficio standard climatizzato mediante un sistema combinato costituito da soffitto radiante e UTA a ventilazione per miscelazione. Un modello numerico in DesignBuilder, basato sugli algoritmi di EnergyPlus, consente simulazioni dinamiche e un’analisi parametrica delle configurazioni dell’aria di mandata.

Le prestazioni del sistema sono valutate secondo tre criteri fondamentali: consumo energetico, prevenzione della condensazione e comfort termico, attraverso specifici indicatori rappresentativi del comportamento operativo del sistema. Una classificazione tramite media ponderata dei punteggi individua la strategia annuale ottimizzata, ottenuta dalla combinazione delle configurazioni stagionali più efficienti.

Rispetto a una strategia di controllo subottimale comune, l'approccio ottimizzato presenta temperature di mandata per il riscaldamento e il raffrescamento più basse, nonché soglie di temperatura esterna più basse per l'attivazione del riscaldamento e del raffrescamento. In assenza di recupero di calore dell’UTA, si osserva un miglioramento moderato dell’efficienza energetica. Nonostante un leggero aumento della domanda energetica totale (+2,0%), aumento della quota coperta dal soffitto radiante (+1,4%) determina una riduzione del 2,3% nel consumo di energia primaria. Più rilevanti risultano gli effetti sulla prevenzione della condensazione, con una riduzione del 98% delle occorrenze annuali, e sul coordinamento del controllo, che registra un calo del 56% dell’energia sprecata per riscaldamento e raffrescamento simultanei. Anche il comfort estivo migliora, con una riduzione del 37% del disagio da raffrescamento nel corso della stagione.

Parole chiave: automazione HVAC, soffitto radiante, Unità di Trattamento dell'Aria, efficienza energetica operativa, condensazione, controllo dell'aria di mandata

Contents

Table of figures

Table of tables

List of acronyms

AHU	Air Handling Unit
HR	Heat Recovery (Air Handling Unit)
ASR	Activated Surface Ratio
ASHRAE	American Society for Heating, Refrigerating and Air-Conditioning Engineers
BCA	Building Commissioning Authority
IAQ	Indoor Air Quality
PMV	Predicted Mean Vote
PPD	Predicted Percentage Dissatisfied
SHC	Simultaneous Heating and Cooling
TABS	Thermally Active Building Systems
VAV	Variable Air Volume

List of symbols

m_a	Air mass flow rate	kg/s
c_{pa}	Air specific heat capacity	kJ/kg.K
$Q_{controller}$	Annual electricity consumption of AHU controllers	kWh
$Ceiling\ H\%$	Ceiling share of heating demand indicator	%
$Ceiling\ C\%$	Ceiling share of cooling demand indicator	%
$Condensation$	Condensation occurrences indicator	h
h_c	Convective heat transfer coefficient	W/m².K
$Discomfort\ C$	Cooling discomfort over the season indicator	%h
q_{cool}	Cooling rate of the hybrid system	kW
$Demand\ C$	Cooling thermal demand indicator	kWh
r	Correlation coefficient	-
T_{dew}	Dew point temperature	°C
ΔT_a	Difference between the input and the output air temperature	°C
ΔT_w	Difference between the input and the output water temperature	°C
$Q_{PE,th}$	District heating and cooling primary energy	kWh,th
$f_{PE,district}$	District heating and cooling primary energy factor	-
$q_{controller}$	Electrical power of an AHU controller	W
$Q_{en,c}$	Electricity or thermal energy consumption of the system component "c"	kWh
$Q_{PE,e}$	Electricity primary energy	kWh,e
$f_{PE,electricity}$	Electricity primary energy factor	-
$P_{int,eq}$	Equipment power density	W/m²
q_{air}	Heat rate absorbed by the supply air	kW
$q_{surface}$	Heat rate exchanged at the cooled surface	kW
q_{water}	Heat rate removed by the internal water circuit	kW
$P_{heating\ coil}$	Heating coil electrical power	kW
$Discomfort\ H$	Heating discomfort over the season indicator	%h
$T_{s,\max heating}$	Heating maximum supply temperature	°C
$Demand\ H$	Heating thermal demand indicator	kWh
$P_{ext,inf}$	Infiltration heat rate	W
$P_{int,light}$	Lighting power density	W/m²
T_a	Mean air temperature	°C
T_{mrt}	Mean radiant temperature	°C

$T_{s,min\ cooling}$	Minimum cooling supply temperature	°C
$N_{controllers}$	Number of AHU controllers	-
$N_{occ\ hours\ i}$	Number of occupied hours during heating or cooling season	h
Δt	Number of operating hours	h
$P_{int,occ,lat}$	Occupants latent power density	W/m²
$P_{int,occ,sens}$	Occupants sensible power density	W/m²
S_{office}	Office space area	m²
T_{op}	Operative temperature	°C
T_o	Outdoor temperature	°C
$T_{o,cooling\ slope}$	Outdoor temperature range of the cooling slope	°C
$T_{o,\mathrm{cooling}}$	Outdoor temperature threshold for cooling	°C
$T_{o,\mathrm{max}\ heating}$	Outdoor temperature threshold for maximum heating	°C
$Discomfort\ i$	Percentage of discomfort hours during heating or cooling season	%h
$f_{PE,en}$	Primary energy factor of electricity or district energy	-
$Q_{PE,en}$	Primary energy consumption	kWh
P_{panel}	Radiant ceiling capacity per active surface	W/m²
$T_{surface}$	Radiant ceiling surface temperature	°C
h_c	Radiative heat transfer coefficient	W/m².K
RH	Relative humidity	%
q_{room}	Room heat rate balance	kW
$S^x_{performance}$	Score for the configuration "x" for a given performance indicator	[0-1]
t	Simulation time step	h
Q_{SHC}	Simultaneous heating and cooling wasted energy	kWh
$SHC\ En\%$	Simultaneous heating and cooling wasted energy in percentage of the total demand	%
$P_{ext,solar}$	Solar radiation power density	W/m²
$T_{amb,summer}$	Summer mean air temperature contractual setpoint	°C
$P_{ext,tr}$	Transmission heat rate through opaque and transparent envelope	W
$Q_{extract}$	Ventilation extract air flow rate	m³/s
Q_s	Ventilation supply air flow rate	m³/s
P_{vent}	Ventilation supply air heat rate	W
T_s	Ventilation supply air temperature	°C
m_w	Water mass flow rate	kg/s
c_{pw}	Water specific heat capacity	kJ/kg.K

T_w	Water temperature	°C
$T_{amb,winter}$	Winter mean air contractual temperature setpoint	°C

1 Introduction

In usual HVAC designs, thermal conditioning is typically provided by a fan coil unit, whereas the present work employs a radiant ceiling. The integration of a radiant ceiling with a ventilation system introduces complex interactions that must be carefully considered; however, these are often overlooked, particularly in the French context of HVAC system sizing.

A standard office space is thermally characterised by heat gains and losses (Table 1.1, Figure 1.1):

Table 1.1: Standard office space heat gains

Gains	Sources	Type
Internal gains	Occupants Lighting Equipment	Latent and sensible Sensible Sensible
External gains	Solar radiation Envelope transmission Infiltration	Sensible Sensible Latent and sensible

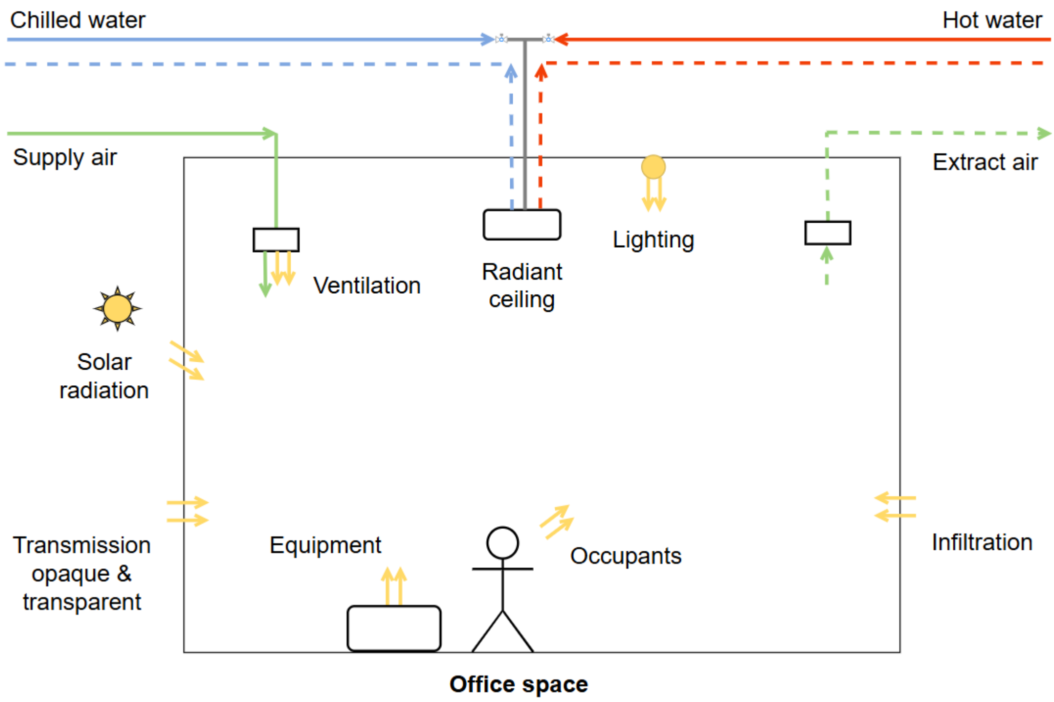

Figure 1.1: Standard office space gains and HVAC system terminal units

The system sizing procedure (Figure 1.2) begins with airflow and thermal balances in order to select an appropriate ventilation and thermal conditioning system:

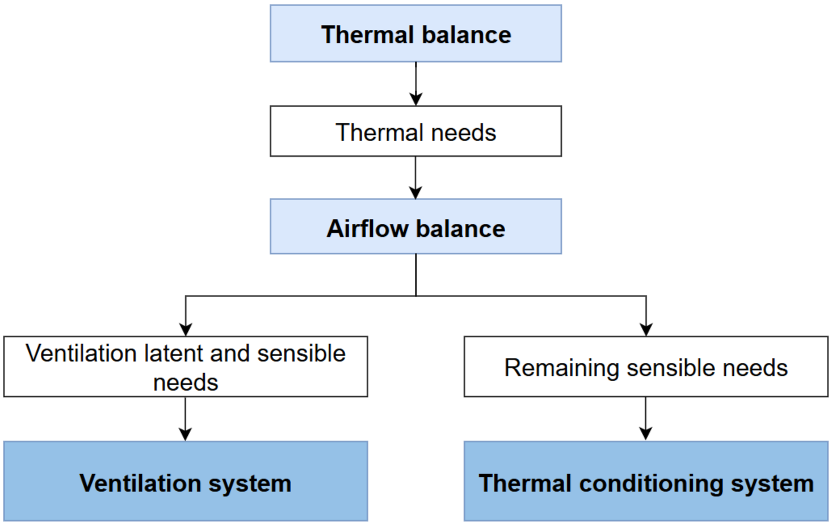

Figure 1.2: HVAC system sizing process

In usual designs (Figure 1.3) where thermal conditioning is provided by a fan coil unit, the thermal capacity must satisfy the required sensible demand and, indirectly by sensible cooling, the majority of latent demand. The ventilation system is an AHU which is responsible for delivering the required indoor air quality (IAQ) airflow rate and some of the latent energy demand by cooling, supplying air at a temperature T_s that ensures thermal comfort while optimising energy consumption.

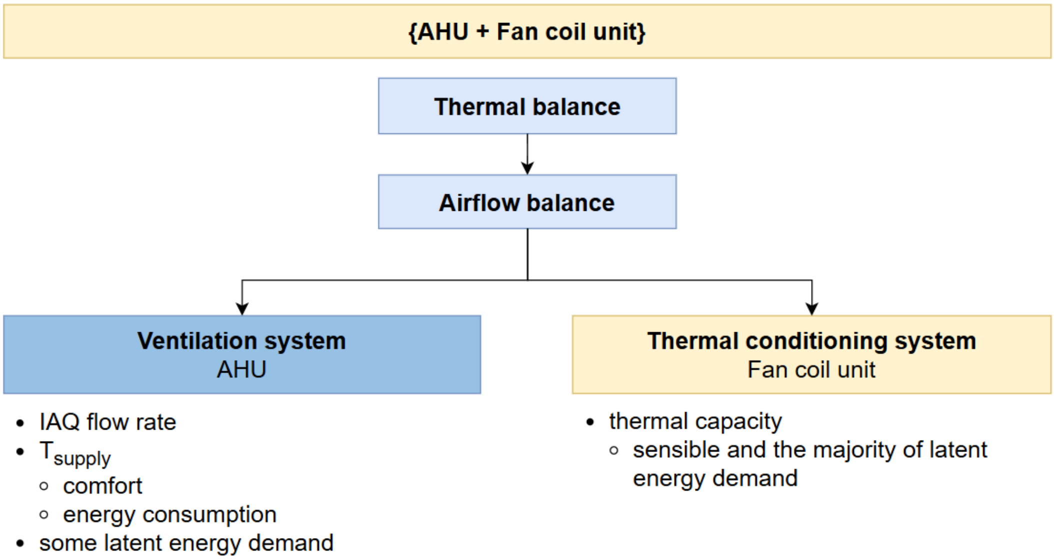

Figure 1.3: Characteristics and system requirements of AHU and fan coil unit combined operation

In this study (Figure 1.4) where thermal conditioning is achieved by a radiant ceiling, the thermal capacity must meet the sensible energy demand and is expressed in W/m² of active surface. However, the ceiling activable surface area is limited, and the ceiling surface temperature must remain above the zone dew point temperature to prevent condensation. These constraints significantly restrict the ceiling capacity, particularly in cooling mode.

Consequently, the AHU is required to assume additional functions, as handling all of the latent energy demand and supplying the remaining portion of sensible demand not met by the radiant ceiling. The resulting interactions between the ventilation and thermal conditioning systems introduce potential risks of overall system performance degradation.

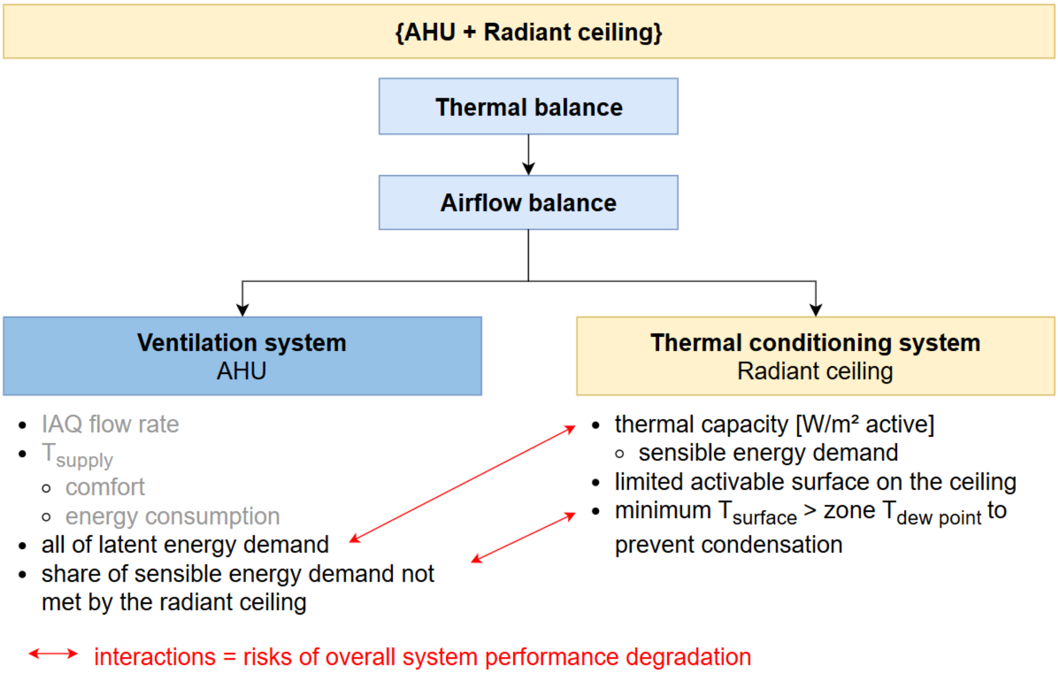

Figure 1.4: Characteristics and system requirements of AHU and radiant ceiling combined operation

In France, the steps involved in HVAC system sizing are typically handled through separate work packages (Figure 1.5) that do not necessarily coordinate with one another, making it difficult to account for interactions between subsystems.

The thermal balance is performed by the company's in-house technical design office, followed by the airflow balance and the selection of the ventilation system by the HVAC package. Finally, the thermal conditioning system is defined by the radiant ceiling package in cooperation with the architect. Moreover, both systems are controlled independently.

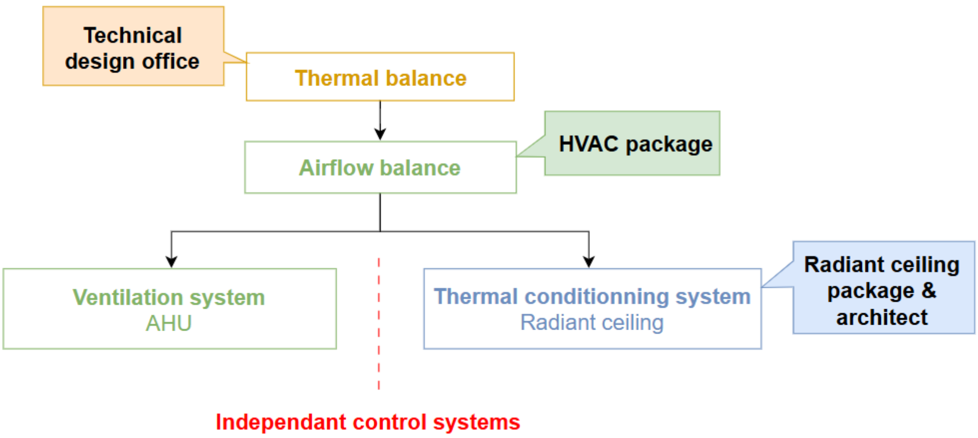

Figure 1.5: Separation of work packages in the HVAC sizing process

These functional separations and the lack of coordination between work packages lead to recurring issues, particularly during summer operation. Drawing on years of professional field experience, HVAC engineers and radiant ceiling manufacturer interviews, such issues include insufficient radiant ceiling capacity, excessive cooling of the supply air resulting in increased energy consumption, and even simultaneous heating and cooling between radiant ceiling and AHU. Conversely, inadequate cooling and dehumidification of the supply air may induce condensation, triggering radiant ceiling shutdown and causing high levels of thermal discomfort.

Therefore, the integrated operation of the AHU and the radiant ceiling is constrained by several scientific and technical barriers related to system operation and coordination, energy efficiency, and indoor environmental control.

The key challenge is to optimise the combined operation of the AHU and radiant ceiling while satisfying several performance requirements:

1. Energy efficiency: avoiding overconsumption by prioritising thermal regulation through the radiant ceiling;
2. Condensation prevention;
3. Control coordination: avoiding energy waste associated with simultaneous heating by the AHU and cooling by the radiant ceiling, and vice versa;
4. Thermal comfort.

During building operation, these requirements are primarily addressed through the optimisation of supply air control strategies.

The purpose of this thesis is to optimise the supply air control (Figure 1.6), by developing a numerical model:

1. For a standard office space;
2. Considering building and HVAC characteristics and limitations;
3. Addressing the above-mentioned requirements, with a particular focus on some requirements for each season;
4. By performing a parametric analysis.

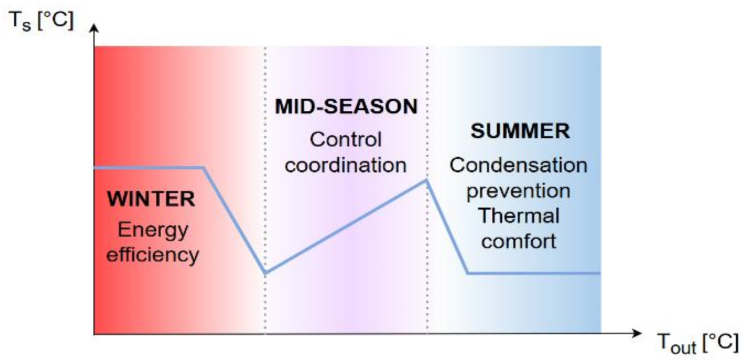

Figure 1.6: Supply air control and main seasonal requirements

The thesis is conducted in Paris, as part of a collaboration with the French company LHIRR. It is an engineering company and Building Commissioning Authority (BCA) specialising in commissioning, retro-commissioning and start-up of tertiary buildings (new constructions and refurbishments), for public and private clients (offices, shopping centres, sports facilities, factories, etc.). It works alongside the client at every project stage—from design and execution to operation—ensuring performance and long-term sustainability (Figure 1.7).

Primarily active in the Île-de-France region, it is a small and medium-sized enterprise with ten employees, valuing rigor, expertise, and environmental responsibility.

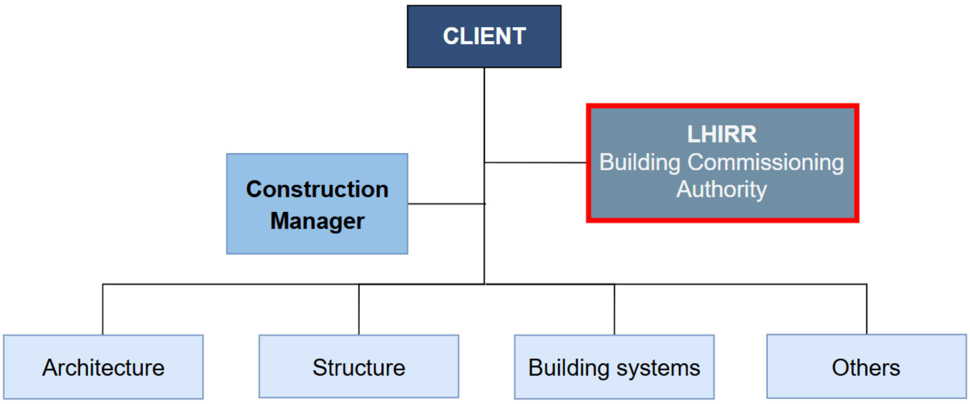

Figure 1.7: Project's hierarchy [internal source]

The main tasks of the BCA are the following:

- Project organisation and monitoring;
- Project optimisation analysis;
- Client support regarding:
  - Functional analysis of the project;
  - Testing and verification of the delivered project;
  - Implementation of change management actions.

In order to carry out these activities, the BCA must possess specific knowledge and skills (Figure 1.8):

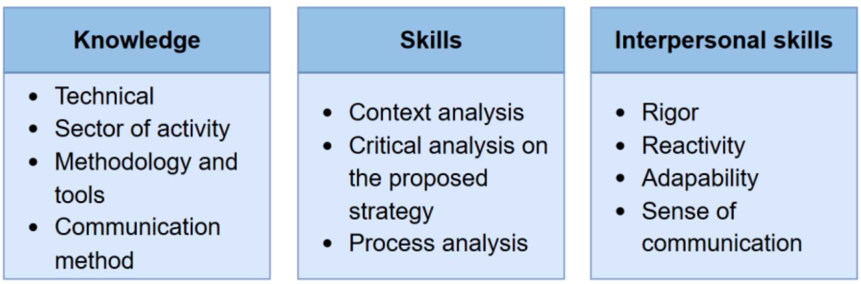

Figure 1.8: Project Management Assistant knowledge and skills [internal source]

In this context, LHIRR is an expert in building HVAC system, building technical management and related fields. The complexity of the technical systems combined with ambitious energy targets, increases the risk of performance losses during design, construction, and operational phases. Commissioning helps mitigate these risks and supports the achievement of the client's objectives in terms of comfort, energy efficiency, and functional performance.

This structured approach aims to translate the client's needs into achievable performance targets that can be measured and verified at each stage of the project. To support this verification process, the team delivers functional analyses based on dynamic simulations, data engineering, and the definition of energy performance contractual commitments.

This thesis first reviews the literature on radiant systems, with particular emphasis on radiant ceilings, covering their main characteristics, their integration with an AHU, and existing strategies for mitigating condensation risk (Chapter 2). The methodology adopted to address the research question is then presented (Chapter 3), followed by a detailed description of the numerical model development (Chapter 4). The performance assessment methodology is presented (Chapter 5), after which the results and analysis leading to supply air control optimisation are discussed (Chapter 6). Finally, the conclusions and perspectives of this study are drawn (Chapter 7).

2 Literature review

The reduction in building energy consumption has driven the development of high-efficiency HVAC solutions, among which radiant systems have gained significant attention for their potential to improve energy efficiency, thermal and acoustic comfort, architectural integration and maintenance.

However, because they rely primarily on radiative and convective sensible heat transfer, radiant systems cannot independently ensure IAQ or humidity control and must therefore be coupled with mechanical ventilation for outdoor air supply and latent load treatment. Their thermal capacity may also be limited in spaces with high internal gains, particularly due to space constraints and the risk of summer condensation.

While the integration with ventilation systems enables complementary operation, it introduces complex interactions that can affect efficiency and occupant comfort, making effective control—especially for condensation prevention in cooling mode—essential.

This literature review covers the main radiant ceiling technologies and their performance characteristics (Section 2.1), the combined operation of radiant ceilings and mechanical ventilation systems (Section 2.2), and existing condensation prevention strategies (Section 2.3). Particular attention is given to the French design context, highlighting the need for further investigation of supply air control strategies based on outdoor air conditions (Section 2.4). The effects of ventilation air diffusion on radiant ceiling capacity and convective heat transfer are beyond the scope of this work and are therefore excluded.

2.1. Radiant ceiling systems

2.1.1. Radiant ceilings history

Radiant ceilings are a long-established technology derived from the Roman hypocaust (Figure 2.1), developed over 2,000 years ago. This early system operated by circulating hot combustion gases from a furnace through cavities beneath raised floors, which then discharged the gases outdoors via wall-mounted flues [1].

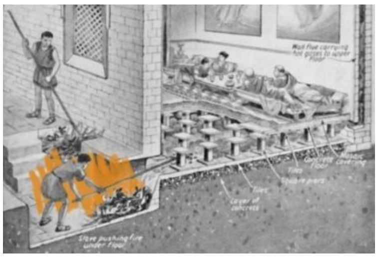

Figure 2.1: Roman hypocaust [2]

The modern development of radiant heating is commonly traced to the early 20th century, when Arthur H. Baker introduced the concept of "panel heating", consisting of small-diameter hot-water pipes embedded within plaster or concrete layers. This innovation marked a significant advancement in radiant heating technology [1].

Nowadays, radiant systems are widely used for building conditioning in several European countries such as Germany, Austria and Denmark, floor heating is particularly prevalent in new residential buildings, and also extends to commercial and industrial sectors. Originally developed for heating in cold climates, radiant systems have progressively expanded to cooling applications and are now implemented in temperate and warm regions worldwide [3]. In the Île-de-France region, radiant ceilings are implemented in approximately 80% of LHIRR's office-building projects [internal source].

2.1.2. Radiant ceilings types

A radiant system is a building conditioning system that regulates indoor thermal comfort through radiation between temperature-controlled surfaces (such as floors, walls, or ceilings) and occupants, by at least 50% of the total heat exchange [4]. The heat carrier can be water, electricity or gas [4] and radiant systems can be classified in several types: radiant panels, embedded systems and Thermally Active Building Systems (TABS) [5].

Radiant panel systems (Figure 2.2 (left)) consist of pipes attached to conductive metallic plates, which are mounted on panels. These assemblies are separated from the supporting surface by an insulation layer in order to direct heat transfer towards the conditioned space and minimise thermal losses to the main building structure.

In embedded radiant systems (Figure 2.2 (right)), pipes are installed within a load-bearing surface layer, enabling the exploitation of the building's thermal mass, while an insulation layer is used to limit heat transfer towards the main building structure.

Embedded radiant floor systems can be classified into two main categories: wet systems where pipes are embedded directly within the screed or concrete layer, and dry systems that feature pipes outside of the screed, typically within the thermal insulation layer and often combined with heat-conducting plates to enhance heat diffusion [5].

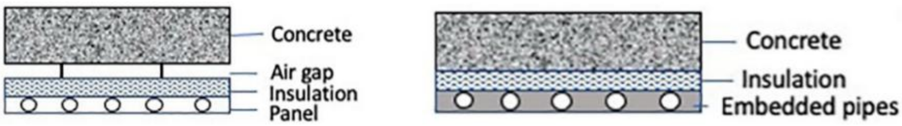

Figure 2.2: Radiant panel systems (left) and embedded radiant systems (right) [6]

In TABS systems (Figure 2.3), the thermal mass of the concrete structure is used to store thermal energy, reducing daytime cooling peak loads by approximately 30–

50% [6]. The stored energy is released at night when the indoor air temperature T_a falls below the slab temperature. The elimination of air plenums allows for reduced interstorey heights; however, this system is generally unsuitable for retrofit applications.

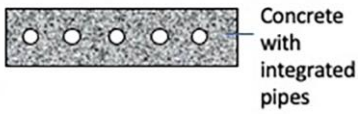

Figure 2.3: Thermally Active Building Systems [6]

2.1.3. Radiant systems advantages

The operative temperature T_{op} is the temperature expressing the combined influence of the two main thermal comfort parameters: the air temperature and the mean radiant temperature [5]. It is “the uniform temperature of an enclosure in which an occupant would exchange the same amount of heat by radiation plus convection as in the existing non-uniform environment”[7]:

$$T_{op} = \frac{h_r \,. T_{mrt} + h_c \,. T_a}{h_r + h_c}$$

With:

- T_a [K] the air temperature;
- T_{mrt} [K] the mean radiant temperature;
- h_c [W/m².K] the convective heat transfer coefficient;
- h_r [W/m².K] the radiative heat transfer coefficient.

For offices with sedentary activity, the comfort range of operative temperature is 19-21 °C in heating, and 25.5-27 °C in cooling [8]. Since radiant systems exchange more than 50% heat by radiation [4], they have a direct influence on the mean radiant temperature T_{mrt} [6], therefore it is possible to achieve the same level of thermal comfort (T_{op}) with lower air temperature in heating and higher air temperature in cooling than with a convective system [4], when heat transfer coefficients are unchanged. As a result, ventilation heat losses and infiltrations are reduced in non-airtight buildings [5].

Moreover, radiative heat exchange is directly perceived by occupants, resulting in a faster thermal response than air convection [6] and heat carrier temperature can be lower in heating and higher in cooling compared with those of conventional air systems [6]. For hydronic radiant ceilings, the typical supply water temperatures are 30-35 °C in heating and 13-14 °C in cooling [9], while fan coil units operate at 45-50 °C in heating and 6-8 °C in cooling [10]. Radiant surface temperatures are close to the comfort setpoint, leading to smaller vertical air temperature gradients and a more uniform thermal environment, which reduce the risk of air drafts and enhance thermal comfort [6].

Low temperatures in heating and high temperatures in cooling allow the use of renewable primary energy sources [6] or even free cooling [11] and increase the operation efficiency of heat generation systems such as chillers [6], heat pumps, solar heating panels and ground heat exchanger [4].

Radiant systems are predominantly hydronic, and because water has a thermal capacity approximately four times higher than that of air (4.18 J/kg.K vs. 1.005 J/kg.K), the same amount of energy can be transported with a lower heat carrier volume, reducing pump energy consumption [6]. Unlike all-air systems, only the minimum required outdoor air per occupant is supplied, eliminating the need for air recirculation to meet thermal loads [6]. As a result, the volume and velocity of air circulating within the zone are significantly reduced—by about 80% [6]—leading to lower fan energy consumption [11]. In cooling, it is possible to achieve a reduction in fan electrical peak power of 75%, and in electrical peak power up to 40% for the entire system (fans and chiller). This allows reduced-size systems and lower capital costs [12]. It is also possible to exploit the building main structure thermal mass to flatten peaks of thermal loads, energy consumption and room air temperature [3].

In buildings with a high-performance envelope conditioned by a hybrid system—radiant ceiling coupled with an outdoor air unit equipped with a wrap-around coil for dehumidification and heat recovery—electricity consumption associated with chillers, fans and pumps can be reduced by up to 40% [13].

Furthermore, radiant ceilings can achieve reductions up to 60% in primary energy consumption and CO_2 emissions compared with conventional all-air systems when combined with an appropriate primary energy system, such as groundwater-based free cooling. These reductions are more pronounced in climates where cooling demands exceed heating demands; however, even in less favourable climates, minimum reductions of approximately 30% have been reported [14].

Moreover, radiant systems can provide superior acoustic comfort compared with fan coil units as they eliminate fan noise within the occupied zone, and enhance IAQ since the absence of wet cooling coils in the occupied space reduces the risk of microbial contamination [4].

Radiant ceiling systems typically require approximately 30 cm of vertical space [9], compared with 40-50 cm for fan coil units [10]. Combined with reduced ductwork requirements, this allows for a reduction in interstorey height [6]. Unlike floor-mounted fan coil units, radiant ceilings do not occupy usable floor area, enabling more efficient space utilisation and greater architectural flexibility [4]. Both the reduction in interstorey height and the preservation of floor space are particularly advantageous in high-cost urban contexts such as Paris, where the cost per square meter is significant [15].

The limited number of moving components and primary equipment, such as pumps and control valves, results in relatively simple maintenance requirements, thereby reducing operational and maintenance costs [16]. In addition, most radiant systems can be readily implemented in retrofit or renovation projects [13].

2.1.4. Radiant systems drawbacks

For radiant ceilings in heating mode, limitations related to radiant asymmetry and vertical air temperature gradients restrict the surface temperature $T_{surface}$ to a maximum of approximately 27 °C, in order to maintain radiant asymmetry below 5 K and ensure thermal comfort [6]. In cooling mode, $T_{surface}$ must remain above the indoor air dew point—typically in the range of 17-19 °C [17]—to prevent condensation, energy overconsumption and IAQ issues [18]. These constraints significantly limit the thermal capacity of radiant ceilings [14], particularly in hot and humid climates where elevated dew point temperatures increase the risk of condensation during summer. In such contexts, the additional energy consumption by the ventilation system can reduce the savings compared with an all-air system [1]. When radiant systems are not complemented by mechanical ventilation for cooling and dehumidification, only low cooling loads can be addressed [17].

Unlike conventional all-air systems, radiant systems are capable of removing only sensible heat and therefore must be combined with a ventilation system to handle latent loads, in addition to supplying the minimum outdoor air flow required to ensure IAQ [3].

The control of radiant systems should be based on operative temperature in order to account for the influence of mean radiant temperature, as heat exchange occurs through radiation by more than 50% [14]. However, in the French context, system control is commonly implemented using air temperature, a cheaper and easier method, and similar to conventional air-based systems.

Moreover, radiant systems generally involve higher initial investment costs compared with traditional air systems, which can limit their range of application [4].

A technical benchmark of radiant ceilings is provided in Appendix A.

2.2. Radiant ceiling and mechanical ventilation system combined operation

2.2.1. Radiant ceiling operation

Radiant systems are complex thermal systems that exchange heat with their environment through multiple mechanisms, including conduction between the water circuit and the radiant surface, as well as radiation with surrounding surfaces and convection with the indoor air [19].

In conventional all-air (convective) systems, radiant heat gains are first absorbed by interior surfaces, furniture, and other thermal masses. Then, once the surface temperatures of these elements exceed the ambient air temperature, the stored heat is released to the space primarily through convection, contributing to the dynamic cooling load [19].

In radiant cooling systems, chilled surfaces directly absorb radiant heat gains, thereby reducing the reliance on other internal thermal masses to buffer radiant loads and increasing direct spatial heat exchange [19]. Due to system thermal inertia, particularly in embedded systems, the instantaneous heat exchange at the cooled surface may differ from the heat transported by the water circuit, unlike suspended radiant panels, which exhibit low thermal inertia [19]. When comparing radiant ceilings and radiant floors, floor systems generally exhibit higher energy consumption than ceiling systems due to their greater thermal inertia and increased risk of overheating or overcooling, particularly in mild climates [14].

For a radiant ceiling, the average total heat transfer is 13.2 W/m².K in cooling and 5.8 W/m².K in heating, so radiant ceilings are more suitable for cooling [20].

On the one hand, the radiative heat transfer coefficient is commonly assumed to be constant, with a typical value of approximately 5.6 W/m².K in both heating and cooling modes. This approximation is generally valid for standard indoor temperature ranges and typical surface emissivity [20].

On the other hand, the convective heat transfer coefficient varies significantly with operating mode, with typical values of about 4.4 W/m².K in cooling and 0.3 W/m².K in heating. Consequently, the cooling capacity of a chilled ceiling can be enhanced by increasing convective heat transfer, for instance through increased surface roughness or by directing ventilation air jets close to the radiant surface [20].

Radiant ceilings can be controlled by a constant water temperature T_w and variable flow rate or variable T_w and constant flow rate [21]. In cooling mode, the heat transfer rate increases with higher water velocities (from approximately 0.05 to 0.45 m/s), and consequently water flow rates, as the temperature difference between the inlet and outlet water decreases, resulting in a lower average chilled water and $T_{surface}$ [18].

With lower T_w, heat transfer may also increase due to the onset of condensation, which adds latent heat transfer to the sensible heat exchange between the capillary tubes and the surrounding air. As a result, a portion of the cooling capacity is consumed by latent heat removal through condensation, also reducing the effective sensible cooling capacity available to meet space cooling demand [18].

The surface temperature of a radiant panel depends not only on T_w on the distribution side but also on the air and surrounding surfaces temperatures within the conditioned zone [17]. Consequently, it is influenced by the cooling load, which is in turn affected by solar and internal heat gains. As a result, condensation does not necessarily occur when outdoor air temperature reaches its maximum and may also take place after chilled water circulation has ceased, due to the thermal inertia of the panel [22].

The degree of subcooling, defined as the difference between the dew point temperature and the chilled-water temperature, serves as an indicator of condensation risk for a given panel material. Experimental results show that gypsum panels exhibit a lower risk of condensation compared with bare tubes and metal panels, as condensation was observed only when the subcooling degree exceeded 6.5 °C, compared with 3.2 °C and 5.4 °C, respectively [18].

2.2.2. Mechanical ventilation operation

The main purpose of mechanical ventilation is to provide fresh air and ensure an adequate IAQ. It can also be used to meet the thermal comfort requirements by maintaining the temperature setpoints (in our case, the latter objective should be dedicated to the radiant system) [4]. Mechanical ventilation can be classified into mixing ventilation and displacement ventilation (in this work, mixing ventilation is implemented).

With mixing ventilation, air is supplied at high velocity above the occupied zone, typically near the ceiling, in order to promote thorough mixing within the space and ensure effective contaminant removal. When used to complement a radiant ceiling for cooling purposes, T_s is set below the room air temperature. However, air velocities in the occupied zone must be limited to avoid draft discomfort [6].

With displacement ventilation, air is supplied at low speed, near the floor in the occupied zone at a temperature close to the ambient temperature, the maximum temperature difference being around 3-5 K [23] to avoid cold drafts [11]. The supply air should also respect the maximum temperature gradient of 3 °C between 0.1 and 1.1 m above the floor to preserve thermal comfort [24].

Contaminant removal is performed exploiting heat plumes, which involves air rising up when heated by the occupants who are also the main contaminant source. It creates a thermal and contaminant stratification, which concentration is higher near the ceiling exhaust, so it can achieve better IAQ compared with mixing ventilation [4].

However, mixing ventilation can be more energy efficient due to lower T_s and the absence of reheating following air dehumidification cooling, leading to energy savings of approximately 17% [6]. It can also achieve a more uniform temperature distribution than in displacement ventilation which relies on vertical temperature gradient [21].

Regardless of the mechanical ventilation strategy, the outside air needs to be first treated either by an AHU or a Dedicated Outdoor Air System (DOAS). In particular, a DOAS supplies the IAQ flow rate through variable or constant air volume, and handles all the space latent load, with cooling coils or desiccant dehumidification.

Moreover, it removes the sensible load with a parallel system, which can be an all-air VAV system, a fan coil unit or a radiant system [4].

2.2.3. Interactions between radiant ceiling and mechanical ventilation system

In a thermal zone conditioned by a combined radiant and ventilation system (Figure 2.4), the cooling rate delivered by the radiant system corresponds to the heat removed by the internal water circuit q_{water}, while the cooling rate delivered by the air system corresponds to the heat absorbed by the supply air q_{air} . The sum of these two contributions represents the total cooling rate of the hybrid system q_{cool} [19]. However, the room heat exchange q_{room} is defined as the sum of the air system cooling rate q_{air} and the heat exchanged at the cooled surface $q_{radiant}$ [19].

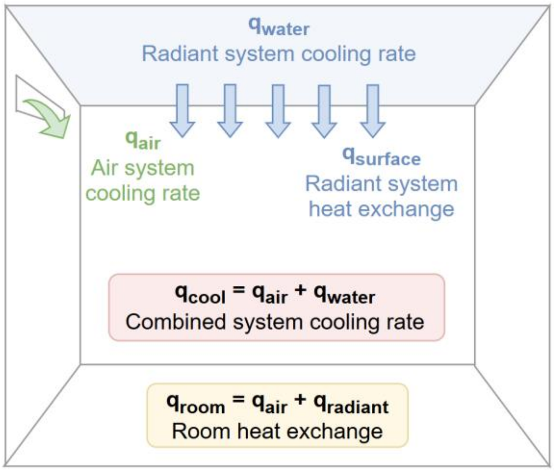

Figure 2.4: Cooling rate of the combined system

The integration of radiant systems with mechanical ventilation makes it possible to benefit from the advantages of both technologies while mitigating their respective limitations, resulting in improved overall system performance [4]. Furthermore, as previously mentioned, positioning ventilation air supply near the radiant surface can enhance the thermal capacity of the system by increasing convective heat transfer, since radiative heat transfer remains relatively constant across different types of radiant systems [6].

While radiant systems are responsible for thermal conditioning, they offer several advantages over all-air systems, except their inability to handle latent loads within the conditioned space, which necessitates the integration with a ventilation system. In the case of a radiant ceiling, the air jet may drop excessively in the occupied zone and cause discomfort, which could be avoided with mixing ventilation [4].

When mixing ventilation is used as the sole cooling system under high cooling load, the combination of high supply air velocity and low T_s may also result in excessive air jet drop and occupant discomfort. In such cases, the use of a radiant system to handle a portion of the sensible cooling load can be beneficial [4]. To complement the ceiling in case of high load, the supply air temperature may be adjusted according to the remaining load, and when air jet velocity exceeds 2 m/s, the cooling capacity of the radiant ceiling can be increased by approximately 5% to 35% due to enhanced convection [25].

When displacement ventilation is used as the sole cooling system, the constraints on T_s limit its achievable cooling capacity. Increasing the air flow to enhance the cooling performance may hinder the contaminant stratification and result in a mixing pattern and require larger diffusers to avoid drafts, neither of which are energy-efficient nor economically viable [4]. Therefore, integrating a radiant ceiling to handle the majority of the sensible cooling load can help overcome these limitations. In this configuration, the displacement ventilation system manages the remaining sensible load, all latent loads, and the supply of outdoor air required to ensure IAQ.

However, if the radiant system removes an excessive portion of the sensible load, the air in contact with the cooled surface may migrate downwards into the occupied zone, compromising both thermal and contaminant stratification. This could lead to a more uniform temperature distribution but also shift the system towards a mixing ventilation regime, reducing IAQ [4].

The integration of a radiant system with ventilation offers an advantage over an all-air system only when the energy required to provide sensible cooling in addition to ventilation exceeds that associated with ventilation alone, and when ventilation by itself is insufficient to meet both sensible cooling and dehumidification demands [26].

2.3. Condensation prevention

To avoid condensation in cooling mode, the radiant ceiling surface temperature should be maintained at least 1 °C above the zone dew point temperature [13].

To ensure this condition, two main strategies may be applied, either individually or in combination:

1. Dehumidification of ventilation air to decrease the zone dew point temperature;
2. Control of the radiant system supply water, either by increasing the water temperature or by interrupting the water flow rate.

2.3.1. Ventilation supply air dehumidification

The most efficient option for supply air dehumidification is to combine the radiant system with a mechanical ventilation system, which provides both air cooling and dehumidification, supplying air at constant temperature and relative humidity (RH) [27]. Indeed, other alternatives studied in the context of radiant floors were found to be less satisfactory, such as isothermal dehumidifier (only dehumidification), dehumidifier with sensible cooling (dehumidification + cooling by the dehumidifier) and fan coils (where dehumidification depends on the chilled water temperature set to 7 °C) [27].

With a radiant floor system, it is appropriate to operate with a constant ventilation airflow rate and T_s = 15 °C and RH = 80% in the Italian climate [27]. T_s may be adjusted to meet any sensible load not covered by the radiant floor; however, T_s is primarily governed by the dehumidification requirement in order to avoid unnecessary and additional energy use for post-heating of the ventilation air [14].

The start-up period is a critical phase, as the local RH at the ceiling surface may exceed 100% due to humidity accumulated overnight through infiltration, combined with the lower ceiling average water temperature resulting from low morning internal gains [28]. To rapidly remove humidity, the Outdoor Air Unit [13] or the AHU [28] should supply air at the lowest temperature (e.g. 16-17 °C for a radiant ceiling in Thailand) [13], while the radiant ceiling system should be brought into operation gradually [21]. The ventilation system may also be started 30 min [29] to 1 h before the radiant system in order to allow for pre-dehumidification and thus avoid condensation, except when the infiltration rate is below 0.05 ach [28].

Increasing the ventilation airflow rate represents another mitigation strategy, continuous and constant overnight ventilation can be beneficial in hot and humid climates, for example by supplying air at T_s = 20 °C and RH = 65% for a radiant ceiling system in the United States [26]. However, this would result in higher energy consumption for coils, fans, and pumps [28].

Coupling radiant ceiling with mixing ventilation has been shown to be more effective compared with displacement ventilation in preventing condensation, due to enhanced air and moisture movement as well as improved temperature uniformity [30]. Nevertheless, when dehumidification is provided by desiccant cooling, a radiant ceiling can be effectively combined with displacement ventilation, as condensation is prevented by supplying fresh air at a fixed temperature (about 5 °C below ambient temperature) to maintain the condition: $T_{surface} = T_{dew} + 1\,°C$ [11].

2.3.2. Ceiling supply water control and new ceiling systems

Control of a radiant floor system, for example, may be based either on the water flow rate (on/off or variable-flow) or on the water supply temperature T_w based on outdoor reset control with T_a feedback [22].

With on/off control, the water valve is fully opened or closed depending on the gap between the measured indoor air temperature T_a and the setpoint, whereas in variable-flow control the water flow rate is modulated proportionally to this temperature deviation. In both approaches, T_w is typically fixed at the minimum value required during the design week with the highest outdoor temperature [22].

With outdoor reset control with T_a feedback, a reset ratio defines the increase in T_w for each degree rise in the outdoor temperature T_o , with additional correction based on T_a feedback [22]. This latter strategy results in smaller fluctuations of the floor $T_{surface}$ and the lowest occurrence of condensation events. Consequently, condensation prevention is most effectively achieved by controlling the water supply temperature based on the highest room dew point, maintaining the surface temperature at least 1°C above it, while on/off control may be used locally for thermal regulation in individual rooms [22].

Nevertheless, for radiant ceiling systems, controlling the water supply pump so that circulation is stopped when T_w becomes too low and the allowable subcooling limit is exceeded has proven to be an effective prevention strategy [18]. To achieve this, radiant ceilings are also equipped with dew point controllers and condensation [internal source].

Moreover, coupling a radiant ceiling with an airbox convector enables an increase in T_w, reducing the risk of condensation while enhancing mixed convection at the ceiling. This is achieved by combining natural convection effects with forced convection generated by the airflow from the convector directly supplied below the ceiling surface [31].

In order to prevent condensation, new radiant ceiling systems have been developed in the last decades featuring an airtight and waterproof membrane transparent to infrared wavelengths (Figure 2.5). This membrane allows the chilled surface temperature to fall below the room dew point while preventing direct contact with the zone humid air, so condensation is avoided on the ceiling surface. Moreover, this technology significantly increases the cooling capacity of radiant ceilings, particularly in hot and humid climates, achieving a reduction in overheating hours of up to 64% compared with conventional radiant systems [32].

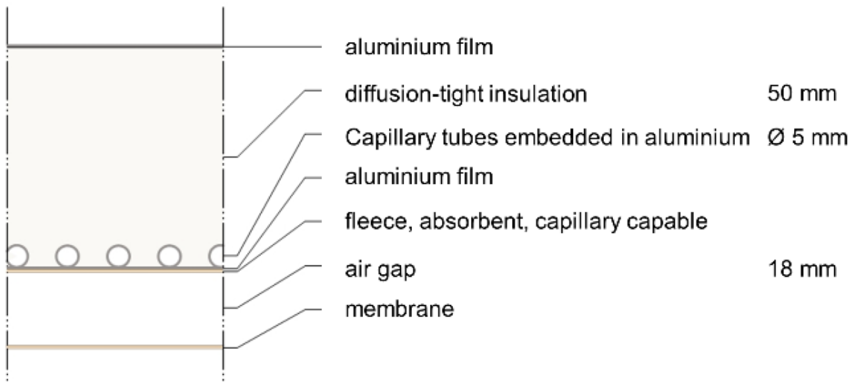

Figure 2.5: Sketch of Interpanel "Climate Panel" [32]

The supply water temperature is generally in the range of 8-12 °C for optimal ceiling cooling performance, though it can drop as low as 6 °C [33].

2.4. Summary and conclusion

This literature review highlights the strong potential of radiant ceiling systems as an alternative to conventional all-air systems, offering improvements in energy efficiency, thermal and acoustic comfort, ease of maintenance activities and architectural flexibility. When integrated with mechanical ventilation, radiant ceilings can provide efficient sensible load management while ventilation ensures IAQ compliance and latent load treatment through appropriate thermal conditioning and dehumidification strategies.

Nevertheless, the combined operation of radiant ceilings and ventilation systems requires careful coordination. In particular, summer operation remains constrained by the risk of surface condensation, which may reduce usable cooling capacity and require conservative control strategies. The most commonly adopted approaches—such as supply air dehumidification, constant air temperature design assumptions, and chilled water modulation—can lead to suboptimal compromises between energy use, comfort, and operational robustness.

Furthermore, within the French design and operational context, the literature provides limited investigation of dynamic supply air temperature control that adapts to outdoor air temperature. This identifies a research gap regarding the optimisation of radiant and ventilation system coordination through adaptive control approaches, with the objective of improving overall energy efficiency, ensuring condensation prevention and maintaining thermal comfort.

3 Research methodology

Following the discussions with company HVAC engineers and industry specialists, and building on the literature review presented in Chapter 2, this thesis identifies a clear gap: while radiant ceilings are well-documented, no established standards or methods currently address the coordination of their combined operation with AHUs via a supply air control that adapts to outdoor air temperature. This thesis therefore aims to address this gap by optimising the combined operation of a radiant ceiling coupled with an AHU through a supply air control strategy that meets specified performance requirements in terms of energy efficiency, condensation prevention, control coordination, and thermal comfort.

These requirements are evaluated through dedicated performance indicators, while accounting for key constraints: radiant ceiling sizing and operational limits (capacity constraints and condensation risk), required indoor air quality flow rates, space heat gains, and building envelope specifications.

In order to find the optimised supply air control, several configurations are tested in a parametric simulation, varying five relevant parameters of the base control curve and splitting it into summer and winter segments (Figure 3.1). The impact of these variations is also assessed.

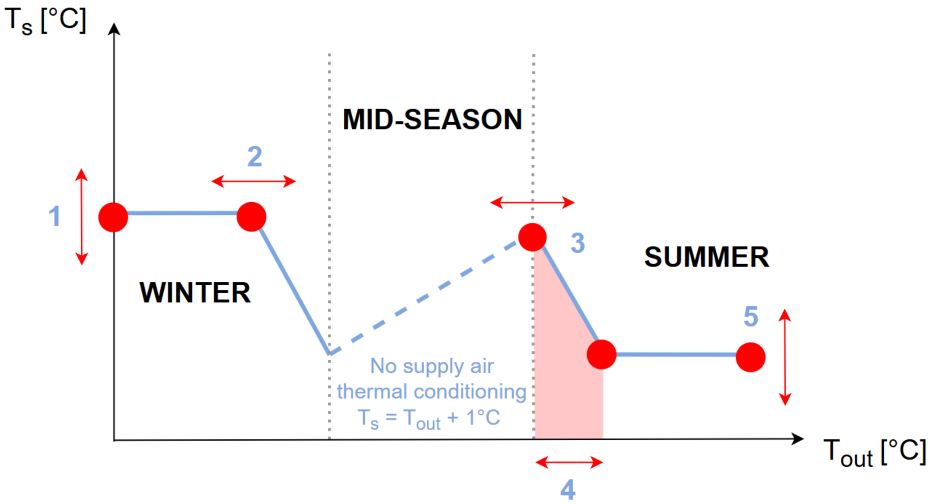

Figure 3.1: Supply air control parameters

Where:

- 1 Maximum heating supply temperature $T_{s,\max heating}$;
- 2 Outdoor temperature threshold for maximum heating $T_{o,\max heating}$;
- 3 Outdoor temperature threshold for cooling $T_{o,cooling}$;
- 4 Outdoor temperature range of the cooling slope $T_{o,cooling\ slope}$;
- 5 Minimum cooling supply temperature $T_{s,min\ cooling}$.

During mid-season, the need for thermal conditioning of supply air for thermal comfort is generally reduced. Therefore, the AHU heating and cooling coils are deactivated, and $T_s = T_{out} + 1$ °C due to the supply fan motor heat loss, which is a common assumption from the company's field experience.

Subsequently, the optimal summer and winter configurations are identified based on a global score defined as a weighted average of all performance indicators, thereby determining the best overall yearly configuration.

Finally, the performance results of the best yearly configuration are compared with a common suboptimal configuration of supply air control.

The methodology (Figure 3.2) starts with the development of the numerical model in DesignBuilder and the checking of the defined hypotheses, followed by parametric simulations and a subsequent analysis of the results, ultimately leading to the design of an optimised supply air control strategy meeting the specified performance requirements:

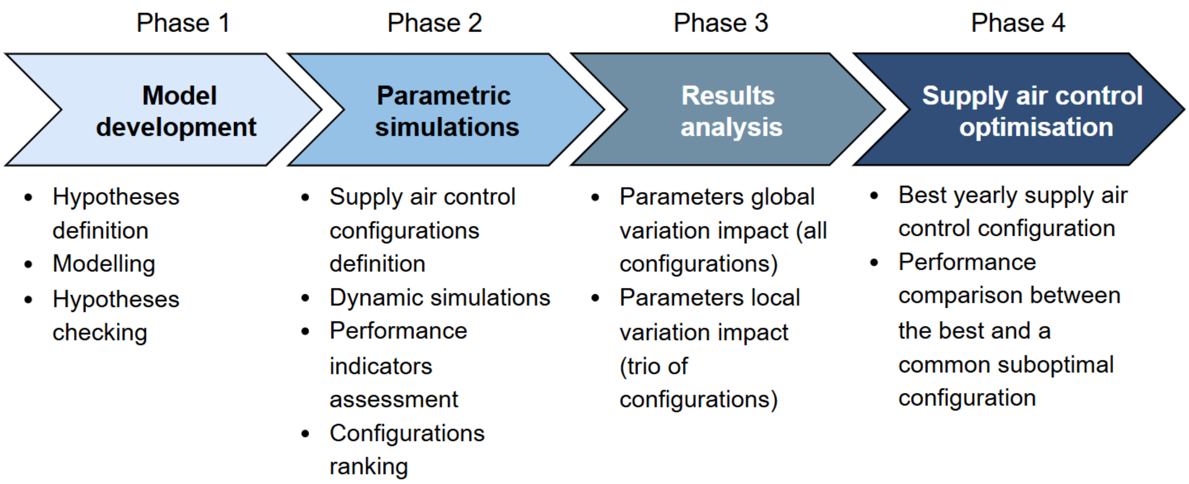

Figure 3.2: Proposed methodology workflow

4 Energy modelling

The numerical model of the standard office space is developed in DesignBuilder to represent the zone's thermal and structural characteristics, and thereby enable detailed dynamic simulations.

4.1. Office building characteristics

The studied space is representative of a standard office building located in Paris:

- Latitude: 48.72°;
- Longitude: 2.38°;
- ASHRAE climate zone: 4A;
- Elevation above sea level: 90 m;
- Exposure to wind: normal;
- Hourly weather data: FRA_PARIS_IWEC.

It is distributed into perimeter offices (Zones 2-5-7-9), each facing a different orientations, and meeting rooms (Zones 3-4) located in the central part of the office plan (Figure 4.1).

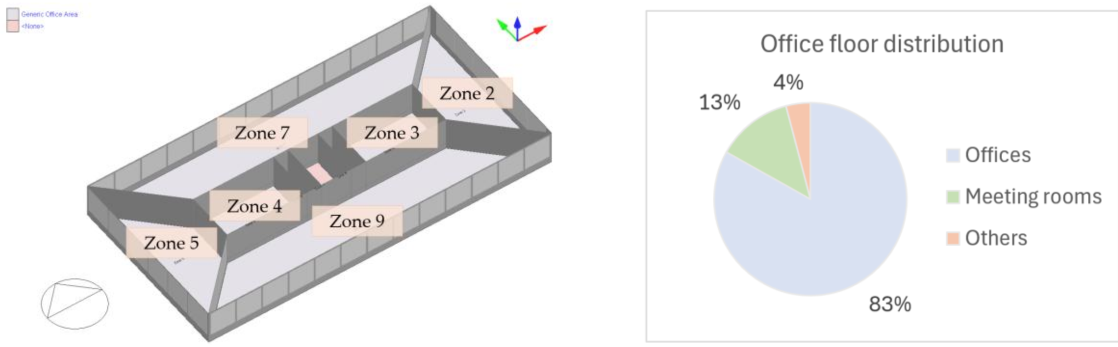

Figure 4.1: Office floor space distribution

The building envelope is made of a simple curtain wall, whose stratigraphy along with the structural components are detailed in Appendix B.

4.2. Standard thermal zone

As previously mentioned in Chapter 1, the typical thermal zone heat gains and losses originate from internal sources such as occupants, lighting and equipment, or from external sources such as solar radiation, envelope transmission and infiltration. The schedules and intensity of these gains (except envelope transmission) are defined in Appendix C.

Although operative temperature, Predicted Mean Vote (PMV) and Predicted Percentage Dissatisfied (PPD) indicators provide more precise and relevant assessments of the radiative heat exchange from radiant ceilings on thermal comfort, the thermal control strategy adopted in this work is based on the zone mean air temperature. This choice is justified by several practical considerations: air temperature is the control variable actually used in office buildings for HVAC regulation and monitoring, it serves as the basis for contractual comfort guarantees, and its use allows to more accurately reflect real operational conditions. Additionally, the 10-15 min response time of black globe thermometers introduces significant measurement delays, making them unsuitable for dynamic control application.

The mean air temperature setpoints follow typical contractual temperature requirements for buildings in France, which vary according to the zone occupancy state (Table 4.1):

Table 4.1: Zone mean air temperature comfort setpoints

Zone air temperature setpoints			
Occupancy state	**Heating**	**Cooling**	**Deadband**
-	**[°C]**	**[°C]**	**[°C]**
Occupancy - 7AM to 8PM	19	26	7
Standby - if no occupant detected during occupied time	18	27	9
Unoccupancy - 8PM to 7AM, all weekends and holidays	17	28	11

The deadband is the temperature range between the heating and cooling setpoints within which no thermal conditioning is delivered.

Figure 4.2 shows the thermal zone heat gains and the radiant ceiling and AHU systems, including their hydronic and air distribution networks:

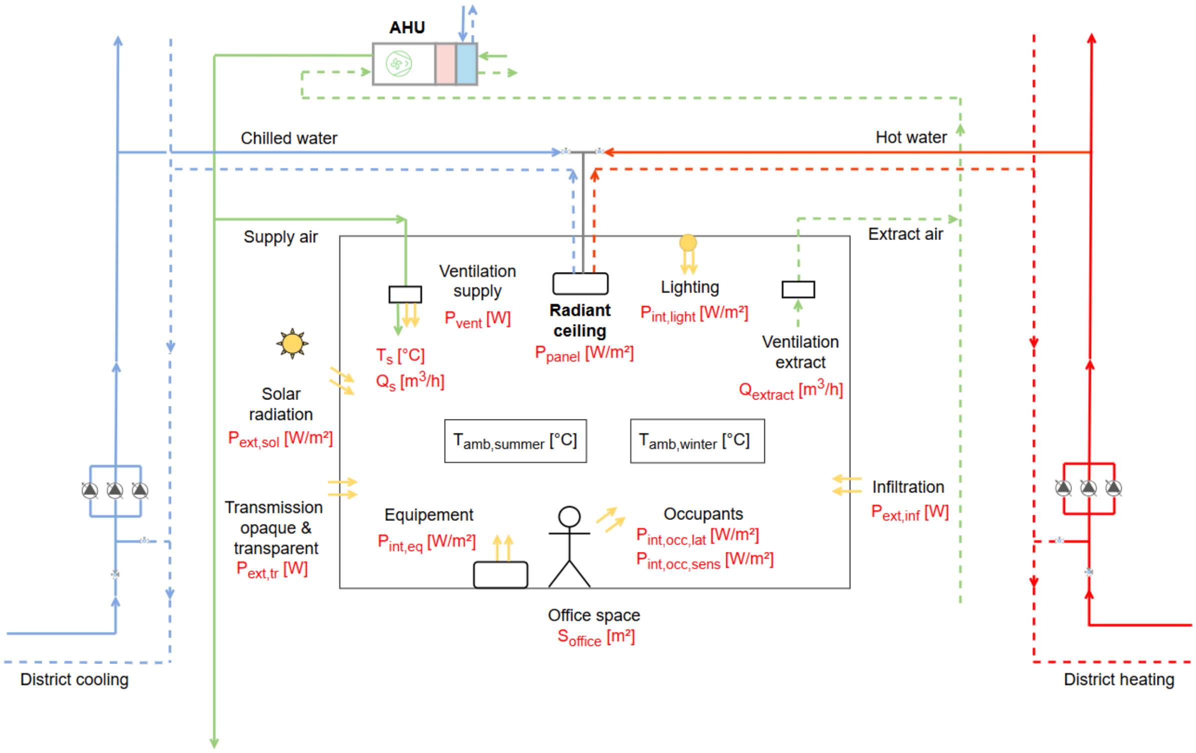

Figure 4.2: Standard office space gains, HVAC system and networks

4.3. HVAC system

4.3.1. Radiant ceiling

The radiant ceiling is modelled with an internal heat source between the glass fibre insulation and the gypsum panel of the intermediate slab (Table 4.2):

Table 4.2: Intermediate slab and radiant ceiling stratigraphy

Intermediate slab and radiant ceiling							
Layers	**λ**	**R**	**U**	**Density**	**cp**	**Thermal mass**	**Thickness**
-	**[W/m.K]**	**[m².K/W]**	**[W/m².K]**	**[kg/m3]**	**[J/kg.K]**	**[kJ/m3.K]**	**[m]**
BOTTOM							
Plaster	0.50	1.00	83	1300	1000	1300	0.006
Internal heat source							
Glass fibre	0.035	1.00	1.00	25	1000	25	0.035
Air gap (plenum)	-	0.23	-	1.2	1.005	-	0.30
Cast concrete	1.13	0.18	5.65	2000	1000	2000	0.20
Air gap	-	0.22	-	1.2	1.005	-	0.10
Wooden particleboard	0.135	0.30	3.38	800	1300	1040	0.04
TOP							
Total	0.31	2.21	0.45	-	-	-	0.681

The thermal capacity is 58.70 W/m² of active surface in heating and 92.95 W/m² in cooling (detailed specifications are in Appendix D). These values are derived from the technical benchmark presented in Appendix A, from discussions with an industry expert, and from the specifications of products installed in an existing project. The radiant ceiling operates continuously to maintain the zone air temperature setpoint based on the occupancy state (Table 4.1).

4.3.2. Air Handling Unit

The ventilation system is a dual-flow AHU, equipped with an electric heating coil and a hydronic cooling coil, whose specifications are in Appendix D.

The AHU delivers the IAQ flow rate—25 m^3/h.person in offices and 30 m^3/h.person in meeting rooms as is typical in standard office buildings in France [23]—through a VAV system, at a temperature T_s determined by the supply air control. The system does not work when the zone is unoccupied.

4.4. Simulation tool and details

The software used for the modelling is DesignBuilder, which relies on the EnergyPlus dynamic simulation engine. The simulations are performed with a time step of 30 minutes, with the following settings:

- General solution algorithm: Conduction Transfer Function (sensible heat-only solution that does not account for moisture storage or diffusion in the construction elements);
- Convection algorithm:
    - Inside convection algorithm: Thermal Analysis Research Program (TARP) by default (which calculates natural convection as a function of temperature difference from ASHRAE algorithm);
    - Outside convection algorithm: DOE-2 by default (combination of the Mobile Window Thermal Test (MoWiTT) and Building Loads Analysis and System Thermodynamics (BLAST) Detailed convection models).

In addition, supply air controls are defined using Energy Management System (EMS) scripts with the DesignBuilder scripting module.

In summary, DesignBuilder enables a detailed representation of internal gains, the building envelope and structural stratigraphy, the HVAC system (production, distribution, and terminal units), as well as the control parameters for the AHU supply air and the radiant ceiling, before running dynamic simulations using the EnergyPlus engine.

5 Performance assessment methodology

The developed numerical model is used to perform a parametric analysis of the relevant supply air control parameters and evaluate the tested configurations in terms of the main performance requirements. For this purpose, the following performance indicators are defined (Figure 5.1):

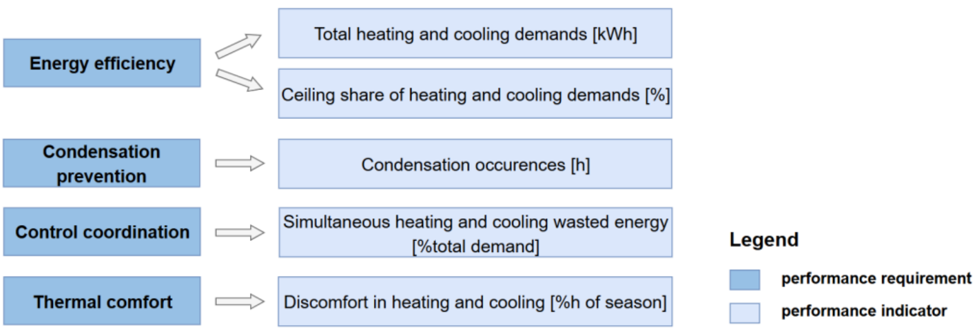

Figure 5.1: Performance requirements assessment through performance indicators

Then, each configuration is ranked based on its overall performance, quantified through a global score defined as a weighted average of the individual scores.

5.1. Model inputs and outputs

The main inputs and outputs of the numerical model concerns the thermal zone, the radiant ceiling and the AHU (Figure 5.2):

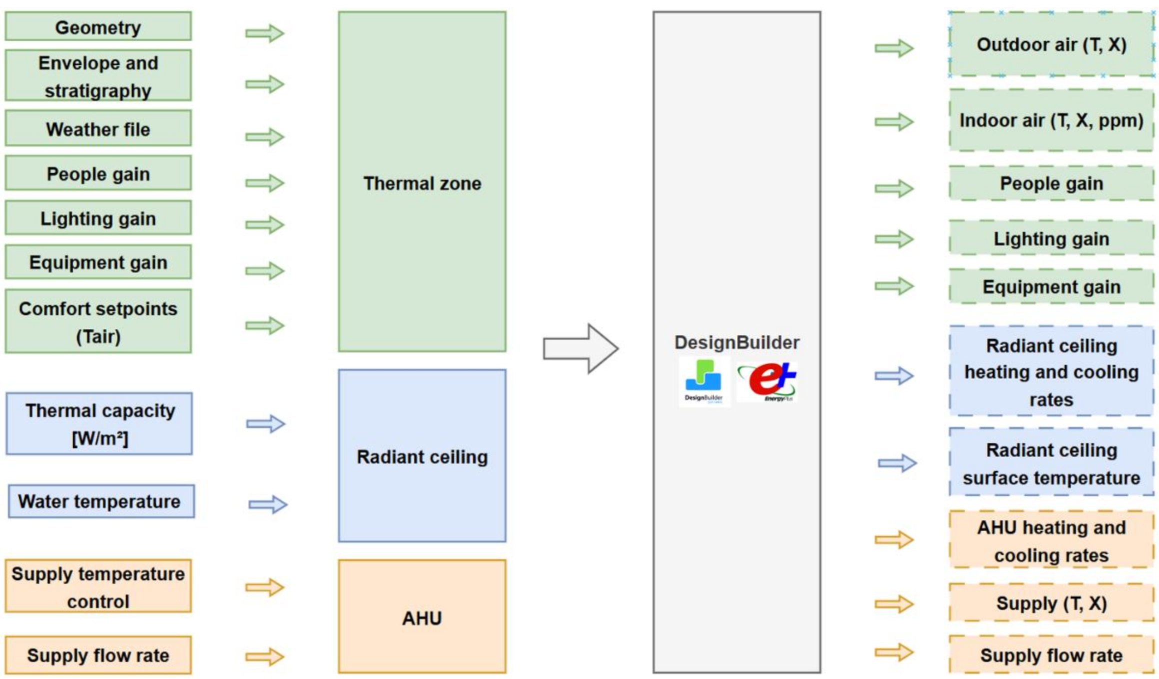

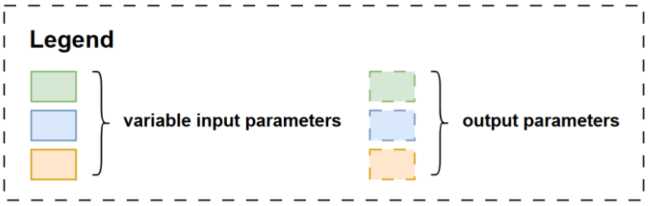

Figure 5.2: Numerical model inputs and outputs

5.2. Tested configurations of the parametric analysis

Variations in the supply air control curve points are explored to assess their impact on performance indicators and improve overall system performance. Supply air control curves result from a distinct heating curve and cooling curve.

The baseline control configuration represents the most refined strategy currently deployed; however, it was developed through years of empirical optimisation based on field experience rather than numerical modelling (Figure 5.3):

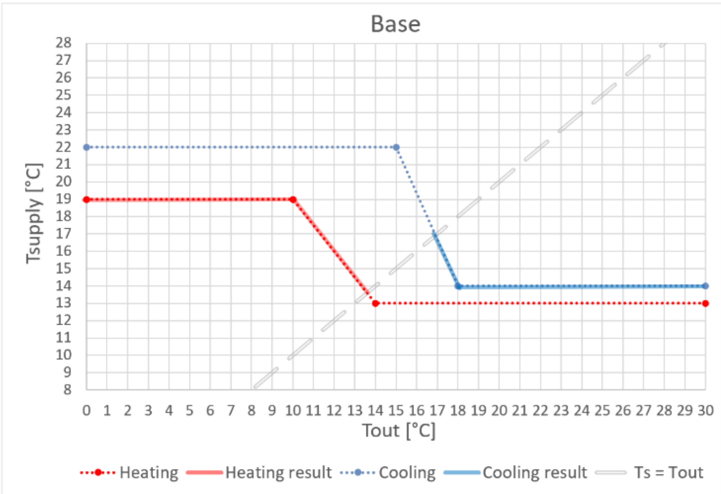

Figure 5.3: Base configuration

For clarity, the winter and the summer sides of the control curve are modified separately; each parameter is varied across a defined range of values, while the others remain constant (Figure 5.4):

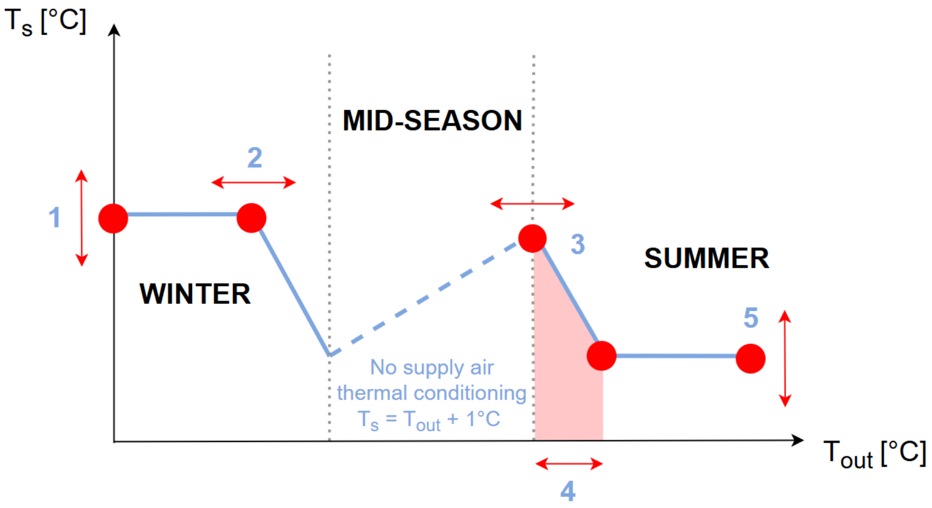

Figure 5.4: Supply air control parameters

Where:

- 1 Maximum heating supply temperature $T_{s,\max heating}$;
- 2 Outdoor temperature threshold for maximum heating $T_{o,\max heating}$;
- 3 Outdoor temperature threshold for cooling $T_{o,cooling}$;
- 4 Outdoor temperature range of the cooling slope $T_{o,cooling\ slope}$;
- 5 Minimum cooling supply temperature $T_{s,min\ cooling}$.

During winter, the main challenge is energy efficiency, as T_s is often higher than required for thermal comfort. Therefore, the variations focus on reducing the maximum heating supply temperature (1) and delaying the heating outdoor temperature threshold as much as possible (2). In addition, some configurations where T_s is above the 19 °C baseline—observed in LHIRR's existing projects—are assessed.

During summer, the main challenges are condensation prevention and thermal comfort. Several configurations are explored to evaluate the impact of increasing the outdoor temperature threshold for cooling (3) and widening the outdoor temperature range defining the cooling slope (4), with the aim of maximising the share of cooling provided by the ceiling. The cooling minimum supply temperature (5) is also varied on both sides of the 14 °C baseline, with an extreme configuration at 12 °C.

During mid-season, the main challenge is system control coordination, therefore the deadband is increased, but only as part of the summer side configurations (3), since the minimum supply air temperature acceptable for thermal comfort on the winter side is around 13 °C.

Configuration name

- WTR — Winter side

  1 $T_{s,y}$ — Heating maximum supply temperature $T_{s,\max heating}$ = y °C;

2 $T_{o,x}$ — Outdoor temperature threshold for maximum heating $T_{o,\max heating}$ = x °C;

- SMR — Summer side

3 T_{o,x_x+1} — Outdoor temperature threshold for cooling $T_{o,cooling}$ = x °C;

4 $T_{o,17\_z}$ — Outdoor temperature range of the cooling slope $T_{o,cooling\ slope}$ = [17;z] °C;

5 $T_{s,y}$ — Cooling minimum supply temperature $T_{s,min\ cooling}$ = y °C.

5.2.1. Winter side configurations

- 1 Heating maximum supply temperature $T_{s,\max heating}$

The configuration name "WTR $T_{s,y}$" means that the heating supply temperature is set to y °C, when the outdoor temperature falls below 10 °C. Above 10 °C, the heating supply temperature decreases linearly from y °C to the point where the heating curve intersects the T_s = T_{out} line, at approximatively 13.5 °C. The tested range of $T_{s,\max heating}$ is from 16 °C to 25 °C, in steps of 1 °C (Figure 5.5):

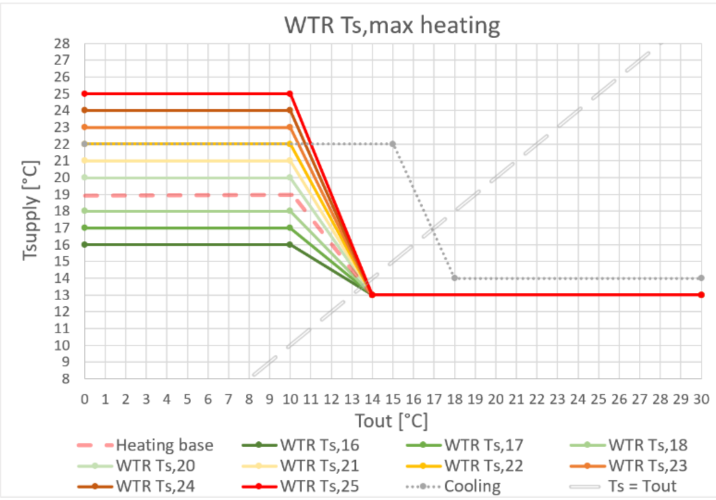

Figure 5.5: Configurations varying the heating maximum supply temperature $T_{s,max\ heating}$

- 2 Outdoor temperature threshold for maximum heating $T_{o,\max heating}$

The configuration name "WTR $T_{s,16} - T_{o,x}$" means that the heating maximum supply temperature (1) is maintained at 16 °C and is applied when the outdoor temperature falls below x °C. The tested range of $T_{o,\max heating}$ is from 2 °C to 8 °C, in steps of 2 °C (Figure 5.6):

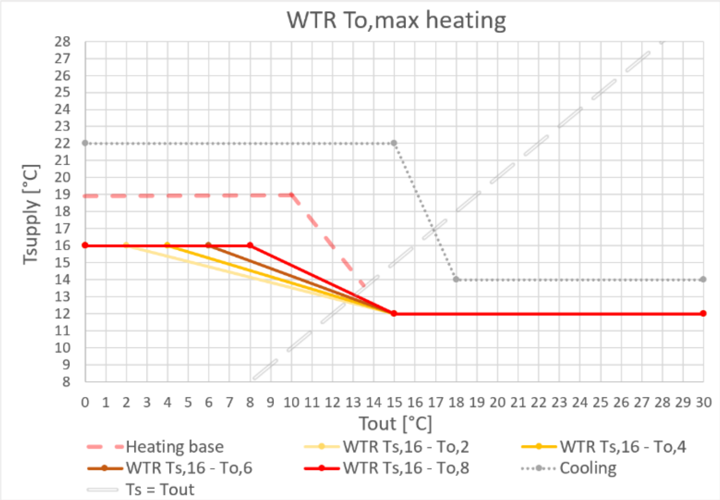

Figure 5.6: Configurations varying outdoor temperature threshold for maximum heating $T_{o,max\ heating}$

5.2.2. Summer side configurations

- **3** Outdoor temperature threshold for cooling $T_{o,cooling}$

The configuration name "SMR T_{o,x_x+1}" means that the outdoor temperature threshold for cooling is x °C; cooling is activated when the outdoor temperature exceed x °C, supplying air at x °C. For outdoor temperatures between x °C and x+1 °C, the cooling supply temperature decreases linearly from x °C to 14 °C. The tested range of $T_{o,cooling}$ is from 18 °C to 21 °C, in steps of 1 °C (Figure 5.7):

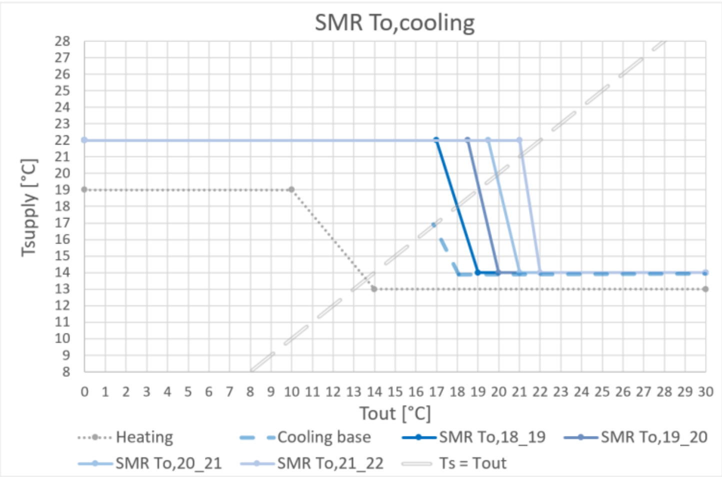

Figure 5.7: Configurations varying the outdoor temperature threshold for cooling $T_{o,cooling}$

- **4** Outdoor temperature range of the cooling slope $T_{o,cooling\ slope}$

The configuration name "SMR $T_{o,17\_z}$" means that the cooling slope is defined for outdoor temperatures between 17 °C (3) and z °C. Over this range, supply temperature decreases linearly from 17 °C to 14 °C. The tested range of $T_{o,cooling\ slope}$ is from 17 °C to 25 °C, in steps of 2 °C (Figure 5.8):

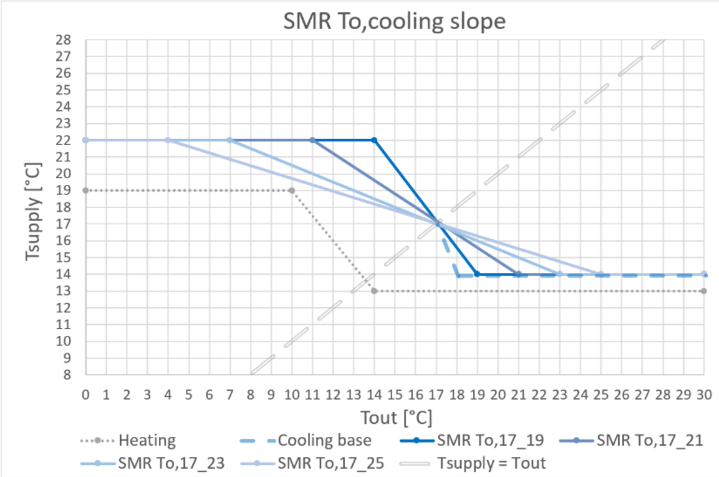

Figure 5.8: Configurations varying the outdoor temperature range of the cooling slope $T_{o,cooling\ slope}$

- **5** Cooling minimum supply temperature $T_{s,min\ cooling}$

The configuration name "SMR $T_{s,y}$" means that the cooling minimum supply temperature is fixed at y °C, when the outdoor temperature exceeds 18 °C. The tested range of $T_{s,min\ cooling}$ is from 12 °C to 16 °C, in steps of 1 °C (Figure 5.9):

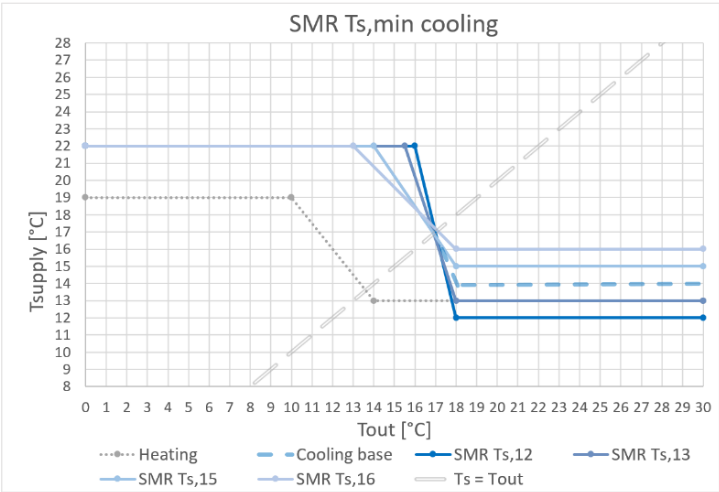

Figure 5.9: Configurations varying the cooling minimum supply temperature $T_{s,min\ cooling}$

5.3. Performance indicators

To assess system performance for each configuration with respect to the defined requirements, several performance indicators have been developed, and the best yearly configuration is compared with the suboptimal one in Section 5.6.

5.3.1. Total heating and cooling demands [kWh]

The ceiling heating and cooling demands are determined by aggregating all zones and applying the following heat transfer formula:

$$Q_{ceiling,heating\ or\ cooling} = \sum_{t}^{z} m_w . c_{pw} . \Delta T_w \ [kWh]$$

With:

- m_w [kg/s] the water mass flow rate;
- c_{pw} [kJ/kg.K] the water specific heat capacity, c_{pw} = 4.18 kJ/kg.K;
- ΔT_w [°C] the difference between the input and the output water temperatures
- t [h] the simulation time step, t = 30 min = 0.5 h;
- z the zone number.

In the event of condensation, ceiling operation is suspended, and no thermal demand is accounted for.

The AHU demands are calculated based on the heating and cooling coil rates. For the electric heating coil, the heating rate is equal to the electrical power input since the efficiency is equal to 1:

$$Q_{heating\ coil} = \sum_{t} P_{heating\ coil} . t \ [kWh]$$

With:

- $P_{heating\ coil}$ [kW] the heating coil electrical power;
- t [h] the simulation time step, t = 30 min = 0.5 h.

The cooling demand of the AHU cooling coil is calculated using the similar to the ceiling formula, but using air as the heat transfer medium:

$$Q_{cooling\ coil} = \sum_{t} m_a . c_{pa} . \Delta T_a \ [kWh]$$

With:

- m_a [kg/s] the air flow rate;
- c_{pa} [kJ/kg.K] the air specific heat capacity, c_{pa} = 1.005 kJ/kg.K;
- ΔT_a [°C] the difference between the input and the output air temperatures;
- t [h] the simulation time step, t = 30 min = 0.5 h.

Therefore, the total heating and cooling demands are:

- $Demand\ H = Q_{heating\ coil} + Q_{ceiling,heating} \ [kWh]$;
- $Demand\ C = Q_{cooling\ coil} + Q_{ceiling,cooling} \ [kWh]$.

And the total thermal demand, which is the thermal energy delivered by the HVAC system, is:

$$Demand\ H\&C = Demand\ H + Demand\ C \ [kWh]$$

The total heating and cooling demand may slightly vary across configurations, as the AHU contribution to thermal conditioning changes with the supply air control. The objective is to minimise overall energy demand while improving the system's global energy efficiency.

5.3.2. Ceiling heating and cooling demands share [%]

For both heating and cooling demands, the ceiling contribution is calculated:

- Heating: $Ceiling\ H\% = \frac{Q_{ceiling,heating}}{Demand\ H} . 100$ [%];
- Cooling: $Ceiling\ C\% = \frac{Q_{ceiling,cooling}}{Demand\ C} . 100$ [%].

The objective is to maximise the ceiling contribution to thermal conditioning, thereby increasing the overall system energy efficiency, since radiant ceilings are more energy efficient than AHUs due to the higher thermal capacity of water compared with air.

5.3.3. Condensation occurrences [h]

The condensation risk is assessed as the number of hours [h] calculated by evaluating all zones simultaneously and counting each time step only once, even if condensation occurs in multiple zones. Condensation occurs when: $T_{surface} < T_{dew}$.

The ceiling surface temperature is estimated as the average water temperature plus 1 °C, following the simplified method commonly used by industrial manufacturers for radiant ceiling sizing:

$$T_{surface} = \frac{T_{w,in} + T_{w,out}}{2} + 1\ [°C]$$

The zone dew point is estimated from the Magnus formula [34]:

$$T_{dew}(\gamma) = \frac{\lambda.\gamma}{\beta - \gamma} [°C]$$

With:

- $\gamma\ (T_a, RH) = \ln\left(\frac{RH}{100}\right) + \frac{\beta.T_a}{\lambda + T_a}$;
- β = 17.62 °C and λ = 243.12 °C, for T_a between -45 °C and 60 °C.

Therefore, the total number of condensation hours is calculated summing the index $I_{condensation}$ returning 0.5 if condensation occurs in one of the zones during the 30 min time step, and 0 otherwise:

$$Condensation = \sum_t I_{condensation}\ [h]$$

Depending on the ventilation supply air temperature T_s, condensation may occur to a greater or lesser extent; the objective is to minimise its occurrence.

In practice, condensation does not occur because radiant systems are equipped with condensation sensors that deactivate the system when a condensation risk is detected, though this may compromise thermal comfort.

5.3.4. Wasted energy due to simultaneous heating and cooling between the AHU and the ceiling [%total demand]

Simultaneous heating and cooling between the AHU and the radiant ceiling panels may occur because the AHU heating and cooling coils are activated based on outdoor temperature rather than season, and outdoor temperatures can fluctuate significantly within a single day. Additionally, radiant ceilings are equipped with 6-way valves (a pair of 3-way valves, one controlling the water inlet and the other the water outlet) that allow rapid alternation between hot and chilled water flow. This enables the ceiling to provide both heating and cooling within the same day, and to meet the contractual indoor air temperature setpoint depending on the zone occupancy (Figure 5.10):

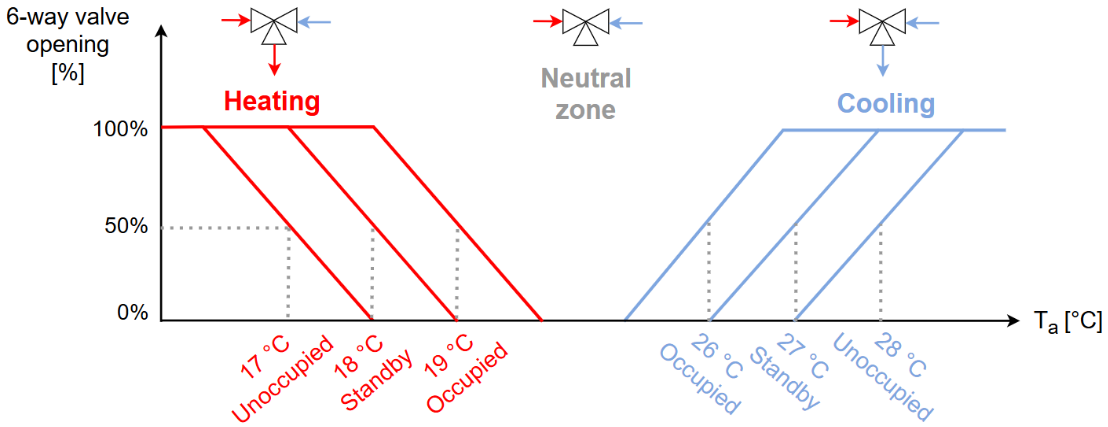

Figure 5.10: Ceiling 6-way valve opening [%] according to the air temperature for each heating and cooling contractual comfort setpoints

Considering that the radiant ceiling throttling range is set to 2 °C (Appendix D), the ceiling's thermal output is given as follows (Figure 5.11):

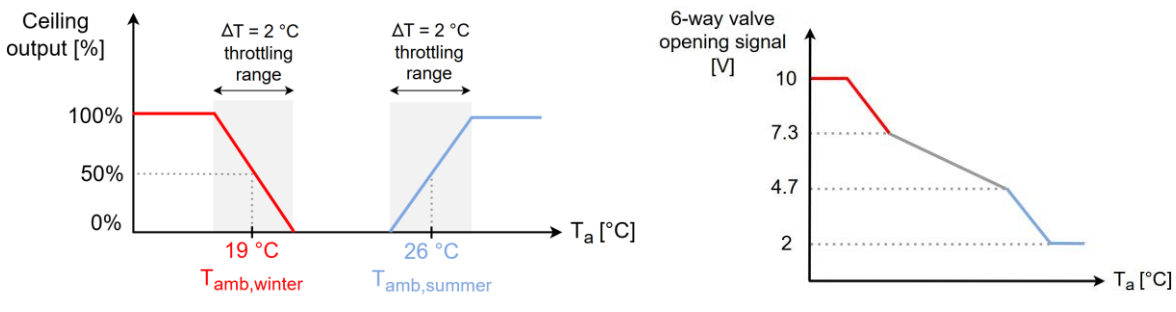

Figure 5.11: Ceiling thermal output [%] (left) and 6-way valve opening signal [V] (right) according to T_a for zone occupied state setpoints

Two scenarios of simultaneous heating and cooling typically occur (Figure 5.12, Appendix G):

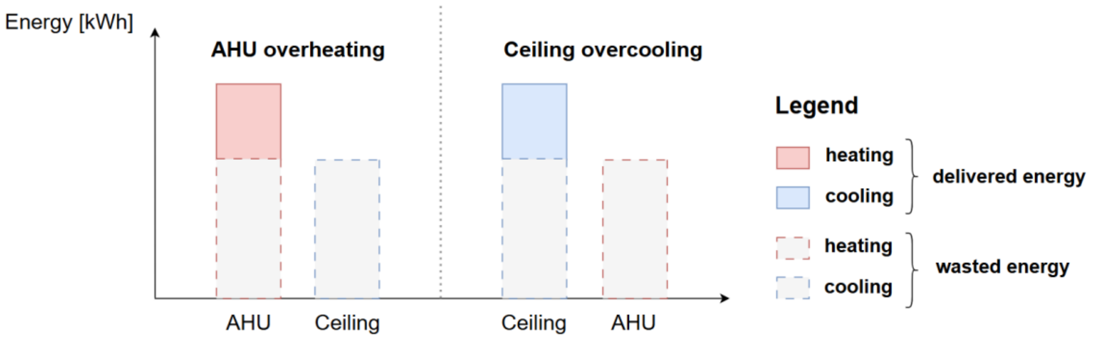

Figure 5.12: Wasted energy for AHU overheating and ceiling overcooling scenarios

1. **AHU overheating:** During winter, inadequate supply air control may result in overheated ventilation air, forcing the radiant ceiling to provide cooling to maintain thermal comfort.
2. **Ceiling overcooling:** During winter, when supply air is heated based solely on outdoor temperature, zones with high internal heat gains (e.g., south-facing spaces or meeting rooms) may require ceiling cooling. In such cases, the ceiling must overcool to compensate for the sensible heating supplied by the AHU. This situation is increasingly common in modern buildings, where highly insulated envelopes mean that thermal demands are not determined solely by outdoor air temperature.

This phenomenon leads to energy waste, as heating and cooling effects counteract each other. The wasted energy is computed as the total cancelled energy from both the AHU and the ceiling, aggregated across all zones:

$$Q_{SHC} = \sum_{t}^{z} Q_{SHC,AHU} + Q_{SHC,ceiling} \ [kWh]$$

With:

- t [h] the simulation time step, t = 30 min = 0.5 h;
- z the zone number.

Then, the corresponding share of the total energy demand is:

$$SHC\ En\% = \frac{Q_{SHC}}{Demand\ H\&C}\ [\%]$$

The objective is to minimise the occurrences of simultaneous heating and cooling, and therefore the associated wasted energy.

5.3.5. Thermal discomfort in heating and cooling [%h]

In this study, within the French context, thermal discomfort is defined as the deviation of the mean air temperature T_a from the specified contractual setpoints (Table 4.1). It is assessed as the percentage of occupied hours of the season [%h] during which discomfort occurs. All zones are evaluated simultaneously, and each time step is counted only once, even if discomfort occurs in multiple zones.

Accounting for the ceiling throttling range (Figure 5.11) and typical control system hysteresis, it is common practice in France to consider that discomfort occurs when the difference between the air temperature and the contractual setpoint exceeds 1 °C. Discomfort is also assumed to occur when condensation is detected, since the ceiling is turned off and cannot meet the sensible cooling demand (Figure 5.13):

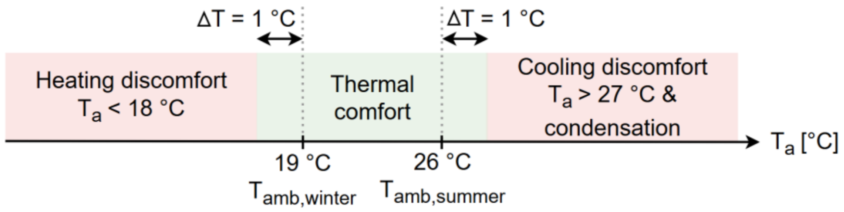

Figure 5.13: Thermal discomfort thresholds

Therefore, the share of discomfort hours is calculated as:

$$Discomfort\ i = \sum_{t}^{z} \frac{I_{discomfort\ i}}{N_{occ\ hours\ i}}\ [\%h]$$

With:

- $Discomfort\ i$ [%h] corresponds to the percentage of discomfort hours during heating or cooling season;
- $I_{discomfort\ i}$ the index returning 0.5 if discomfort occurs in one of the zones during the 30 min time step, and 0 otherwise;
- $N_{occ\ hours\ i}$ $[h]$ the number of occupied hours during heating or cooling season, where heating season is from November to April (1419 h) and cooling season from May to October (1452 h).

The objective is to minimise thermal discomfort occurrences and to keep the percentage of discomfort below 10% of occupied hours for each zone and season individually, a threshold inspired by comfort category II of the ISO standard [35]. However, an initial overall discomfort evaluation, aggregating all zones, is first conducted to identify the best summer and winter configurations. A more detailed zone-level analysis is then performed for the best and the suboptimal configurations only.

It can be noted that some of the indicators are interrelated:

- The total demand, the ceiling demand share and the wasted energy due to simultaneous heating and cooling are interdependent and broadly related to energy efficiency;
- Condensation directly affects thermal comfort, the ceiling's total cooling demand and demand share.

These performance indicators are calculated from the DesignBuilder model outputs and are used to assess the tested supply air control configurations (for both summer and winter operation), as well as to develop the optimised yearly supply air control (Figure 5.14):

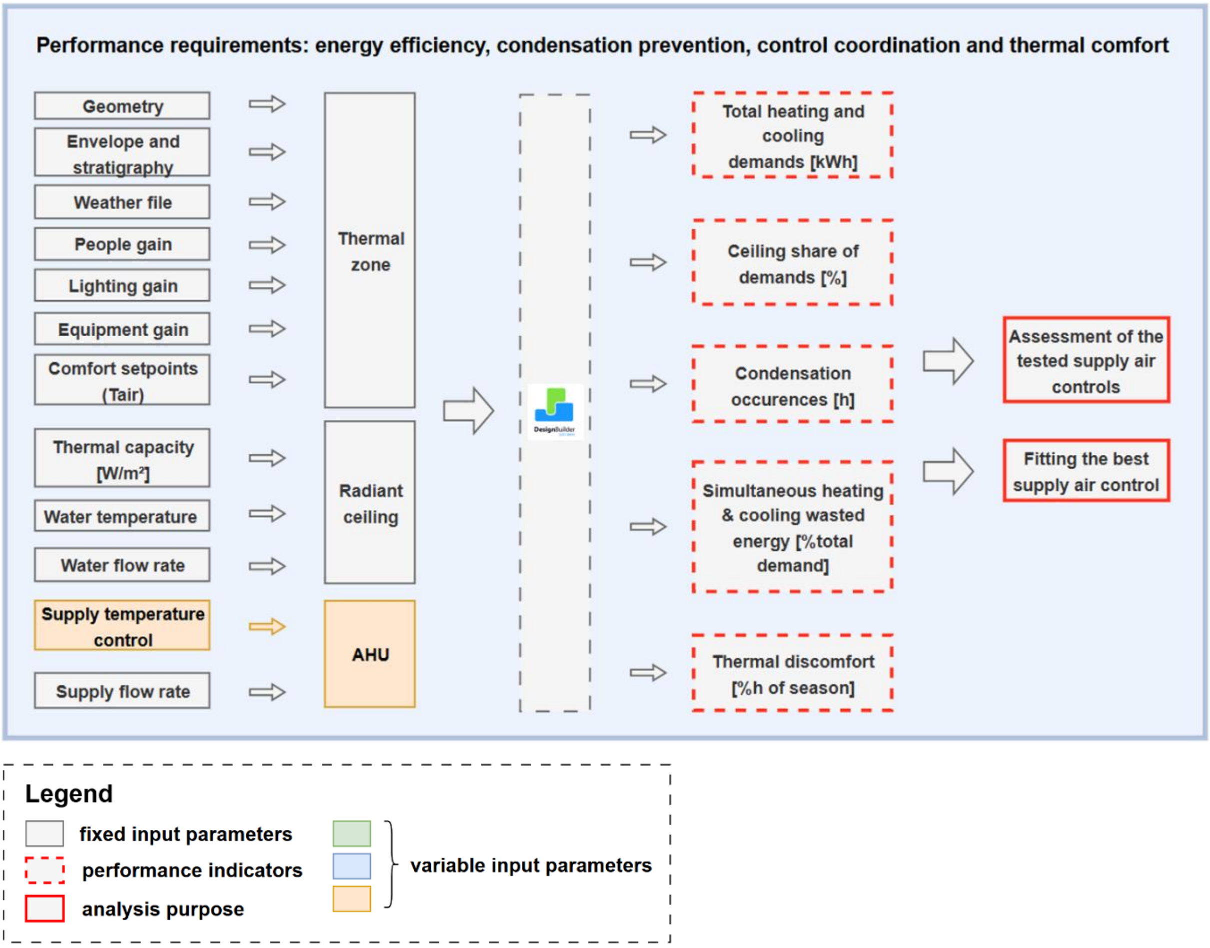

Figure 5.14: Parametric analysis performance indicators

5.4. Configurations ranking

To rank the tested winter and summer configurations based on their overall performance, a score—absolute or relative—is assigned to each performance indicator. The scoring methodology varies across indicators depending on the characteristics of the underlying results, in order to ensure meaningful differentiation between configurations. A global performance score is then computed as a weighted average of the individual indicator scores.

5.4.1. Total heating and cooling demands [kWh]

For the total heating and cooling demands, the score is calculated for each configuration “x” as follows:

$$S^{x}_{Demand\ i} = 1 - \frac{Demand\ i^{x} - Demand\ i^{min}}{Demand\ i^{max} - Demand\ i^{min}}\ [0-1]$$

With:

- $Demand\ i^{x}$ [kWh] the heating or cooling demand of configuration "x";
- $Demand\ i^{max}$ [kWh] the maximum heating or cooling demand among all the tested configurations;
- $Demand\ i^{min}$ [kWh] the minimum heating or cooling demand among all the tested configurations.

In this way, the configuration with the lowest heating or cooling demand obtains the highest score 1, while the one with the highest demand receives a score of 0.

5.4.2. Ceiling heating and cooling demands share [%]

For the ceiling share of demands, the scoring is based the same principle as for the total heating and cooling demands:

$$S^{x}_{Ceiling\ i\%} = \frac{Ceiling\ i\%^{x} - Ceiling\ i\%^{min}}{Ceiling\ i\%^{max} - Ceiling\ i\%^{min}}\ [0-1]$$

With:

- $Ceiling\ i\%^{x}$ [%] the ceiling share of heating or cooling total demand of configuration "x";
- $Ceiling\ i\%^{max}$ [%] the maximum ceiling share of heating or cooling total demand among all the tested configurations;
- $Ceiling\ i\%^{min}$ [%] the minimum ceiling share of heating or cooling total demand among all the tested configurations.

In this way, the configuration with the maximum ceiling heating or cooling demand share obtains the highest score 1, while the one with the minimum ceiling demand share receives a score of 0.

5.4.3. Condensation occurrences [h]

For condensation occurrences, the scoring approach is designed to reflect the highly negative impact of condensation on thermal comfort; therefore, a decreasing exponential function is used. The relationship shown between the score value and the number of condensation hours is defined as follows (Figure 5.15):

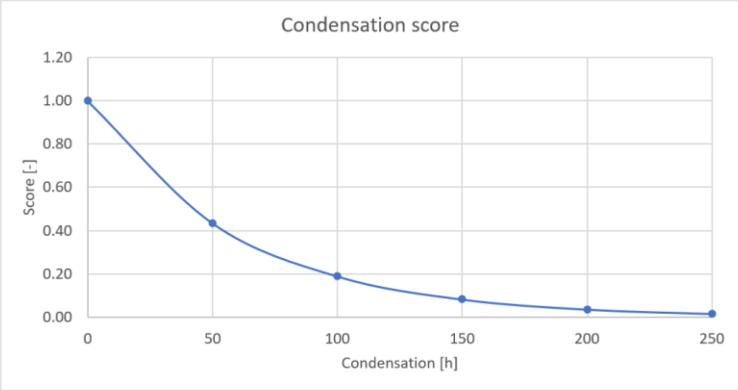

Figure 5.15: Condensation score curve

Therefore, the condensation score is calculated with the following function:

$$S^{x}_{Condensation} = e^{-Condensation^{x}/60}\ [0-1]$$

With $Condensation^{x}$ [h] the number of condensation hours of configuration "x".

In this way, a pronounced drop in the score is observed as condensation duration increases from 0 to 100 h, whereas the rate of decrease becomes less steep for durations exceeding 100 h.

5.4.4. Wasted energy due to simultaneous heating and cooling between the AHU and the ceiling [%total demand]

For the wasted energy, the score is calculated as follows:

$$S^{x}_{SHC\ En\%} = 1 - \frac{SHC\ En\%^{x} - SHC\ En\%^{min}}{SHC\ En\%^{max} - SHC\ En\%^{min}}\ [0-1]$$

With:

- $SHC\ En\%^{x}$ [%] the wasted energy share of total demand of configuration "x";
- $SHC\ En\%^{max}$ [%] the maximum wasted energy share of total demand among all the tested configurations;
- $SHC\ En\%^{min}$ [%] the minimum wasted energy share of total demand among all the tested configurations.

In this way, the configuration with the minimum wasted energy obtains the highest score 1, while the one with the maximum value receives a score of 0.

5.4.5. Thermal discomfort in heating and cooling [%h]

For thermal discomfort, the score is calculated as follows:

$$S^{x}_{Discomfort\ i} = 1 - \frac{Discomfort\ i^{x} - Discomfort\ i^{min}}{Discomfort\ i^{max} - Discomfort\ i^{min}}\ [0-1]$$

With:

- $Discomfort\ i^{x}$ the discomfort hours percentage [%h] during heating or cooling season of configuration "x";
- $Discomfort\ i^{max}$ = 20% the maximum seasonal discomfort percentage in heating or cooling;
- $Discomfort\ i^{min}$ = 10% the minimum seasonal discomfort percentage in heating or cooling.

In this way, the score is set to 1 if the percentage of discomfort hours is less than or equal to 10% of the occupied hours, and to 0 if it exceeds 20%, considering all zones concurrently. For the zone-level analysis (Subsection 6.3.5), a more stringent upper limit is applied and set at 10% to comply with comfort category II of the ISO standard [35].

5.4.6. Global score

The weights attributed to each of the performance scores are determined to reflect the relative importance of the corresponding performance indicator (Table 5.1):

Table 5.1: Weight attribution for the global performance score

Performance indicator	Score weight
Total heating demand [kWh]	1
Total cooling demand [kWh]	1
Ceiling share of heating demand [%]	1
Ceiling share of cooling demand [%]	1
Condensation occurrences [h]	4
Wasted energy [%total demand]	2
Discomfort in heating [%h]	1.25
Discomfort in cooling [%h]	1.25

The condensation occurrences score has the highest weight of 4 because such events do not only interrupt ceiling operation but also adversely impact multiple indicators, including total energy demand, ceiling demand share, and thermal discomfort. Furthermore, condensation represents a critical operational constraint: modern condensation sensors can tolerate only one to two detection events before requiring replacement, unlike earlier technologies based on gold-plated sheets, which could withstand several hundred occurrences without degradation. Simultaneous heating and cooling is weighted at 2, as wasted energy must be avoided? The remaining energy-efficiency-related indicators are weighted at 1 since they are numerous and their effects are relatively comparable. Discomfort is weighted at 1.5, as such occurrences represent failures to meet the contractual performance requirements.

Therefore, the global performance score for each configuration "x" is calculated as:

$$S^{x}_{global} = (1 * S^{x}_{Demand\ H} + 1 * S^{x}_{Demand\ C} + 1 * S^{x}_{Ceiling\ H\%} + 1 * S^{x}_{Ceiling\ C\%} + 4 * S^{x}_{Condensation} + 2 * S^{x}_{SHC\ En\%} + 1.5 * S^{x}_{Discomfort\ H} + 1.5 * S^{x}_{Discomfort\ C})/13$$

The parametric analysis on the supply air control is conducted by varying the heating maximum supply temperature $T_{s,\max heating}$, the outdoor temperature threshold for maximum heating $T_{o,\max heating}$, the outdoor temperature threshold for cooling $T_{o,cooling}$, the outdoor temperature range of the cooling slope $T_{o,cooling\ slope}$ and the minimum cooling supply temperature $T_{s,min\ cooling}$.

The performance of tested configurations is assessed through performance indicators: total heating and cooling demands [kWh], ceiling share of demands [%], condensation occurrences [h], wasted energy due to simultaneous heating and cooling [%total demand] and thermal discomfort [%h].

The configurations are then ranked based on a global score, defined as a weighted average of the individual performance indicator scores. Condensation is assigned the highest weight (4/13) given its strong adverse impact on system operation and other indicators.

6 Results and analysis

A detailed analysis is performed to assess the influence of each supply air control parameter on system performance. The yearly performance of the optimal configuration is then compared with that of a commonly used suboptimal configuration.

6.1. Supply air control impact on system performance

At building commissioning, the supply air control parameters (Figure 6.1) are established; however, building operators can subsequently modify them. While such modifications occur frequently in practice, their effects on building performance are largely overlooked. This study therefore aims to evaluate the impact of these parameter variations on the performance indicators.

To this end, score variations for each performance indicator are evaluated using two approaches: first, by aggregating all configurations to capture the full range of variations; second, by examining a selected trio of configurations for detailed analysis over a restricted range.

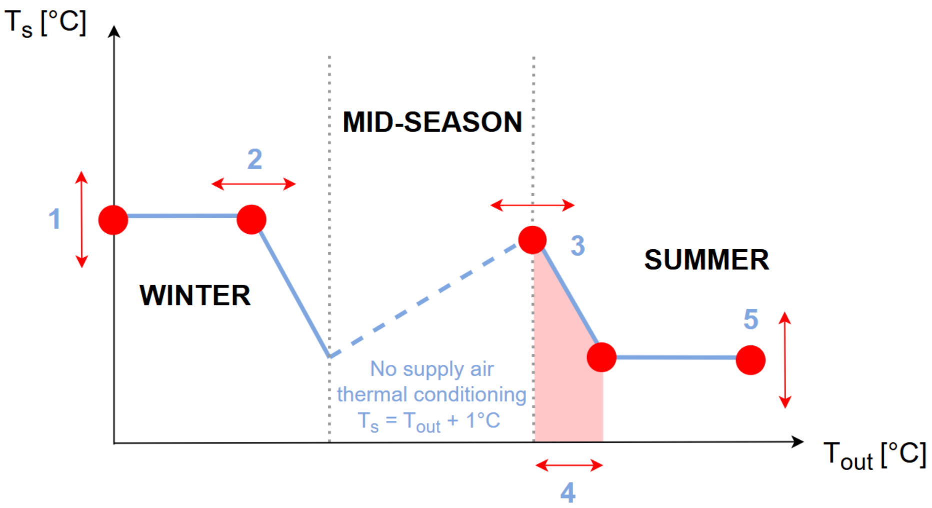

Figure 6.1: Supply air control parameters

Configuration name

- WTR — Winter side

  1 $T_{s,y}$ — Heating maximum supply temperature $T_{s,\max heating}$ = y °C;

  2 $T_{o,x}$ — Outdoor temperature threshold for maximum heating $T_{o,\max heating}$ = x °C;

- SMR — Summer side

  3 T_{o,x_x+1} — Outdoor temperature threshold for cooling $T_{o,cooling}$ = x °C;

  4 $T_{o,17\_z}$ — Outdoor temperature range of the cooling slope $T_{o,cooling\ slope}$ = [17;z] °C;

  5 $T_{s,y}$ — Cooling minimum supply temperature $T_{s,min\ cooling}$ = y °C.

Performance indicators

- Demand H/C — Total heating/cooling demand [kWh]
- Ceiling H%/C% — Ceiling share of cooling and heating demand [%]
- Condensation — Condensation occurrences [h]
- SHC En% — Simultaneous heating and cooling wasted energy [%total demand]
- Discomfort H%/C% — Heating/cooling discomfort occurrences [%h]

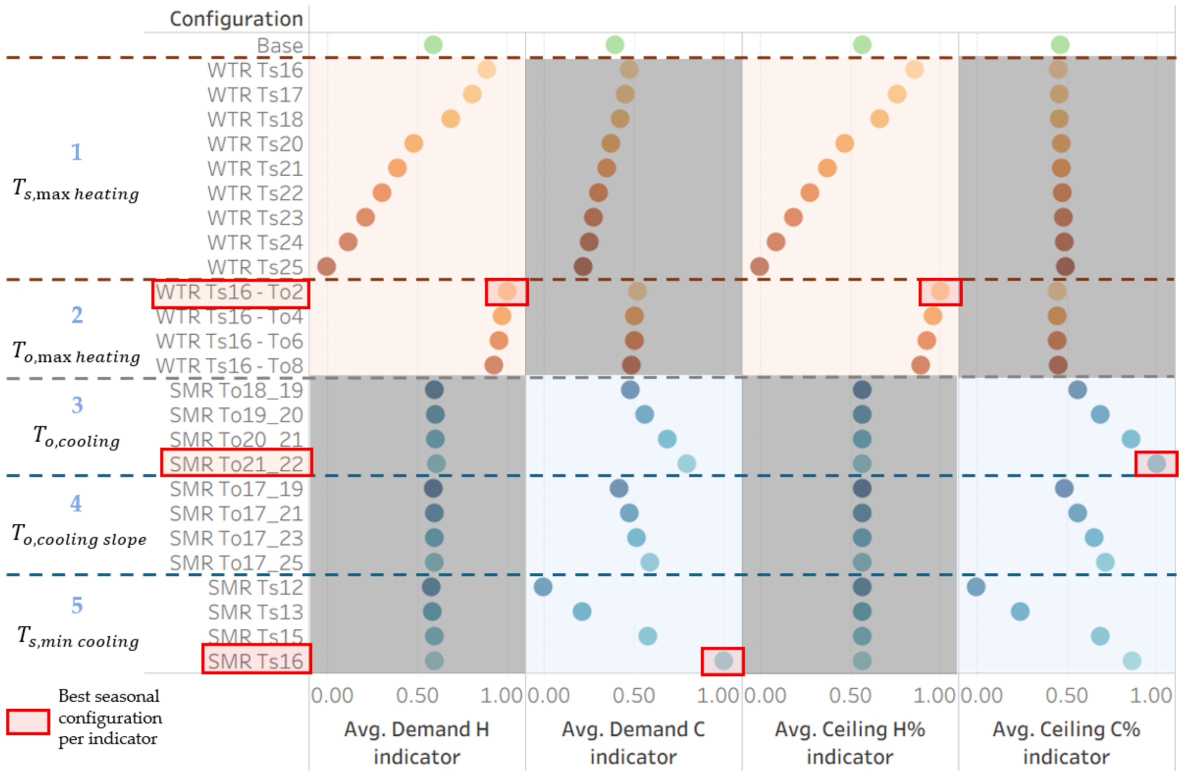

Figure 6.2: Configurations score for the total heating and cooling demands and ceiling demands share indicators

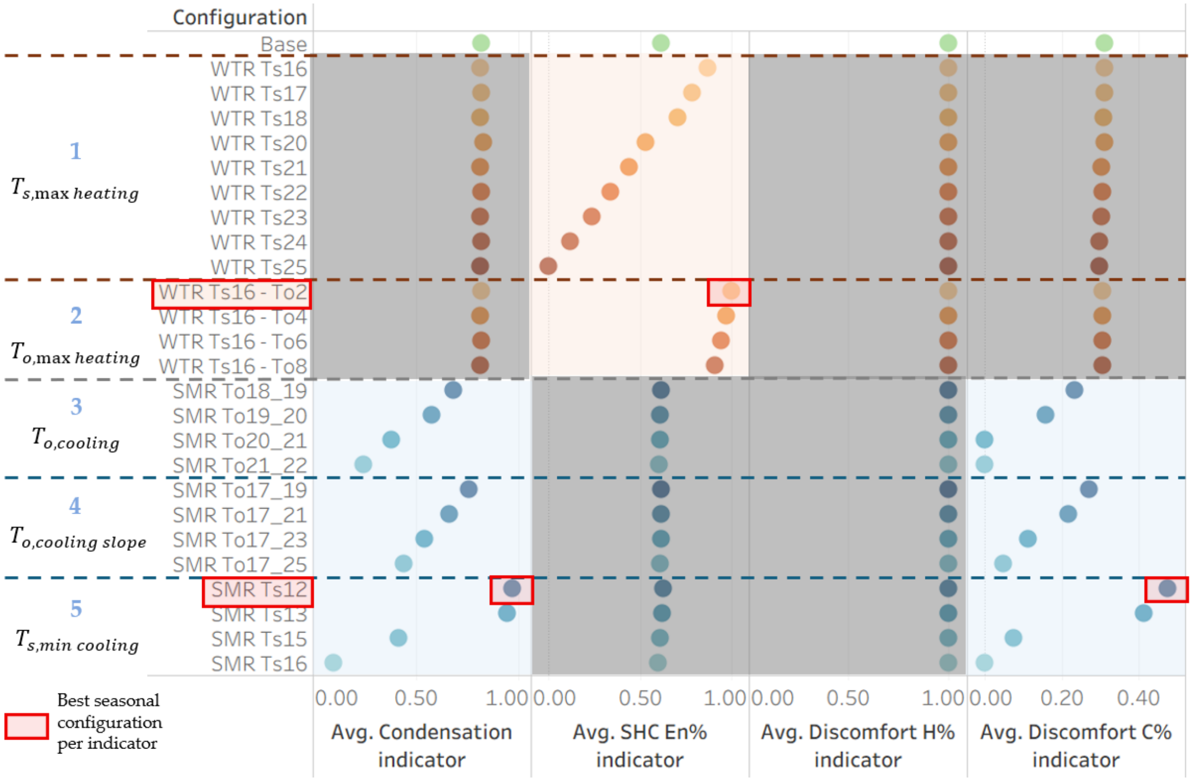

Figure 6.3: Configurations score for simultaneous heating and cooling, condensation and heating and cooling discomfort indicators

For the detailed analysis, three adjacent configurations—defined by consecutive values of each supply air control parameter—are selected:

- A middle configuration “x,middle”, defined as the reference configuration;
- A top configuration “x,top”, corresponding to a parameter variation $\Delta parameter = v\,°C$ relative to “x,middle”;
- A bottom configuration “x,bottom”, corresponding to a parameter variation $\Delta parameter = -v\,°C$ relative to “x,middle”.

The score variation is calculated as follows:

- For the top configuration: $\Delta S_{global}^{x,top-x,middle} = \frac{S_{global}^{x,top} - S_{global}^{x,middle}}{\Delta parameter}$;
- For the bottom configuration: $\Delta S_{global}^{x,bottom-x,middle} = \frac{S_{global}^{x,bottom} - S_{global}^{x,middle}}{|\Delta parameter|}$.

With $|\Delta parameter| = \Delta parameter = v\,°C$, the absolute value of the parameter variation.

A colour scale (Table 6.1) is assigned to each score variation, ranging from red indicating a strongly negative score drop, to green, indicating a strongly positive score increase:

Table 6.1: Colour scale for the score variation intensity

Score variation range	Variation intensity
] -inf ; -0.05]	- -
] -0.05 ; -0.02]	-
] -0.02 ; 0.02]	/
] 0.02 ; 0.05]	+
] 0.05 ; +inf]	+ +

6.1.1. Winter side configurations

For winter configurations, the following indicators exhibit a strong correlation, with a correlation coefficient r approaching 1 (Figure 6.4):

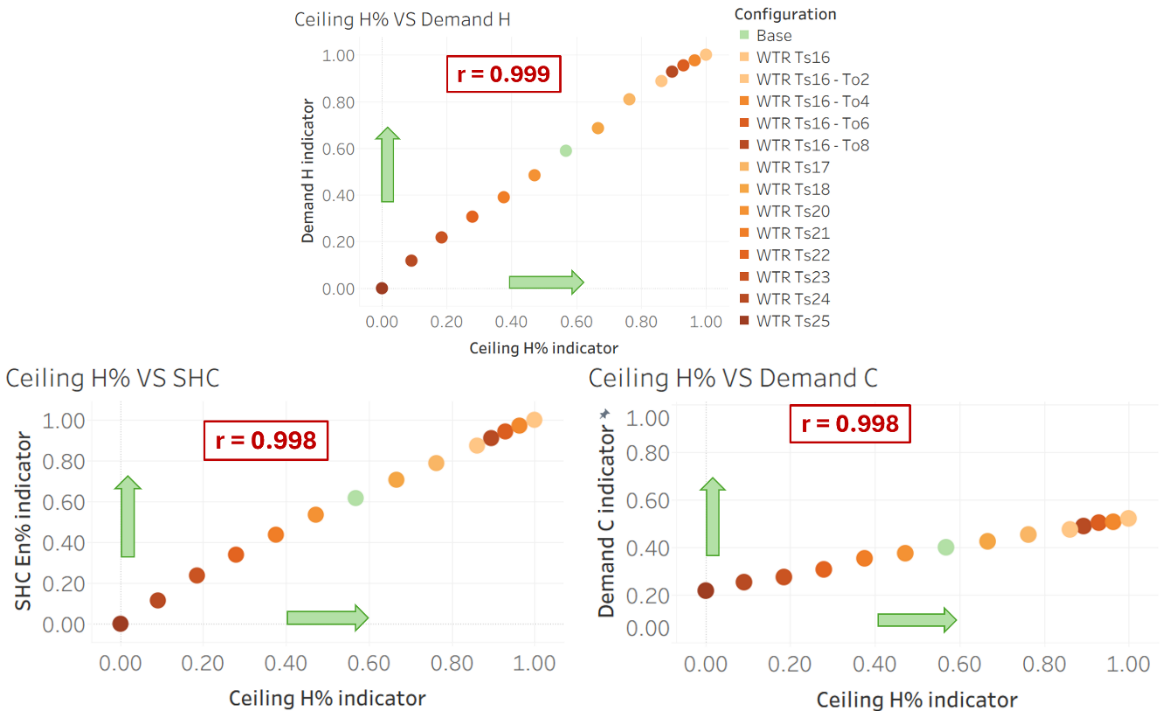

Figure 6.4: Relationship between ceiling share and heating demand (top), ceiling heating share and simultaneous heating and cooling (bottom left), ceiling heating share and cooling demand (bottom right) performance indicators

6.1.1.1. Heating maximum supply temperature (1)

As $T_{s,\max heating}$ (1) increases, performance scores of Demand H, Ceiling H% and SHC En% decrease significantly (Figure 6.2, Figure 6.3) indicating that both system energy efficiency and control coordination are reduced (Figure 6.4 (top), Figure 6.4 (bottom left)).

When the heating maximum supply temperature increases by 1 °C (Table 6.2), the ceiling heating share decreases significantly and the heating demand increases, as the AHU provides more heating than needed. Wasted energy also increases since the radiant ceiling needs to compensate for the AHU overheating by delivering cooling, leading to poorer subsystems coordination (Appendix G). This mechanism explains the increase in cooling demand (Figure 6.4 (bottom right), Table 6.2). As a result, the average impact of this variation on the system performance is negative.

Conversely, when the supply temperature decreases by 1 °C, the opposite effects are observed with similar magnitude.

Table 6.2: $T_{s,max\ heating}$ impact on the performance indicators

		Parameter	WTR Ts,max heating								
		Performance indicator	Avg. Demand H indicator	Avg. Demand C indicator	Avg. Ceiling H% indicator	Avg. Ceiling C% indicator	Avg. Condensation indicator	Avg. SHC En% indicator	Avg. Discomfort H% indicator	Avg. Discomfort C% indicator	Avg. Indicator
		Performance requirement	Energy efficiency	Energy efficiency	Energy efficiency	Energy efficiency	Condensation prevention	Operation coordination	Thermal comfort	Thermal comfort	
Δparameter [°C]	**1**	**WTR Ts18**	- -	-	- -	/	/	- -	/	/	-
	0	**WTR Ts17**									
	-1	**WTR Ts16**	+ +	+	+ +	/	/	+ +	/	/	+

6.1.1.2. Outdoor temperature threshold for maximum heating (2)

Over the whole range of outdoor temperature threshold for heating $T_{o,\max heating}$ (2), the impact on each performance indicator score is minimal (Figure 6.2, Figure 6.3, Table 6.3); therefore, this parameter appears to be of limited relevance to the overall system performance.

Table 6.3: $T_{o,max\ heating}$ impact on the performance indicators

		Parameter	WTR To,max heating								
		Performance indicator	Avg. Demand H indicator	Avg. Demand C indicator	Avg. Ceiling H% indicator	Avg. Ceiling C% indicator	Avg. Condensation indicator	Avg. SHC En% indicator	Avg. Discomfort H% indicator	Avg. Discomfort C% indicator	Avg. Indicator
		Performance requirement	Energy efficiency	Energy efficiency	Energy efficiency	Energy efficiency	Condensation prevention	Operation coordination	Thermal comfort	Thermal comfort	
Δparameter [°C]	**1**	**WTR To8**	/	/	/	/	/	/	/	/	/
	0	**WTR To6**									
	-1	**WTR To4**	/	/	/	/	/	/	/	/	/

6.1.2. Summer side configurations

For summer configurations, the following indicators exhibit a strong correlation, with a correlation coefficient r approaching 1 (Figure 6.5):

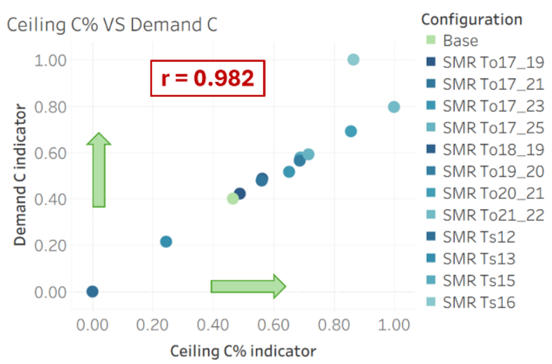

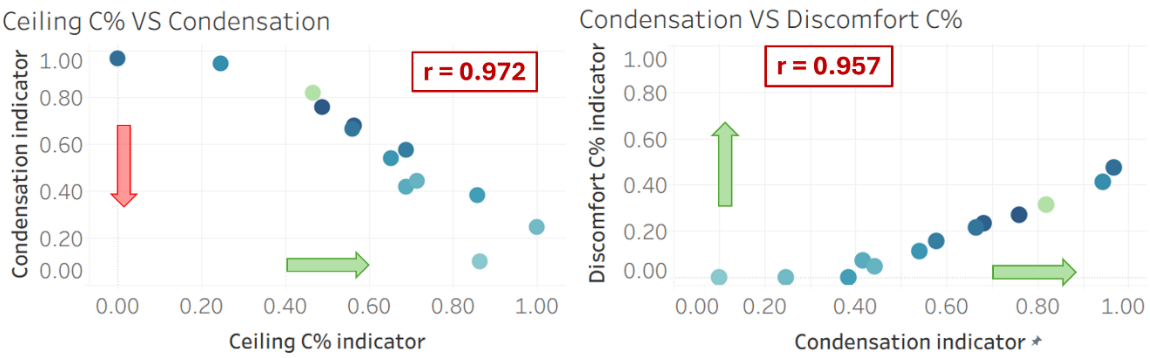

Figure 6.5: Relationship between ceiling share and cooling demand (top), ceiling cooling share and condensation (bottom left), condensation and cooling discomfort (bottom right) performance indicators

6.1.2.1. Outdoor temperature threshold for cooling (3)

As the outdoor temperature cooling threshold $T_{o,cooling}$ (3) increases, the scores of Demand C and Ceiling C% increase (Figure 6.2), whereas Condensation and Discomfort C% scores decrease (Figure 6.3)—particularly for thresholds above 19 °C. This suggests that improved energy efficiency is associated with reduced condensation prevention and diminished thermal comfort (Figure 6.5). Therefore, to ensure effective condensation prevention and satisfactory thermal comfort, $T_{o,cooling}$ should not exceed 19 °C.

When the outdoor temperature threshold for cooling increases by 1 °C (Table 6.4), the AHU provides less cooling; consequently the ceiling cooling share increases while the cooling demand decreases, as the AHU deadband becomes wider. However, condensation occurrences increase significantly. As a result, although the system energy efficiency is enhanced, condensation risk becomes substantial. Since this indicator carries the highest weight, the overall impact on the system performance is negative.

Conversely, when the outdoor temperature threshold decreases by 1 °C, the opposite effects are observed for the previously mentioned indicators. In addition, cooling discomfort decreases significantly, resulting in a strongly positive impact on the overall system performance.

Table 6.4: $T_{o,cooling}$ impact on the performance indicators

		Parameter	**SMR To,cooling**								
		Performance indicator	Avg. Demand H indicator	Avg. Demand C indicator	Avg. Ceiling H% indicator	Avg. Ceiling C% indicator	Avg. Condensation indicator	Avg. SHC En% indicator	Avg. Discomfort H% indicator	Avg. Discomfort C% indicator	Avg. Indicator
		Performance requirement	Energy efficiency	Energy efficiency	Energy efficiency	Energy efficiency	Condensation prevention	Operation coordination	Thermal comfort	Thermal comfort	
Δparameter [°C]	**1**	**SMR To21_22**	/	+ +	/	+ +	- -	/	/	/	-
	0	**SMR To20_21**									
	-1	**SMR To19_20**	/	- -	/	- -	+ +	/	/	+ +	+ +

6.1.2.2. Outdoor temperature range of the cooling slope (4)

As the cooling slope magnitude $T_{o,cooling\ slope}$ (4) increases, the scores of Demand C and Ceiling C% show moderate improvement (Figure 6.2), whereas Condensation and Discomfort C% scores decrease (Figure 6.3). This suggests that enhanced system energy efficiency is associated with reduced condensation prevention and diminished thermal comfort (Figure 6.5). The effects appear slightly more pronounced when transitioning from "SMR $T_{o,17\_21}$" to "SMR $T_{o,17\_23}$".

When the outdoor temperature range defining the cooling slope increases by 2 °C (Table 6.5), the ceiling cooling share increases moderately, as the AHU reaches the cooling minimum temperature $T_{s,min\ cooling}$ (5) at a higher outdoor temperature threshold, so it contributes less to cooling. However, cooling discomfort increases significantly, indicating that the ceiling cooling capacity is insufficient to meet the cooling demand. Condensation occurrences also increase substantially, since the supply air is insufficiently dehumidified and the zone dew point exceeds the ceiling surface temperature. Consequently, the overall impact on the system performance is negative.

Conversely, when the outdoor temperature range of the cooling slope decreases by 2 °C, the opposite effect is observed for the ceiling share. However, for discomfort and condensation indicators, the positive effect is less pronounced than the negative one. This suggests that condensation varies substantially not only for $T_{o,cooling}$ between 19 °C and 20 °C (Paragraph 6.1.2.1) but also for $T_{o,cooling\ slope}$ between 21 °C and 23 °C.

Table 6.5: $T_{o,cooling\ slope}$ impact on the performance indicators

		Parameter	SMR To,cooling slope								
		Performance indicator	Avg. Demand H indicator	Avg. Demand C indicator	Avg. Ceiling H% indicator	Avg. Ceiling C% indicator	Avg. Condensation indicator	Avg. SHC En% indicator	Avg. Discomfort H% indicator	Avg. Discomfort C% indicator	Avg. Indicator
		Performance requirement	Energy efficiency	Energy efficiency	Energy efficiency	Energy efficiency	Condensation prevention	Operation coordination	Thermal comfort	Thermal comfort	
Δparameter [°C]	2	SMR To17_23	/	/	/	+	- -	/	/	- -	-
	0	SMR To17_21									
	-2	SMR To17_19	/	-	/	-	+	/	/	+	/

6.1.2.3. Cooling minimum supply temperature (5)

As the cooling minimum supply temperature $T_{s,min\ cooling}$ (5) increases, Demand C and Ceiling C% scores increase substantially (Figure 6.2), whereas Condensation and Discomfort C% scores decrease significantly (Figure 6.3). A particularly large gap is observed between supply temperatures of 14 °C (baseline) and 15 °C, suggesting that improved energy efficiency is associated with reduced condensation prevention and diminished thermal comfort (Figure 6.5). Therefore, to ensure effective condensation prevention and satisfactory thermal comfort, $T_{s,min\ cooling}$ should not exceed 14 °C. Below 13 °C, further improvement in condensation prevention appear negligible.

When the cooling minimum supply temperature increases by 1 °C, ceiling cooling share increases significantly, as the AHU supplies warmer air and contributes less to cooling, and cooling demand decreases since the AHU is not overcooling. However, thermal discomfort and condensation—which has the highest weight in the global score—increase significantly, resulting in a strongly negative impact on the global system performance.

Conversely, when the cooling minimum supply temperature decreases by 1 °C, the opposite effects are observed, but the resulting positive effect is negligible.

Table 6.6: $T_{s,min\ cooling}$ impact on the performance indicators

		Parameter	**SMR Ts,min cooling**								
		Performance indicator	Avg. Demand H indicator	Avg. Demand C indicator	Avg. Ceiling H% indicator	Avg. Ceiling C% indicator	Avg. Condensation indicator	Avg. SHC En% indicator	Avg. Discomfort H% indicator	Avg. Discomfort C% indicator	Avg. Indicator
		Performance requirement	Energy efficiency	Energy efficiency	Energy efficiency	Energy efficiency	Condensation prevention	Operation coordination	Thermal comfort	Thermal comfort	
Δparameter [°C]	**1**	**SMR Ts15**	/	+ +	/	+ +	- -	/	/	- -	- -
	0	**Base (Ts14)**									
	-1	**SMR Ts13**	/	- -	/	- -	+ +	/	/	+ +	/

Therefore, when each indicator is considered individually (Figure 6.2,Figure 6.3), "WTR $T_{s,16} - T_{o,2}$" delivers the best results in minimising total heating demand, increasing the ceiling heating share, and reducing simultaneous heating and cooling. Moreover, "SMR $T_{s,16}$" achieves the highest performance in terms of minimising cooling demand, "SMR $T_{o,21-22}$" performs best with respect to ceiling cooling share and "SMR $T_{s,12}$" provides the highest condensation prevention and cooling thermal comfort.

Furthermore, each supply air control parameter exhibits a different degree of influence on the performance indicators:

- Demand H, Ceiling H% and SHC En% are primarily influenced by $T_{s,\max heating}$, while $T_{o,\max heating}$ has only a slight impact on performance indicators. When both parameters increase, energy efficiency and control coordination decrease.
- Demand C, Ceiling C%, Condensation and Discomfort C% are mostly impacted by $T_{s,min\ cooling}$, followed by $T_{o,cooling}$ and lastly by $T_{o,cooling\ slope}$. When these parameters increase, energy efficiency increases whereas condensation prevention and cooling thermal comfort deteriorate.

The main values of each performance indicators are provided in Appendix E and a more detailed analysis is provided in Appendix F.

6.2. Best and suboptimal configurations

6.2.1. Best configuration

According to the global score ranking, and compared with the base configuration score of 0.65, the best winter configuration is "WTR $T_{s,16} - T_{o,2}$", with a score of 0.78 (Figure 6.6). The best summer configuration is "SMR $T_{s,13}$" (Figure 6.7) with a score of 0.67:

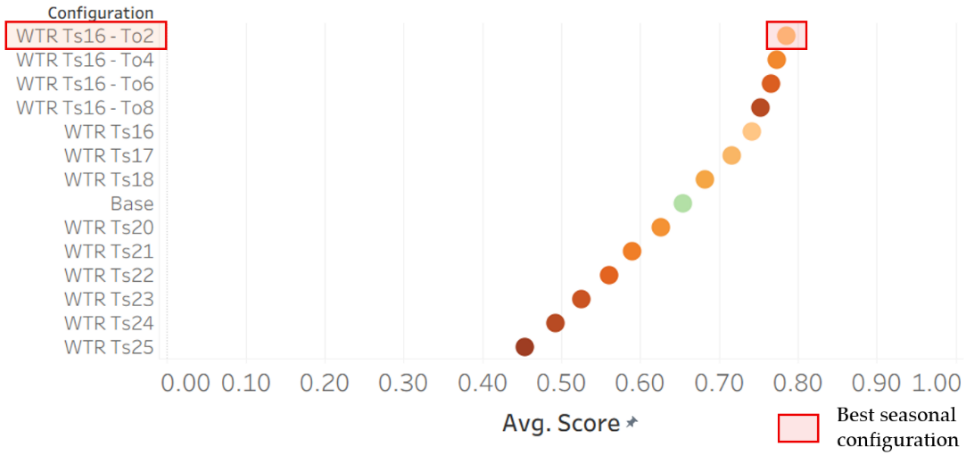

Figure 6.6: Winter configurations ranking based on global performance score

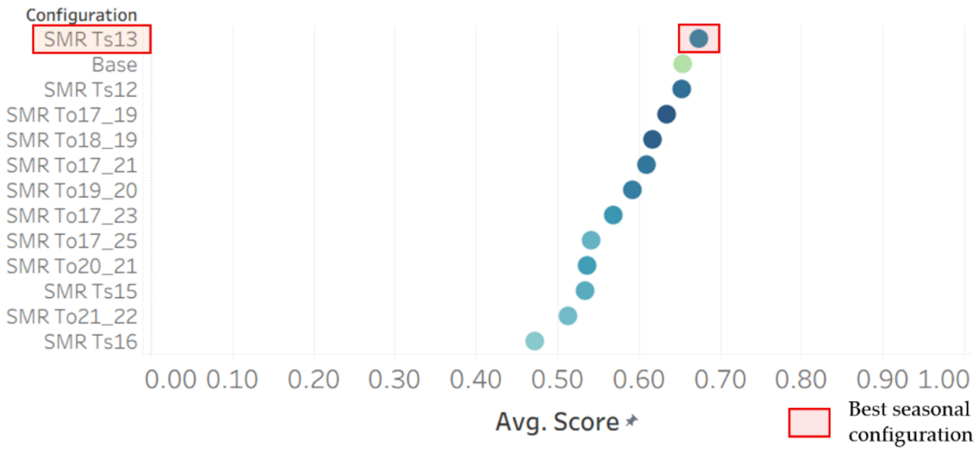

Figure 6.7: Summer configurations ranking based on global performance score

However, based on field experience, supply air temperatures should remain above 14 °C in summer and 18 °C in winter to ensure thermal comfort, unless using high-performance diffusers, as assumed in this study.

Therefore, the optimised annual configuration combines the best winter and summer configurations (Figure 6.8):

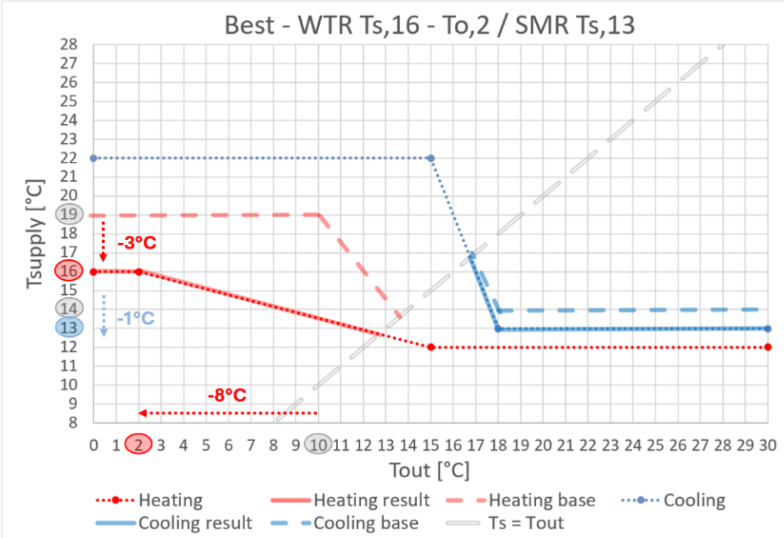

Figure 6.8: Best configuration - Optimised supply air control

6.2.2. Suboptimal configuration

The suboptimal configuration selected for the performance comparison with the best configuration is based on several of the company's existing projects. Comparing the two configurations, the better-performing one features lower heating supply and outdoor threshold temperatures, lower cooling supply and outdoor threshold temperatures, and a narrower cooling slope range (Figure 6.9):

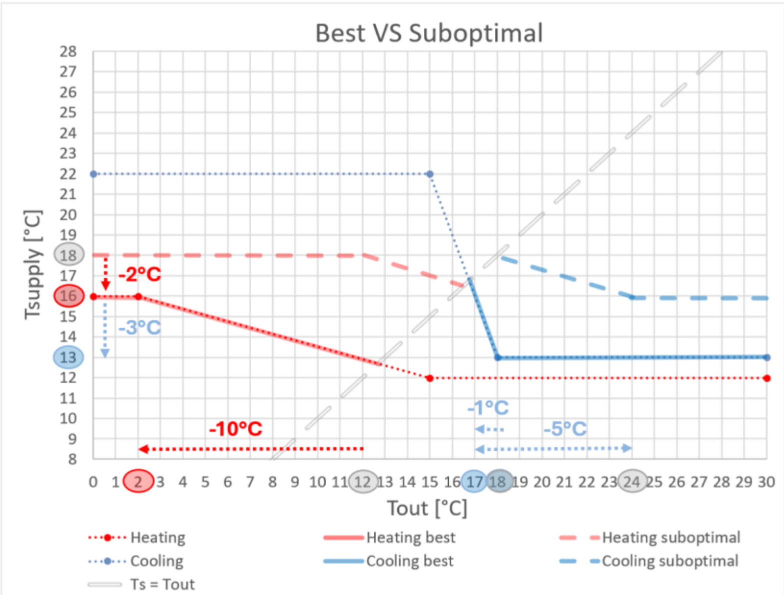

Figure 6.9: Best VS Suboptimal configuration

6.3. Comparison of the best configuration with the suboptimal configuration

Once the optimal (best) yearly configuration is obtained, a detailed comparison with the suboptimal configuration is performed for each performance indicators: total heating and cooling demands in [kWh] and [kWh/m²] with primary energy consumption [kWh], ceiling demands share [%], condensation occurrences [h], wasted energy due to simultaneous heating and cooling [%total demand], and seasonal thermal discomfort [%h] with PPD [%] comfort index. The seasonality and intensity of each indicator are assessed at both floor and zone levels. Regarding the energy efficiency indicators, an additional comparison is conducted between cases with AHU heat recovery enabled and disabled.

6.3.1. Total heating and cooling demands in [kWh] and [kWh/m²] and primary energy consumption [kWh]

6.3.1.1. Total heating and cooling demand in [kWh] and [kWh/m²]

For the suboptimal configuration (Figure 6.10), the heating demand amounts to 37,375 kWh (63% of total) and the cooling demand reaches 21,893 kWh (37% of total), resulting in a total thermal demand of 59,268 kWh or 98.84 kWh/m².

For the best configuration (Figure 6.10), the heating demand amounts to 36,481 kWh (60% of total) and the cooling demand to 23,954 kWh (40% of total) resulting in a total thermal demand 60,435 kWh or 100.79 kWh/m². Compared with the suboptimal configuration, this represents a 2.4% reduction in heating demand and a 9.4% increase in cooling demand, leading to a slight overall increase of 2.0% in total thermal demand:

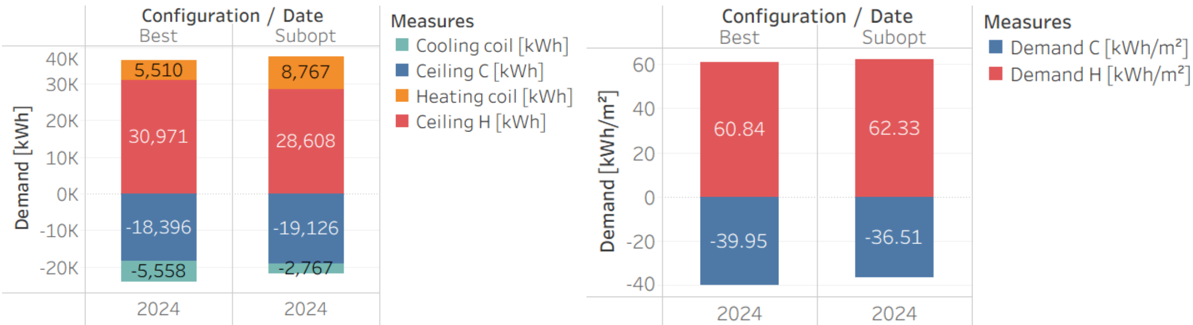

Figure 6.10: Total heating and cooling demand in [kWh] (left) and in [kWh/m²] (right) over a year

Moreover, there is practically no heating in summer months of June to August but some cooling—mainly provided by the ceiling—remains present throughout winter and mid-season months (around 400-500 kWh from November to March, and 1,000-1,300 kWh in April and October), explaining the simultaneous heating and cooling detailed in Subsection 6.3.4 (Figure 6.11).

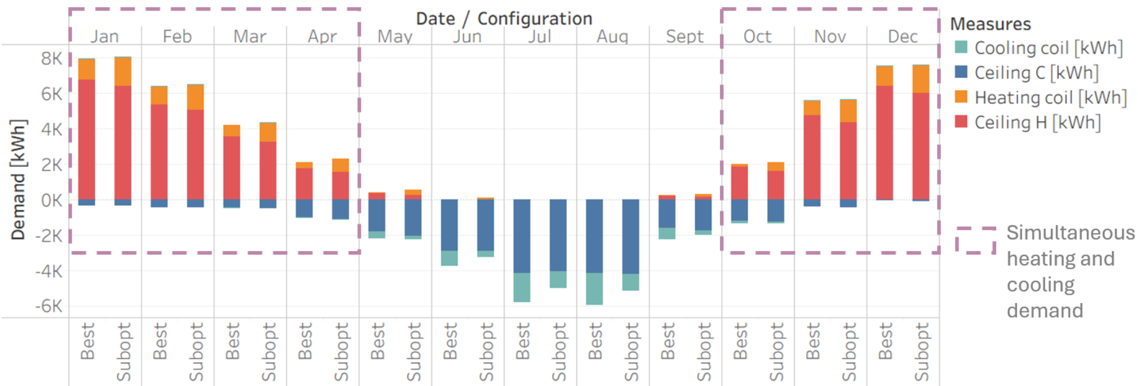

Figure 6.11: Total heating and cooling demand in [kWh] per month

Considering zones individually (Figure 6.12), south-oriented Zone9 requires significantly more cooling than Zone7 which has the same area but is oriented north due to higher solar gains:

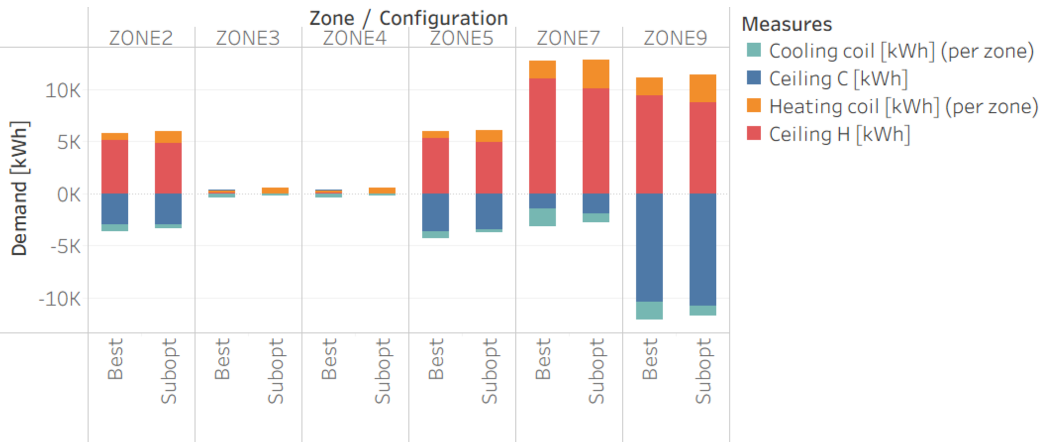

Figure 6.12: Total heating and cooling demand in [kWh] per zone

When AHU heat recovery (HR) is enabled, following the settings detailed in Appendix D, the recovery wheel takes priority for thermally conditioning the supply air, with the coils engaged only when necessary.

With heat recovery (Figure 6.13), heating coil demand is nearly suppressed and total heating demand amounts to 28,618 kWh (57% of total) for the suboptimal configuration and 30,966 kWh (56% of total) for the best, hence a reduction in heating demand of 23.4% and 15.1% respectively compared with the case without heat recovery. Total cooling demand amounts to 21,824 kWh (43% of total) for the suboptimal configuration and 23,887 kWh (44% of total) for the best, hence a reduction of 0.3% for both configurations. This results in a total demand of 84.13 kWh/m² for the suboptimal and 91.48 kWh/m² for the best, hence a reduction of 14.9% and 9.2% respectively compared with the no heat recovery scenario.

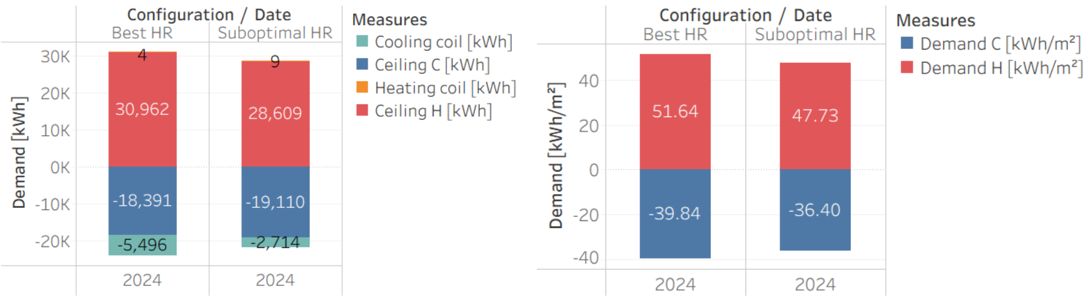

Figure 6.13: Total heating and cooling demand with AHU heat recovery in [kWh] (left) and in [kWh/m²] (right) over a year

The reduction in demand is greater for the suboptimal configuration, as its heating coil share—which is higher than that of the best configuration prior to heat recovery activation (Figure 6.10)—is entirely replaced by the recovery wheel. Compared with the suboptimal configuration, the best configuration exhibits a higher energy demand by 8.7%, primarily due to the ceiling heating demand, which is not offset by the recovery wheel.

6.3.1.2. Primary energy consumption in [kWh]

The primary energy demand associated with electricity use (heating coil, AHU supply and extract fans, cooling coil and ceiling pumps, AHU controllers) and with district heating and cooling (cooling coil and ceiling water loops) is assessed, along with the breakdown by component (Figure 6.14). The hydronic and air distribution network losses are neglected in this analysis.

The annual electricity consumption of AHU controllers is estimated at 525.6 kWh,e as follows:

$$Q_{controller} = N_{controller} \cdot q_{controller} \cdot \Delta t \text{ [kWh]}$$

With:

- $N_{controller} = 12$, since each controller supervises an area of 50 m², and the whole office floor represents 600 m² of conditioned area;
- $q_{controller} = 5\ W$, the electrical power of a controller [36]
- $\Delta t = 8760$ h, the operating number of hours in a year.

In France, the primary energy factor for electricity is $f_{PE,electricity} = 1.9$ and for district energy is $f_{PE,district} = 1$ [37]. Hence, the primary energy consumption is calculated as:

$$Q_{PE,en} = \sum_{c} Q_{en,c} \cdot f_{PE,en} = Q_{PE,e} \cdot f_{PE,electricity} + Q_{PE,th} \cdot f_{PE,district}\ [kWh]$$

With:

- $Q_{en,c}\ [kWh]$ the electricity or thermal energy consumption of the system component "c";
- $f_{PE,en}$ the primary energy factor of electricity or district energy;

- $Q_{PE,e}$ [kWh,e] the electricity primary energy;
- $Q_{PE,th}$ [kWh,th] the district heating and cooling primary energy.

For the suboptimal configuration (Figure 6.14), the primary energy consumption amounts to 74,816 kWh, while for the best configuration it decreases to 73,058 kWh, corresponding to a moderate reduction of 2.3%. This reduction is primarily driven by a lower heating demand (Figure 6.10), which accounts for a 5.1% reduction in total primary energy (3,826 kWh) relative to the suboptimal configuration (Figure 6.15). This improvement allows to partially offsets the higher cooling demand (Figure 6.10), which contributes to a 2.8% increase in primary energy consumption (2,061 kWh).

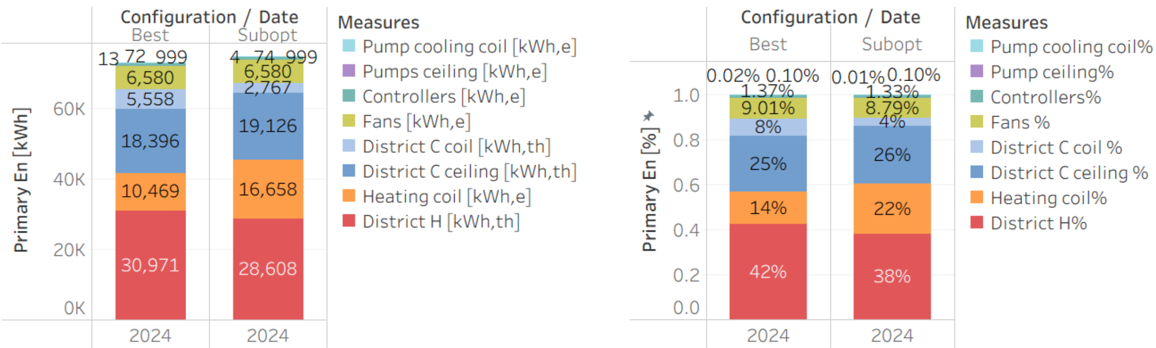

Figure 6.14: Combined AHU and radiant ceiling primary energy consumption in [kWh] (left) and components breakdown [%] (right) over a year

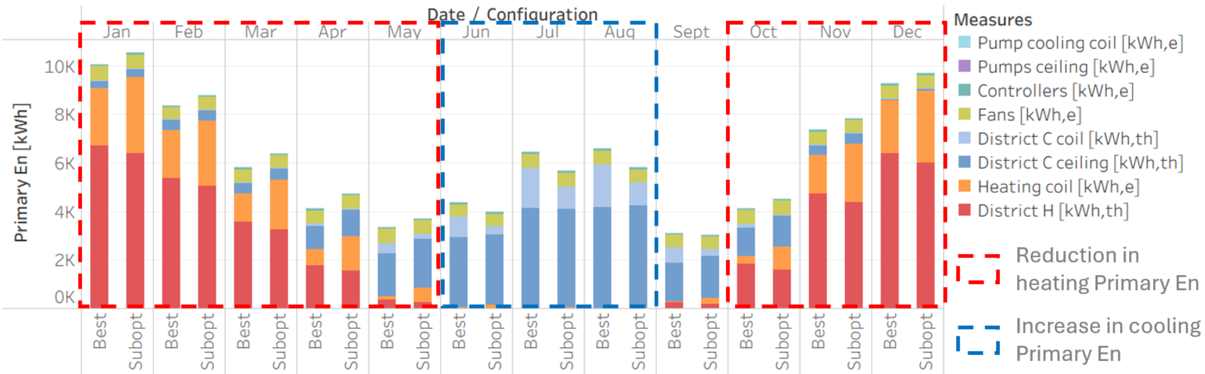

Figure 6.15: Total primary energy consumption in [kWh] per month

Moreover, the lower contribution of the electric heating coil is offset by the use of the hydronic radiant ceiling that consumes less primary energy per unit of thermal energy delivered ($f_{PE,district} < f_{PE,electricity}$). Thereby, for the best configuration, while the ceiling share of heating demand is 5.7 times higher than the heating coil's (Figure 6.17), the associated primary energy share is only 3 times higher (Figure 6.14).

As expected from the heating and cooling demand distribution (Figure 6.10), the components breakdown (Figure 6.14) shows that district heating for the radiant ceiling represents the highest share of primary energy consumption, followed by district cooling for the ceiling and electricity for the heating coil. Furthermore, it should be noted that the reported primary energy for pumps does not accurately represent real-world performance, as DesignBuilder's modelling of pumps electricity consumption is significantly underestimated. When estimating pump electricity consumption based on a consumption of 100 Wh/m^3 of water flow rate, a usual value used by the company’s engineers, the overall system consumes around 1,100 kWh and 1,016 kWh of primary energy for the best and the suboptimal configuration respectively, hence it represents around 1.4% of the total primary energy consumption.

With AHU heat recovery, the primary energy consumption amounts to 58,106 kWh for the suboptimal configuration and to 62,522 kWh for the best, hence a reduction of 22% and 14% respectively compared with the scenario without AHU heat recovery (Figure 6.16):

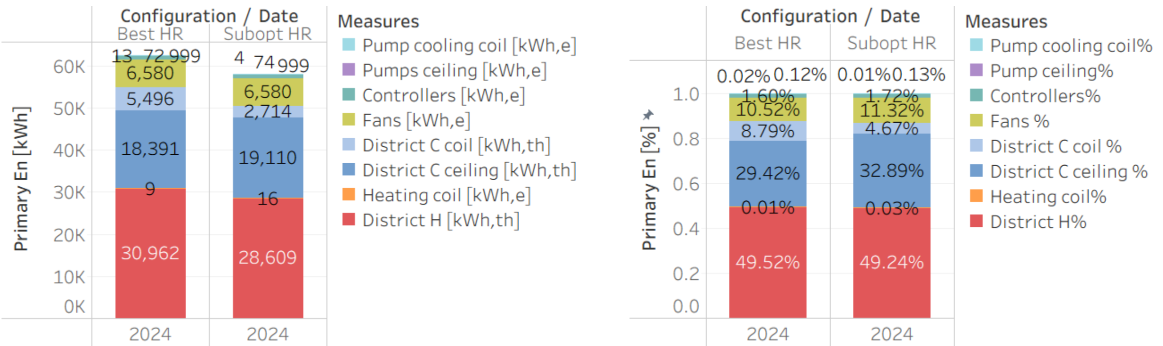

Figure 6.16: Combined AHU and radiant ceiling primary energy consumption with AHU heat recovery in [kWh] (left) and components breakdown [%] (right) over a year

Compared with the suboptimal configuration, the ceiling contribution in heating of the best configuration increases but is not offset by the AHU recovery wheel, leading to an 8.7% rise in total demand (Paragraph 6.3.1.1). However, the primary energy consumption increases only by 7.6% since the radiant ceiling is more energy-efficient than the AHU.

6.3.2. Ceiling heating and cooling demands share [%]

The best configuration (Figure 6.17) shows an increase of 8% in ceiling heating share, owing to lower heating supply and threshold temperatures (Figure 6.9), and a reduction of 10% in ceiling cooling share, owing to lower cooling supply and threshold temperatures. Compared with the suboptimal configuration, this results in an increase of 1.4% in the ceiling share of total demand:

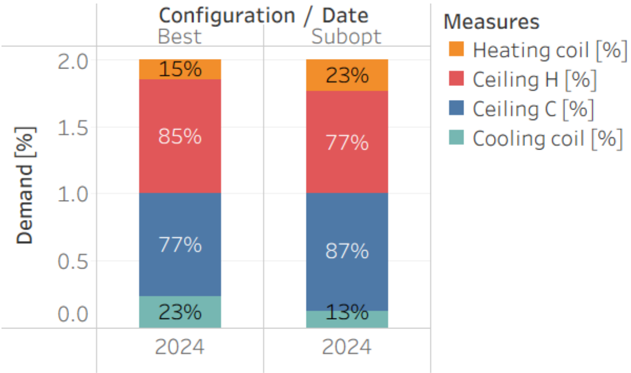

Figure 6.17: Ceiling heating and cooling demand share in [%] between ceiling and AHU

Considering zones individually (Figure 6.18), in Zone2, Zone5 and Zone9, the majority of thermal conditioning is provided by the ceiling. Ceiling heating contribution is higher in the best configuration since AHU supply temperature is lower, whereas it is lower in cooling since supply air temperature is lower. Therefore, for the best configuration, meeting rooms benefit—albeit to a negligible extent—from radiant ceiling heating. Furthermore, the ceiling's contribution to thermal demand varies across zones even under the same control configuration. In north-facing Zone7, the ceiling's contribution to cooling is significantly lower than other zones, as cooling demand is reduced and the supply air handles most of the sensible cooling load.

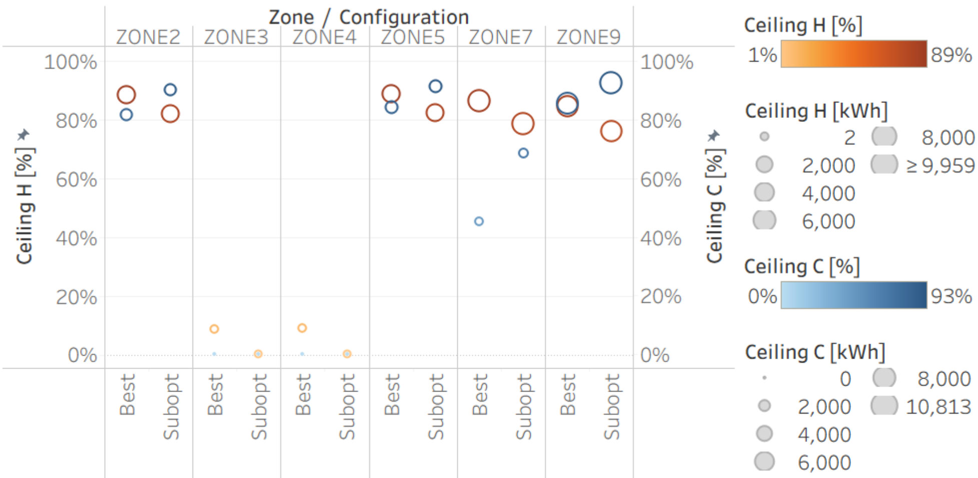

Figure 6.18: Ceiling demand share in [%] per zone

When AHU heat recovery is enabled, as expected from the energy demand analysis in Subsection 6.3.1, the radiant ceiling covers all of the heating demand and the supply air is almost exclusively heated by the recovery wheel (Figure 6.19):

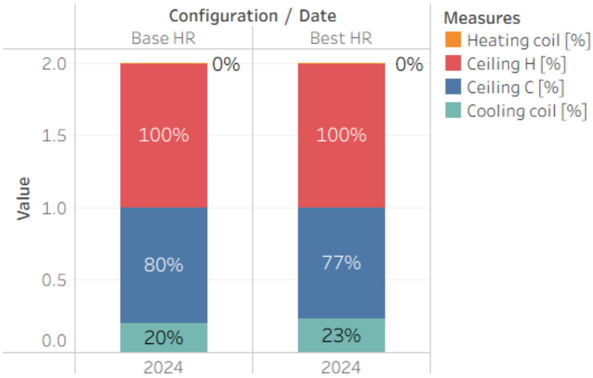

Figure 6.19: Ceiling heating and cooling demand share with AHU heat recovery in [%] between ceiling and AHU

6.3.3. Condensation occurrences [h]

For the suboptimal configuration, condensation hours amount to 177.5 h considering all zones concurrently, while for the best configuration, the number drops to 3.5 h, hence a reduction of 98% (Figure 6.20):

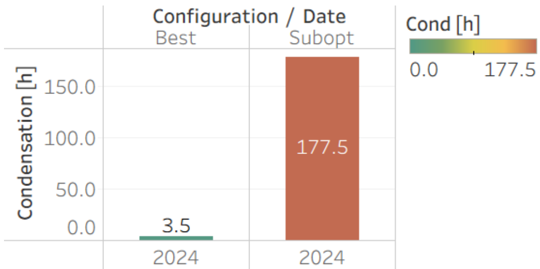

Figure 6.20: Condensation occurrences in [h] for all zones concurrently per year

This improvement is achieved through a colder and more dehumidified supply air: the cooling minimum supply temperature is lower by 3 °C, the outdoor temperature threshold for cooling is lower by 1 °C and the outdoor temperature range of the cooling slope is between T_{out} = 17-18 °C instead of T_{out} = 18-24 °C, therefore cooling at minimum temperature starts from T_{out} = 18 °C instead of T_{out} = 24 °C (Figure 6.9).

For the suboptimal configuration, condensation occurs mostly in September (10.5 h), between 4PM and 5PM (Figure 6.21). For the best configuration, it occurs equally in June, July and September (1-1.5 h), without any specific peak hours.

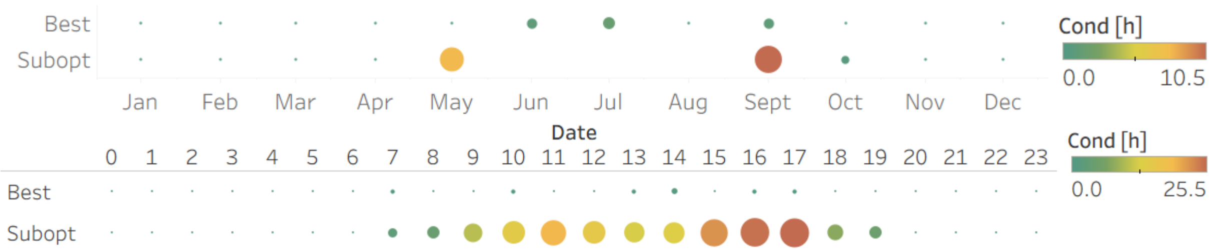

Figure 6.21: Condensation occurrences in [h] for all zones concurrently per month (above) and for each hour of the day over a year (below)

Moreover, in a single day (Figure 6.22), the most frequent scenario corresponds to 30 min/day (possibly even less since simulations run at a time step of 30 min), for 8 days for the suboptimal and only 3 days for the best, hence a reduction of 63% in frequency. The maximum condensation intensity is 1 h/day for the best, while for the suboptimal it is 12 h/day (all zones considered, on 3rd of July), hence a reduction of 92% in intensity.

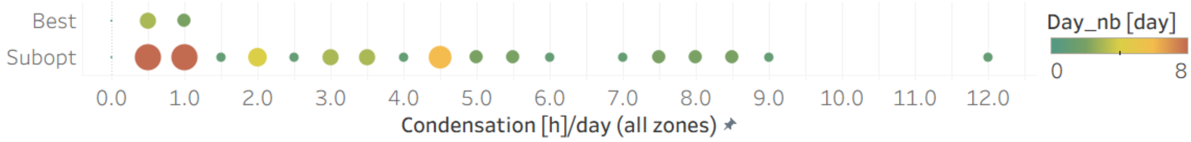

Figure 6.22: Condensation occurrences in [h/day] for all zones concurrently and the corresponding number of days

Considering zones individually (Figure 6.23), for the suboptimal configuration, condensation seems to occur mostly in the offices and particularly in Zone5, which is west-oriented, for 89.5 h. For the best configuration, condensation occurs exclusively in the offices, with a maximum duration of only 1 h, hence a reduction of 99%.

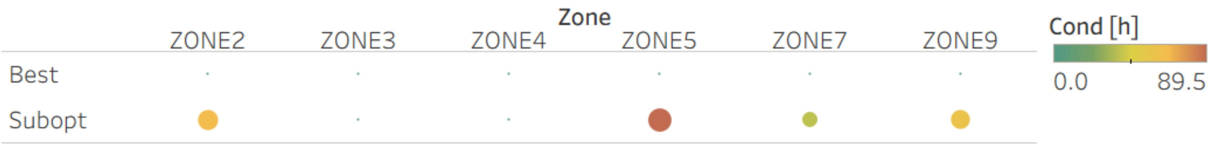

Figure 6.23: Condensation occurrences in [h] per zone

6.3.4. Wasted energy due to simultaneous heating and cooling between the AHU and the ceiling [%total demand]

For the suboptimal configuration (Figure 6.24), simultaneous heating and cooling wasted energy represents 1.25% of the total demand (738.5 kWh), while for the best configuration, it drops to 0.55% (330 kWh), representing a reduction of 56%:

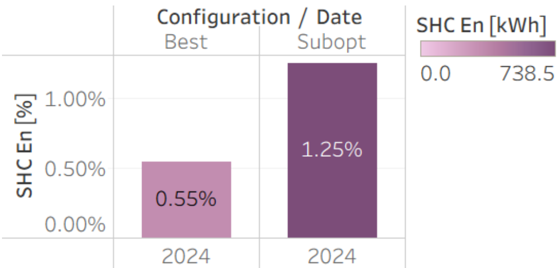

Figure 6.24: Simultaneous heating and cooling wasted energy in [%total demand] aver a year

Simultaneous heating and cooling occurs mainly during winter and mid-season months (Figure 6.11, Figure 6.25), when the AHU is overheating and the ceiling compensates with cooling (Appendix G), which occurs less for the best configuration since the heating maximum supply air temperature is lower by 3 °C. It also happens mostly between 11AM and 3PM for both configurations (Figure 6.26), when solar heat gains are the highest:

Figure 6.25: Simultaneous heating and cooling wasted energy in [%monthly demand]

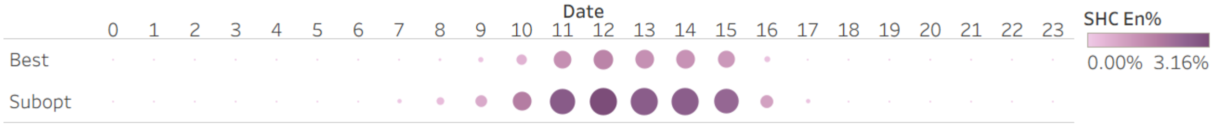

Figure 6.26: Simultaneous heating and cooling wasted energy in [%hourly demand] per hour of the day over a year

Considering zones individually (Figure 6.27), the phenomenon occurs primarily in Zone9, south-oriented, for both configurations:

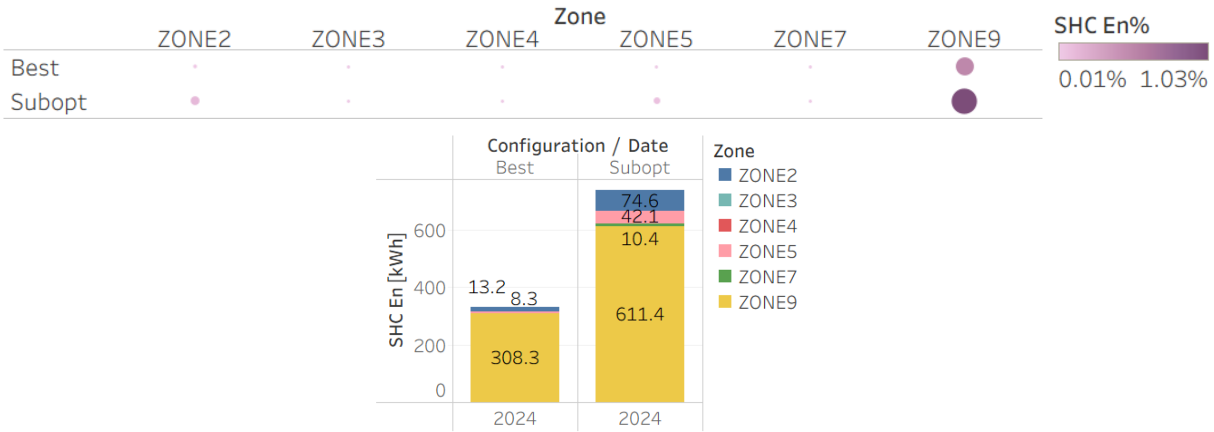

Figure 6.27: Simultaneous heating and cooling wasted energy in [%total demand] per zone with the corresponding amount in [kWh]

This effect is probably due to solar heat gains, particularly high in the south-oriented zone around midday as mentioned previously (Figure 6.26), while the outdoor air temperature is rather low. As a result, the AHU is providing heating while the ceiling is cooling. A possible solution would be to define a specific supply air control for the south-oriented zone.

With AHU heat recovery, wasted energy almost disappears, since it is mostly due to AHU overheating caused by heating coil operation (Figure 6.28):

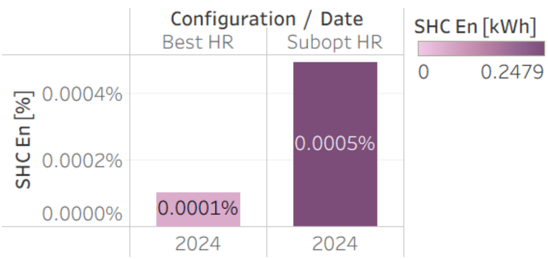

Figure 6.28: Simultaneous heating and cooling wasted energy with AHU heat recovery in [%total demand] over a year

6.3.5. Thermal discomfort in heating and cooling [%h] and PPD [%] index

For the suboptimal configuration (Figure 6.29), there is no heating thermal discomfort but cooling discomfort represents 25% of the season (376 h) for all zones considered simultaneously. For the best configuration, a negligible amount of heating discomfort of 30 min occurs, while cooling discomfort decreases to 16% (237 h) owing to lower cooling supply air temperatures, hence a relative reduction of 37% compared to the suboptimal configuration.

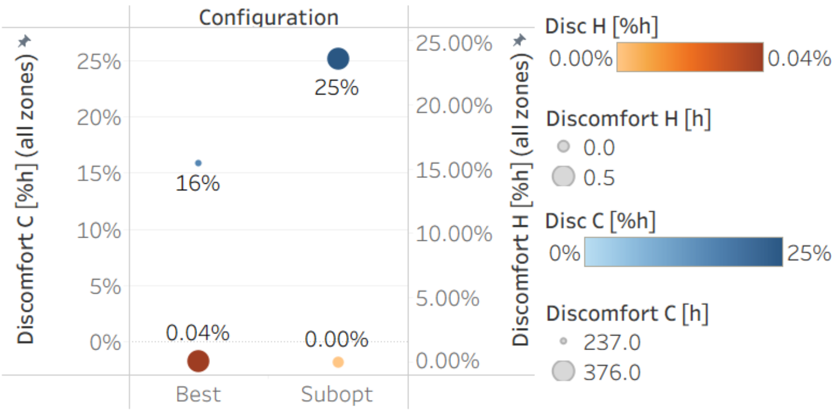

Figure 6.29: Heating and cooling discomfort in [%h] over the corresponding season with the corresponding number of hours [h]

Heating discomfort occurs in December at 8AM (Figure 6.30) for 30 min (Figure 6.31), while cooling discomfort occurs primarily in August between 3PM and 5PM, for 122 h (8% of monthly occupied hours) for the suboptimal configuration and 77.5 h (5% of monthly occupied hours) for the best, hence a reduction of 36% during the warmest month, when all zones are considered simultaneously.

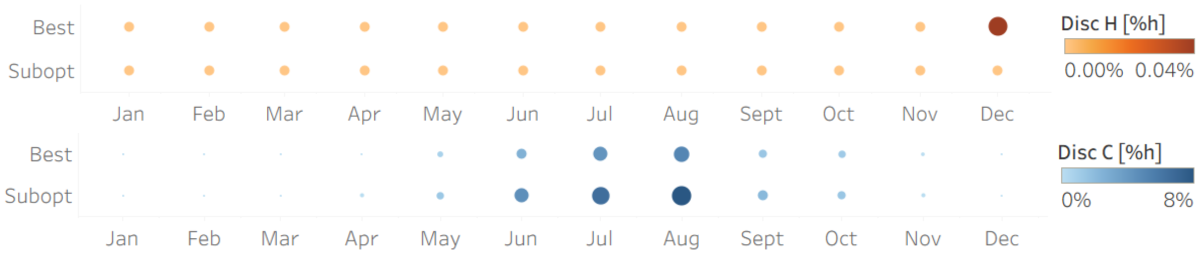

Figure 6.30: Heating and cooling discomfort in [h] per month with the associated [%h] over the season

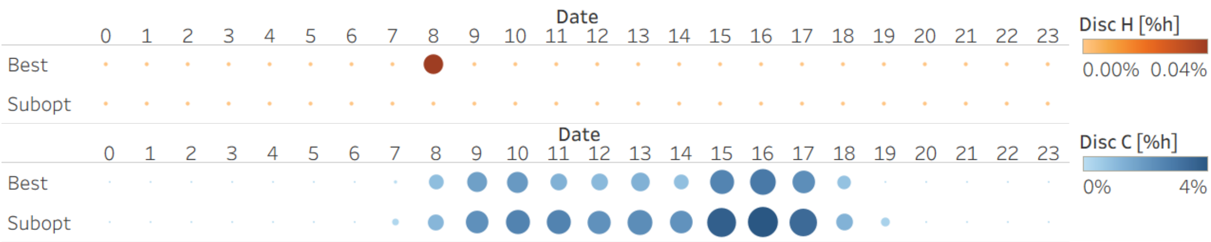

Figure 6.31: Heating and cooling discomfort in [h] for each hour of the day with the associated [%h] over the season

Moreover, in a single day (Figure 6.32), the most critical scenario of cooling discomfort is 12 h/day (for 1 day) for the suboptimal, and 9.5 h/day (for 2 days) for the best configuration, hence a reduction of 21% in daily intensity.

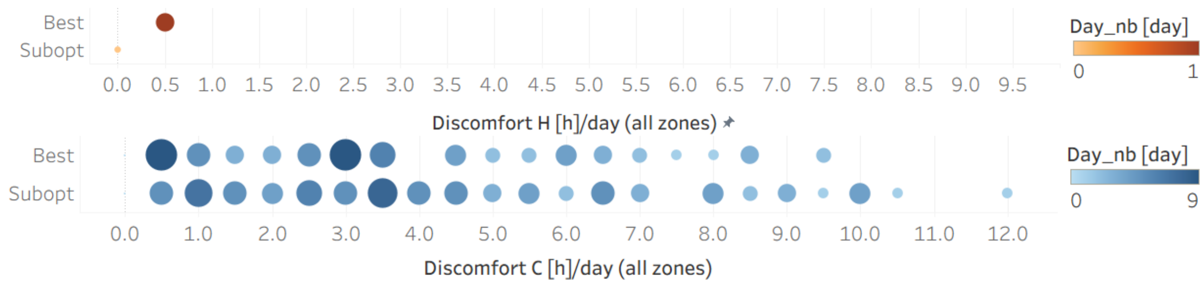

Figure 6.32: Heating and cooling discomfort in [h]/day with the corresponding number of days

Considering zones individually (Figure 6.33), heating discomfort occurs for the best configuration for 0.04% of the season (30 min) and exclusively in offices (Zone2 and Zone5), which are oriented to the east and west respectively. For cooling discomfort, the most critical zone is Zone5 for 12% of the season for the suboptimal (174.5 h) and for 8% (111 h) for the best, which is still acceptable considering the defined limit (Subsection 5.3.5), hence a reduction of 36%.

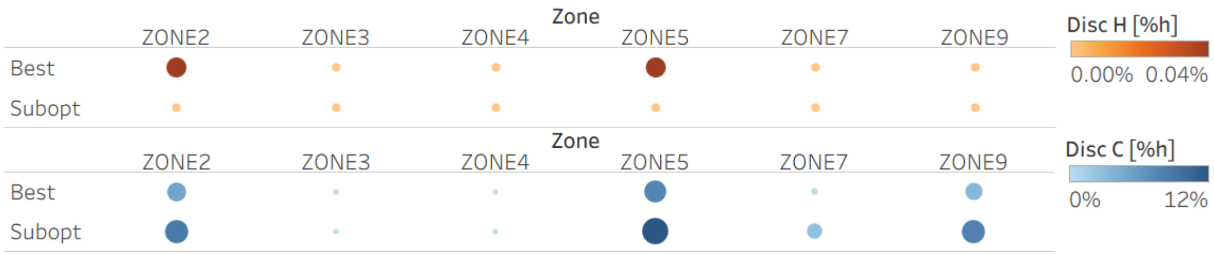

Figure 6.33: Heating and cooling discomfort in [%h] of the season per zone

The PPD cumulative distribution function (Figure 6.34) shows that, for both configurations, the PPD remains below 10%, thereby comfort category II of the ISO standard [35] is achieved for at least 73% of the yearly occupied hours across all zones. Although previous analyses based on air temperature deviation from the contractual setpoints show that the suboptimal configuration yields higher discomfort, the PPD-based assessment reveals the contrary: compared to the best configuration, the cumulative share of hours is higher for any given PPD value, and the maximum PPD in each zone consistently remains below that of the best configuration.

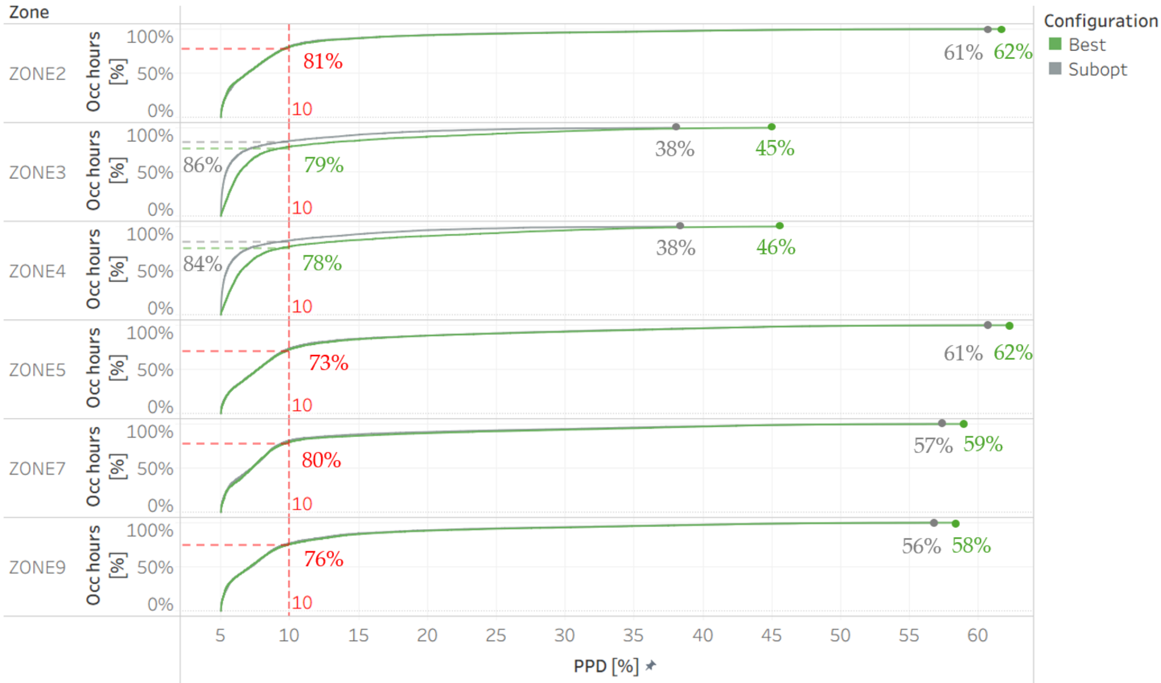

Figure 6.34: Cumulative distribution function of PPD [%] per zone during occupied hours over a year

For the best configuration in Zone5 (Figure 6.34), comfort contractual setpoints are not met for around 4% of yearly occupied hours (when converting both seasonal discomforts to a yearly scale). However, the PPD remains below 10% for 73% of hours, so comfort category II [35] is not met for 28% of the year. This suggests that the PPD-based assessment reflects a higher level of discomfort than the air temperature deviation from contractual setpoints alone. This may be explained by how radiant and convective heat exchanges are interpreted within the PMV/PPD framework. The PMV index accounts for mean air temperature, mean radiant temperature, and air velocity — all parameters directly affected by cooler supply air, which simultaneously reduces the contribution of radiant ceiling cooling and, consequently, lowers radiative heat exchange.

It should be kept in mind that diffusion effects at low supply temperature ($T_{s,\max\, heating}$ = 16 °C in heating and $T_{s,min\ cooling}$ = 13 °C in cooling) are neglected in this study. Consequently, even though high-quality diffusers capable of supplying air at 13 °C are employed, the discomfort assessment may not fully capture the associated thermal conditions.

The main yearly performance indicators when AHU heat recovery is not activated—heating and cooling demands [kWh], ceiling share [%], primary energy consumption [kWh] and components breakdown [%], condensation occurrences [h], simultaneous heating and cooling wasted energy [%total demand], heating and cooling discomfort [%h]—of all winter, summer and yearly configurations are provided in Appendix E.

6.3.6. Discussion

According to the results analysis, each supply air control parameter has a different degree of influence on the performance indicators and requirements:

- Demand H, Ceiling H% and SHC En% are primarily influenced by $T_{s,\max heating}$, while $T_{o,\max heating}$ has only a slight impact on performance indicators. When both parameters increase, energy efficiency and control coordination decrease.
- Demand C, Ceiling C%, Condensation and Discomfort C% are mostly impacted by $T_{s,min\ cooling}$, followed by $T_{o,cooling}$ and lastly by $T_{o,cooling\ slope}$. When these parameters increase, energy efficiency increases while condensation prevention and cooling thermal comfort deteriorate.
- Discomfort H% exhibits negligible variation across the tested configurations, as its occurrences remain marginal throughout the season.

Based on the global performance score, in which condensation carries the highest weight (4/13), followed by simultaneous heating and cooling (2/13), thermal discomfort (1.5/13) and energy demand and ceiling share indicators (1/13), the best-performing seasonal configurations are "WTR $T_{s,16} - T_{o,2}$" for winter and "SMR $T_{s,13}$" for summer. Within the scope of this study, this yields the best-performing yearly configuration as a combination of both, while successful real-world implementation would depend on the use of high-performance diffusers.

Compared with the suboptimal configuration, the best configuration achieves improved overall performance:

1. **Energy efficiency**: A 3 °C reduction in AHU heating maximum supply temperature and a 10 °C decrease in the corresponding outdoor temperature threshold lead to a slight improvement in energy efficiency when AHU heat recovery is not activated. Although the total energy demand slightly increases (+2.0%), the ceiling's share of total demand rises (+1.4%), driven by a significant increase in its contribution to heating (+8%). As a result, primary energy consumption decreases by 2.3%, reflecting the higher energy efficiency of the radiant ceiling relative to the AHU.
2. **Condensation prevention:** With a reduction of 98% in yearly occurrences, this substantial improvement results from a decrease of 3 °C in the cooling minimum supply temperature, of 1 °C in the outdoor temperature threshold, and of 5 °C in the outdoor temperature range of the cooling slope, collectively sufficiently dehumidifying the air to lower the zone dew point.
3. **Control coordination:** Simultaneous heating and cooling, occurring mainly during winter and mid-season months, is also significantly reduced thanks to the lowered heating temperature, leading to a 56% decrease in wasted energy and enhanced control coordination.

4. **Thermal comfort:** The lower cooling minimum supply temperature and outdoor temperature threshold for cooling allow a reduction in cooling discomfort by 37% over the season and by 36% during the warmest month. Despite a negligible amount of heating discomfort (30 min), thermal comfort relative to contractual setpoints is significantly improved.

7 Conclusions and perspectives

This thesis investigates the combined operation of radiant ceiling systems coupled with mechanical ventilation systems as a promising alternative to conventional all-air HVAC systems. The literature review highlights that radiant ceilings can provide substantial benefits in terms of energy efficiency, thermal and acoustic comfort, maintenance reduction, and architectural flexibility. When combined with mechanical ventilation systems, radiant systems can effectively manage sensible loads, while the air system ensures indoor air quality compliance and supports latent load control through dehumidification. However, the combined use of radiant ceilings and ventilation requires careful control coordination, particularly in summer conditions, where condensation risk remains a major limiting factor. Conventional design approaches—such as intensive dehumidification and chilled water modulation—often lead to suboptimal compromises between energy use, comfort, and operational robustness. In the French context, the literature provides limited analysis of dynamic supply air temperature control strategies that adapt to outdoor conditions, identifying a research gap in the optimisation of system control coordination through adaptive control.

To address this gap, a dynamic numerical model of a standard office space in Paris is developed using DesignBuilder. The objective is to identify an optimised supply air control capable of meeting the four key performance requirements: energy efficiency, condensation prevention, control coordination, and thermal comfort. For this purpose, a parametric analysis is conducted by varying five parameters of the supply air temperature control curve, distinguishing winter and summer sides: the heating maximum supply temperature $T_{s,\max heating}$, the outdoor temperature threshold for maximum heating $T_{o,\max heating}$, the outdoor temperature threshold for cooling $T_{o,cooling}$, the outdoor temperature range of the cooling slope $T_{o,cooling\ slope}$ and the cooling minimum supply temperature $T_{s,min\ cooling}$.

System performance is quantified through a set of developed performance indicators: total heating and cooling demands [kWh], radiant ceiling demands share [%], condensation occurrences [h], wasted energy due to simultaneous heating and cooling [%total demand], and seasonal thermal discomfort [%h]. For each of these indicators, a score is computed, either as a relative score compared across configurations or as an absolute threshold-driven score; then each configuration is ranked with a weighted global scoring method prioritising condensation prevention (4/13), followed by control coordination (2/13), thermal comfort (1.5/13) and energy efficiency (1/13). Then, the best-performing seasonal strategies are combined to define the optimised yearly control strategy.

On the one hand, the results show that heating performance indicators—including heating demand, ceiling heating share, and simultaneous heating and cooling—are mostly influenced by the maximum heating supply temperature. While the diffusion phenomenon is neglected, heating discomfort remains negligible across all configurations. Lower heating maximum temperature and outdoor temperature threshold for maximum heating lead to improved energy efficiency and control coordination in winter. On the other hand, cooling performance indicators—including cooling demand, ceiling cooling share, condensation, and cooling discomfort—are mainly governed by the minimum cooling supply temperature. Lower outdoor temperature threshold for cooling, shorter outdoor temperature range of the cooling slope and lower cooling minimum supply temperature lead to decreased energy efficiency in summer, but to enhanced condensation prevention and cooling thermal comfort.

Compared with the suboptimal configuration, the optimised approach features a 2 °C lower heating maximum temperature, a 10 °C lower outdoor temperature threshold for maximum heating, a 3 °C lower cooling minimum supply temperature, a 1 °C lower outdoor temperature threshold for cooling, and a 5 °C smaller outdoor temperature range of the cooling slope. When AHU heat recovery is not activated, the best configuration achieves a modest improvement in energy efficiency. Although the total energy demand slightly increases (+2.0%), the ceiling's share of total demand increases (+1.4%), driven by a significant increase in its contribution to heating (+8%). This leads to a 2.3% decrease in primary energy consumption, reflecting the higher energy efficiency of the radiant ceiling relative to the AHU. Most notably, condensation prevention improves significantly with a 98% reduction in yearly occurrences, and control coordination is enhanced with a 56% decrease in energy wasted through simultaneous heating and cooling. Summer thermal comfort also improves with a 37% reduction in cooling discomfort over the season.

Overall, this work demonstrates that adaptive ventilation supply air control, tuned seasonally and coordinated with radiant ceiling operation, can substantially improve the system performance. These findings support the relevance of dynamic control strategies as a pathway to unlocking the full potential of radiant ceilings in office buildings under the Paris climate and, more broadly, within the HVAC design context.

Several avenues could further strengthen the findings of this thesis and extend the optimisation of radiant ceiling and ventilation system coordination. These include the experimental validation of the numerical model, the development of adaptive ceiling water temperature control based on the zone dew point temperature, and the assessment of the ventilation and pre-ventilation strategies covering airflow rate, duration, and supply air temperature. Further improvements could also be achieved through a refinement of the model with zone-specific internal gain schedules, reflecting realistic variations in occupancy and usage patterns. Collectively, these extensions would enable a broader evaluation of how advanced control strategies and operational parameters affect key system performance requirements.

8 Bibliography and web-links

[1] C. Stetiu, "RadiantCooling in U.S. OfficeBuildings: Towards Eliminating the¨Perception of Climate-Imposed Barriers," Jan. 1998.

[2] S. A. Lloyd, "The ancient Romans had central heating.," https://historyfacts.com/science-industry/fact/the-ancient-romans-had-central-heating/. Accessed: Jan. 22, 2026. [Online]. Available: https://historyfacts.com/science-industry/fact/the-ancient-romans-had-central-heating/

[3] K. N. Rhee and K. W. Kim, "A 50 year review of basic and applied research in radiant heating and cooling systems for the built environment," *Build. Environ.*, vol. 91, pp. 166–190, Sep. 2015, doi: 10.1016/j.buildenv.2015.03.040.

[4] F. Causone and S. P. Corgnati, *Radiant cooling combined with ventilation systems*. Nova Science Publishers, Inc., 2011.

[5] J. Babiak, B. W. Olesen, and D. Petráš, "Low temperature heating and high temperature cooling," 2009.

[6] A. Hesaraki and N. Huda, "A comparative review on the application of radiant low-temperature heating and high-temperature cooling for energy, thermal comfort, indoor air quality, design and control," Feb. 01, 2022, *Elsevier Ltd*. doi: 10.1016/j.seta.2021.101661.

[7] British Standards Institution, *BS EN ISO 7726:2025 Ergonomics of the thermal environment-Instruments for measuring and monitoring physical quantities*. 2025.

[8] British Standards, *BS EN 15251:2007 Indoor environmental input parameters for design and assessment of energy performance of buildings addressing indoor air quality, thermal environment, lighting and acoustics*. European committee for Standardization, 2007.

[9] Plafometal, "Zenith® par PLAFOMETAL : l'alliance parfaite du confort, du design et de la performance Fabrication française," Nov. 2025. [Online]. Available: www.plafometal.fr

[10] Daikin, "Fan Coil Unit Product Catalogue," 2014. Accessed: Jan. 25, 2026. [Online]. Available: https://www.daikin.com.sg/resources/ck/files/catalogue/Chilled%20Water%20Fan%20Coil%20Unit.pdf?

[11] X. Hao, G. Zhang, Y. Chen, S. Zou, and D. J. Moschandreas, "A combined system of chilled ceiling, displacement ventilation and desiccant dehumidification," *Build. Environ.*, vol. 42, no. 9, pp. 3298–3308, Sep. 2007, doi: 10.1016/j.buildenv.2006.08.020.

[12] H. E. Feustel and C. Stetiu, "EPIE&GY Hydronic radiant cooling-preliminary assessment *," 1995.

[13] A. Aryal, P. Chaiwiwatworakul, and S. Chirarattananon, "An experimental study of thermal performance of the radiant ceiling cooling in office building in Thailand," *Energy Build.*, vol. 283, p. 112849, Mar. 2023, doi: 10.1016/j.enbuild.2023.112849.

[14] E. Fabrizio, S. P. Corgnati, F. Causone, and M. Filippi, "Numerical comparison between energy and comfort performances of radiant heating and cooling systems versus air systems," *HVAC and R Research*, vol. 18, no. 4, pp. 692–708, Aug. 2012, doi: 10.1080/10789669.2011.578700.

[15] CBRE, "Bureaux à Paris : un m², combien d'euros ?" Accessed: Jan. 25, 2026. [Online]. Available: https://immobilier.cbre.fr/blog/bureaux/prix-des-loyers-de-bureaux-a-paris-2/

[16] T. H. M. Eltayib, "Design of a radiant panel cooling system for summer air conditionning," Dec. 2008.

[17] J. Miriel, L. Serres, and A. Trombe, "Radiant ceiling panel heating-cooling systems: experimental and simulated study of the performances, thermal comfort and energy consumptions," 2002. [Online]. Available: www.elsevier.com/locate/apthermeng

[18] Y. L. Yin, R. Z. Wang, X. Q. Zhai, and T. F. Ishugah, "Experimental investigation on the heat transfer performance and water condensation phenomenon of radiant cooling panels," *Build. Environ.*, vol. 71, pp. 15–23, Jan. 2014, doi: 10.1016/j.buildenv.2013.09.016.

[19] R. Hu, S. Sun, J. Liang, Z. Zhou, and Y. Yin, "A Review of Studies on Heat Transfer in Buildings with Radiant Cooling Systems," Aug. 01, 2023, *Multidisciplinary Digital Publishing Institute (MDPI)*. doi: 10.3390/buildings13081994.

[20] F. Causone, S. P. Corgnati, M. Filippi, and B. W. Olesen, "Experimental evaluation of heat transfer coefficients between radiant ceiling and room," *Energy Build.*, vol. 41, no. 6, pp. 622–628, Jun. 2009, doi: 10.1016/j.enbuild.2009.01.004.

[21] A. Novoselac and J. Srebric, "A critical review on the performance and design of combined cooled ceiling and displacement ventilation systems."

[22] J. H. Lim, J. H. Jo, Y. Y. Kim, M. S. Yeo, and K. W. Kim, "Application of the control methods for radiant floor cooling system in residential buildings," *Build. Environ.*, vol. 41, no. 1, pp. 60–73, Jan. 2006, doi: 10.1016/j.buildenv.2005.01.019.

[23] CEN (European Committee for Standardization), "EN 16798-1:2019 Energy performance of buildings – Ventilation for buildings – Part 1: Indoor environmental input parameters for design and assessment of energy performance of buildings addressing indoor air quality, thermal environment, lighting and acoustics," 2019.

[24] ASHRAE, "ANSI/ASHRAE Standard 55-1992: Thermal Environmental Conditions for Human Occupancy," *American Society of Heating, Refrigerating and Air-Conditioning Engineers*, 1996.

[25] J. W. Jeong and S. A. Mumma, "Ceiling radiant cooling panel capacity enhanced by mixed convection in mechanically ventilated spaces," *Appl. Therm. Eng.*, vol. 23, no. 18, pp. 2293–2306, Dec. 2003, doi: 10.1016/S1359-4311(03)00211-4.

[26] C. Stetiu, "Energy and peak power savings potential of radiant cooling systems in US commercial buildings," 1999.

[27] A. Zarrella, M. De Carli, and C. Peretti, "Radiant floor cooling coupled with dehumidification systems in residential buildings: A simulation-based analysis," *Energy Convers. Manag.*, vol. 85, pp. 254–263, 2014, doi: 10.1016/j.enconman.2014.05.097.

[28] L. Z. Zhang and J. L. Niu, “Indoor humidity behaviors associated with decoupled cooling in hot and humid climates,” 2003. [Online]. Available: www.elsevier.com/locate/buildenv

[29] G. Ge, F. Xiao, and S. Wang, “Neural network based prediction method for preventing condensation in chilled ceiling systems,” *Energy Build.*, vol. 45, pp. 290–298, Feb. 2012, doi: 10.1016/j.enbuild.2011.11.017.

[30] C. Teodosiu, V. Ilie, and R. Teodosiu, “Numerical Prediction of Thermal Comfort and Condensation Risk in a Ventilated Office, Equipped with a Cooling Ceiling,” in *Energy Procedia*, Elsevier Ltd, 2016, pp. 550–558. doi: 10.1016/j.egypro.2015.12.243.

[31] M. K. Kim and H. Leibundgut, “A case study on feasible performance of a system combining an airbox convector with a radiant panel for tropical climates,” *Build. Environ.*, vol. 82, pp. 687–692, Dec. 2014, doi: 10.1016/j.buildenv.2014.10.012.

[32] K. Helder, M. Hiller, R. Koenigsdorff, M. Bauer, and F. Thumm, “Modeling, simulation and performance analysis of radiant cooling panels operating below the dew point.”

[33] Interpanel, “The world´s coldest ceiling.” Accessed: Feb. 20, 2026. [Online]. Available: https://www.interpanel.com/produkt/innovation/

[34] Sensiron, “Application Note Dew-point Calculation,” 2006. [Online]. Available: www.sensirion.com

[35] British Standards Institution, “BS EN ISO 7730:2025 Ergonomics of the thermal environment — Analytical determination and interpretation of thermal comfort using calculation of the PMV and PPD indices and local thermal comfort criteria,” 2025.

[36] Distech Controls, “Eclypse TM Connected Terminal Unit Controller Overview,” 2025. [Online]. Available: https://builder.distech-controls.com.

[37] Connaissance des Energies, “Qu’est-ce que le coefficient de conversion de l’électricité en énergie primaire ?” Accessed: Feb. 02, 2026. [Online]. Available: https://www.connaissancedesenergies.org/questions-et-reponses-energies/quest-ce-que-le-coefficient-de-conversion-de-lelectricite-en-energie-primaire

Appendix A Radiant ceiling benchmark

Table A.1: Radiant ceiling benchmark

N°	Brand	Model	Technology	Dimensions [mm]	Tube material	Capacity [W/m²] (ΔT [°C]) Activated Surface Ratio (ASR)	Maintenance	Height [mm]	Weight [kg/m]	Advantages
1	**PLAFOMETAL**	Zénith SC 110- SC 140	Simple reversible ceilings, autoportants ou suspended	Width: 300-800 Lenght: 600-2,000	Copper	Heating: 114,9 (15) Cooling: 106,6 (10)	Removable or Sliding	35 - 55 Suspension: 100 - 160	n/a	Thermal comfort (consistent temperature), acoustic comfort (silent), aesthetic appeal (integrated, customisable installations), health and safety comfort (no draughts, low VOC), sustainability (water temperature min/max 14/45°C, renewable energy, 40% lower consumption, 100% recyclable materials), low maintenance, new projects or renovations, diversity of buildings
2	**Zehnder**	Zehnder ZFP	Simple reversible ceilings, suspended	Width: 300 – 1,500 Lenght: 2,000 - 6,000	Galvanised steel	For width 300/1500 Heating: 39 - 61 W/m (15) Cooling: 29 - 129 W/m (8.5) So Heating: 130/26 - 203/41 Cooling: 97/19 - 430/86	Removable	55 Min suspension: 141 - 392	4.4-21kg/m (with water)	Volumes up to 50m high, 60% energy savings (compared to air heater or gas radiant heating), reduced heat loss due to air stratification, corrosion resistant (galvanised), lightweight (suitable for roofs), no convection, simple installation, renewable energy, low operating costs.
3	**Interalu**	Easy KlimaPlus	Simple reversible ceilings	Width: 150 – 250 Lenght: 75 – 250	Steel	Heating: 96 (15) Cooling: 74-78 (10)	Removable	50	n/a	Acoustic and thermal comfort, durable, easy to install, flexible, safe, low cost
4	**Barcol-Air**	CAURUS	Composant Reversible hybrid ceilings			Max 20W/m² stored in thermal mass	Removable	30 - 50 Supension: 80 - 200	n/a	Convection (forced air drawn from the room transfers heat to the concrete above), can be combined with Convector Wings to increase the exchange surface area, Class A acoustic performance (acoustic power Lw < 30dB) for silent air supply without draughts.
5	**Barcol-Air**	AQUILO	Composant Reversible hybrid ceilings			Max 10W/m² (open panel), max 5W/m² (closed panel) stored in thermal mass	Removable	30 - 50 Supension: 150 - 220	n/a	Integrated air supply (highly efficient ventilation), Class A acoustic performance (acoustic power Lw < 25dB) for silent air supply without draughts, increased convection through air flow at the rear of the panel without creating draughts (through perforations), can be combined with Convector Wings to increase the exchange surface area
6	**Barcol-Air**	A11-S (open island system)	Simple or hybrid reversible ceiling	Width: 400 – 1,200 Lenght: 800 - 3,000	Copper	Heating: max 117 (15) Cooling: max 122 (8) with convector wings (max 105W/m² without) At 85% ASR With CAURUS: 125 at 85% ASR With AQUILO: Heating 138, Cooling 122 at 85% ASR	Removable	30 - 50 Min suspension: 80	n/a	High thermal and acoustic performance (class A), activation registers (connection between copper pipes and aluminium heat-conducting rails) laser-welded and then bonded to metal plates using a special adhesive, easy installation, low system weight, Convector Wings + AQUILO or CAURUS convector (no insulation above)
7	**Barcol-Air**	Spectra M-S (open island system)	Simple or hybrid reversible ceiling	Width: 400 – 1,200 Lenght: 600 - 3,000	Copper	Heating: max 102 (15) Cooling: max 91 (8) At 85% ASR With CAURUS: 125 W/m² at 85% ASR With AQUILO: Heating 138, Cooling 122 at 85% ASR	Removable	30 - 40 Min suspension: 80	n/a	High thermal and acoustic performance (class A), magnetic connection between the activation register and the ceiling panel (independent elements, therefore possibility of prefabrication of the two components and use for renovation with subsequent activation of panels), tool-free assembly and disassembly + AQUILO or CAURUS convectors

N°	Brand	Model	Technology	Dimensions [mm]	Tube material	Capacity [W/m²] (ΔT [°C]) Activated Surface Ratio (ASR)	Maintenance	Height [mm]	Weight [kg/m]	Advantages
8	**Barcol-Air**	SPECTRA M-C (closed system)	Simple or hybrid reversibe ceiling	Width: 400 – 1,200 Lenght: 600 - 3,000	Copper	Heating: max 87 (15) Cooling: max 83 (8) At 75% ASR With AQUILO: Heating 114, Cooling 113 at 75% ASR	Removable	30 - 40 Min suspension: 100	n/a	Thermal comfort, good acoustic efficiency (class B), activation system such as SPECTRA M-S, tool-free assembly and disassembly + AQUILO convectors
9	**Barcol-Air**	VARICOOL UNI (closed system)	Simple reversibe ceiling	Width: 180 – 1,000 Lenght: 500 - 1,500	Copper	Heating: max 103 (15) Cooling: max 77 (8) At 65% ASR	Removable	27 Min suspension: 120	n/a	All surfaces can be activated because the activation profiles are directly targeted at the cladding. Plasterboard, expanded glass granule panels and aluminium honeycomb panels can be used, but acoustic performance is lower (class C).
10	**Barcol-Air**	ALBATROS	Simple reversibe ceiling	Width: 290 – 990 Lenght: 600 - 2,500 Tubes spacing: 100	Copper	Heating: max 303 (15) Cooling: max 241 (8)	Removable	150 Min suspension: 220	n/a	High thermal capacity, slotted aluminium fins, acoustic comfort (class A), possibility of achieving high convection cooling performance combined with an air circulation system.
11	**Uponor Corporation**	Uponor Renovis	Simple reversibe ceiling	Width: 625 Lenght: 1200 - 2,000 Tubes spacing: 50	PE-Xa	Heating: max 97 (15) Cooling: max 52 (8)	Removable	15 Min suspension: 50	12.7kg/m² (with water) And 12kg/m² (empty)	Thermal comfort, integrated lighting, durable (minimum heating temperature = 35°C; Trange = 15-50°C), quick installation, suitable for renovation projects
12	**Messana Radiant Cooling**	Ray Magic® Quad Metal	Simple reversibe ceiling	Width: 610 Lenght: 1,830	Copper	Heating: 110 (15) Cooling: 83 (8)	Removable	32	9.16kg/panel (with water) so 8.2kg/m² And 9kg/panel (empty) so 8.1 kg/m²	High heating and cooling performance, high sound absoprtion (when micro-perforated), easy installation, durable and 100% recyclable
13	**SPC**	Thermatile TWELVE	Simple reversibe ceiling	Width: 600 Lenght: 1800 - 3,600	Copper	Heating: max 179 (20)	Removable	Around 25 Min suspension: 75	n/a	Rigid panel with low deflection, lightweight, flexible waterway, customisable finish, easy installation with hanging wire kits
14	**Giacomini**	GK-V Ultra (open island system)	Simple reversibe ceiling	Width: 675 Lenght: 1,350	Copper	Heating: 150 (15) Cooling: 124 (8)	Removable	65 Min suspension: around 195	12.2kg/panel so 13.4kg/m² (empty)	High thermal performance, activation with aluminium diffusers, acoustic insulation, ceiling design enhances convection effect without discomfort, easy to install and desinstall for maintenance (snap-on system)
15	**Hunter Douglas**	PareauLux-30BD aluminium	Simple reversibe ceiling	Width: 600 Lenght: 800 - 6,000	Copper	Heating: 78 (15) Cooling: 123 (8)	Removable	50-100 Min suspension: around 205	n/a	Thermal capacity, acoustic insulation (absorbent panels), integrated lighting and ventilation, low operating costs, durability, activation with aluminium diffusers
16	**Interpanel**	Climatelight	Simple reversible ceiling	Width: 1,064 Lenght: 2,159	/	Heating: 184 (5) Cooling: 200 (4)	Removable	100 Min suspension: 180	12kg/m²	No dew point shutt-off, reduced ceiling coverage, no additional energy for air dehumidification, simple control, high thermal and acoustical performance, lighting integration, easy installation

Appendix B Geometry and envelope

Zone	Type	Conditionned	Net area	Percentage of total net area	Net volume	Interstorey height
-	-	-	[m²]	[%]	[m3]	[m]
Zone 1	Concrete core	No	13	2%	39	2.97
Zone 2	Office	Yes	73	12%	215	
Zone 3	Meeting room	Yes	40	6%	119	
Zone 4	Meeting room	Yes	40	6%	119	
Zone 5	Office	Yes	73	12%	215	
Zone 6	Corridor	No	6	1%	18	
Zone 7	Office	Yes	187	30%	556	
Zone 8	Corridor	No	6	1%	18	
Zone 9	Office	Yes	187	30%	556	
Total	-	-	625	100%	1856	
Total conditionned	-	Yes	600	96%	1780	

Table B.1: Office floor space distribution

Curtain wall - glazing

Zone	Ucw	Uglazing	Uwall	Solar factor	Visible transmittance	Solar protection type	Shading coefficient SC	Shading solar transmittance	WWR	Area of one window (DB average)
-	[W/m²·K]	[W/m²·K]	[W/m².K]	[0-1]	[0-1]	-	[0-1]	[0-1]	[%]	[m²]
Zone 2 & 5	1.57	1.10	2.84	0.30	0.60	textile	0.15	0.13	82%	7.26
Zone 7 & 9										6.83

Curtain wall - opaque wall

Layers	λ	R	U	Density	cp	Thermal mass	Thickness
-	[W/m.K]	[m².K/W]	[W/m².K]	[kg/m3]	[J/(kg.K)]	[kJ/m3.K]	[m]
IN							
Aluminium	230	0.000043	23000	2700	880	2376	0.010
Standard insulation	0.040	1.83	0.548	12	840	10	0.073
Aluminium	230	0.000043	23000	2700	880	2376	0.010
OUT							
Total	0.26	0.35	2.84	-	-	-	0.093

Intermediate slab

Layers	λ	R	U	Density	cp	Thermal mass	Thickness
-	[W/m.K]	[m².K/W]	[W/m².K]	[kg/m3]	[J/(kg.K)]	[kJ/m3.K]	[m]
BOTTOM							
Plaster	0.50	1.00	83	1300	1000	1300	0.006
Glass fibre	0.035	1.00	1.00	25	1000	25	0.035
Air gap (plenum)	-	0.23	-	1.2	1.005	-	0.300
Cast concrete	1.13	0.18	5.65	2000	1000	2000	0.200
Air gap	-	0.22	-	1.2	1.005	-	0.100
Wooden particleboard	0.135	0.30	3.38	800	1300	1040	0.040
TOP							
Total	0.31	2.21	0.45	-	-	-	0.681

Concrete core							
Layers	**λ**	**R**	**U**	**Density**	**cp**	**Thermal mass**	**Thickness**
-	**[W/m.K]**	**[m².K/W]**	**[W/m².K]**	**[kg/m3]**	**[J/kg.K]**	**[kJ/m3.K]**	**[m]**
IN							
Glass fibre	0.035	3.43	0.29	25	1000	25	0.12
Cast concrete	1.13	0.18	5.65	2000	1000	2000	0.20
OUT							
Total	0.52	0.61	1.64	-	-	-	0.32

Internal partitions							
Layers	**λ**	**R**	**U**	**Density**	**cp**	**Thermal mass**	**Thickness**
-	**[W/m.K]**	**[m².K/W]**	**[W/m².K]**	**[kg/m3]**	**[J/kg.K]**	**[kJ/m3.K]**	**[m]**
IN							
Gypsum plasterboard	0.25	0.10	10.00	900	1000	900	0.025
Air gap	-	0.15	-	1.2	1.005	-	0.010
Gypsum plasterboard	0.25	0.10	10.00	900	1000	900	0.025
OUT							
Total	0.10	0.61	1.64	-	-	-	0.060

Internal thermal mass										
Zone	**Type of thermal mass**	**Net zone area**	**%/m² area**	**Equivalent material area**	**Equivalent material**	**Thermal conductivity**	**Density**	**Specific heat**	**Thermal mass**	**Thickness**
-	**-**	**[m²]**	**[%]**	**[m²]**	**-**	**[W/m.K]**	**[kg/m3]**	**[J/kg.K]**	**[kJ/m3.K]**	**[m]**
Zone 2 & 5	Furniture	73	43%	31	Wooden particleboard	0.135	800	1300	1040	0.040
Zone 9 & 7	Furniture	187	43%	81						
Zone 3 & 4	Furniture	40	42%	17						

Thermal bridges		
Zone	**Type**	**Ψ**
-	**-**	**[W/m.K]**
Zone 2 & 5 - 7 & 9	Wall-intermediate slab	0.18
Zone 2 & 5	Lintel above window	0.09
	Sill below window	0.09
	Jamb at window	0.09
Zone 9 & 7	Lintel above window	0.11
	Sill below window	0.11
	Jamb at window	0.11
Zone 2 & 5 - 7 & 9	Wall-wall corner	0.13

Infiltration	
Type	**Infiltration rate**
-	**[m3/h.m²ext]**
Façade	1.2

Table B.2: Envelope and main structure stratigraphy

Appendix C Thermal zone

Table C.1: Internal gains schedule and power density [W/m²]

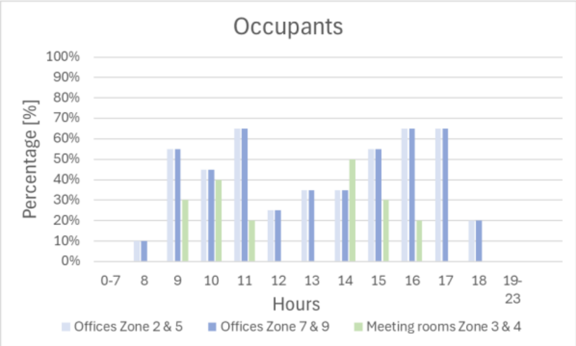

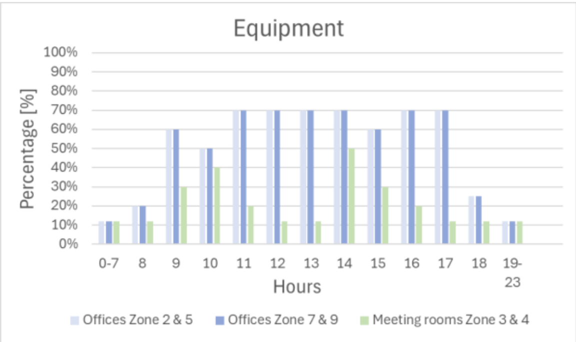

	Offices Zone 2 & 5	Offices Zone 7 & 9	Meeting rooms Zone 3 & 4
Power density [W/m²]	3.90	3.90	3.90
Power max [W]	283	730	156

	ASHRAE value	
	Without metabolic factor	With metabolic factor = 0,93
Sensible [W]	81	75
Latent [W]	59	55
Total [W]	140	130
Latent fraction [-]	42%	42%

	Offices Zone 2 & 5	Offices Zone 7 & 9	Meeting rooms Zone 3 & 4
Density [p/m²]	0.095	0.095	0.50
Occupation rate [m²/p]	10.6	10.6	2.0
Capacity max [p]	6.9	17.7	20

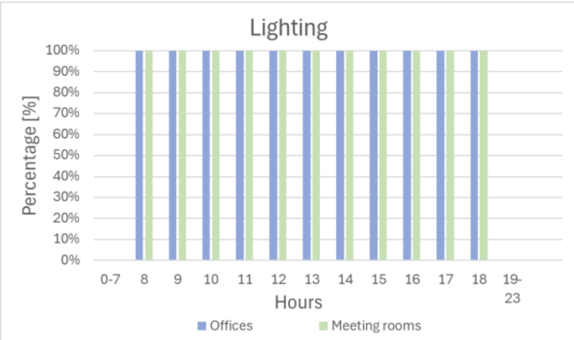

Full power density	Set point	Irradiance limit	Glare limit
[W/m²]	[lux]	[W/m²]	-
4	300	200	19

The occupancy, lighting and equipment schedules and power density are based on existing building assumptions and operational data.

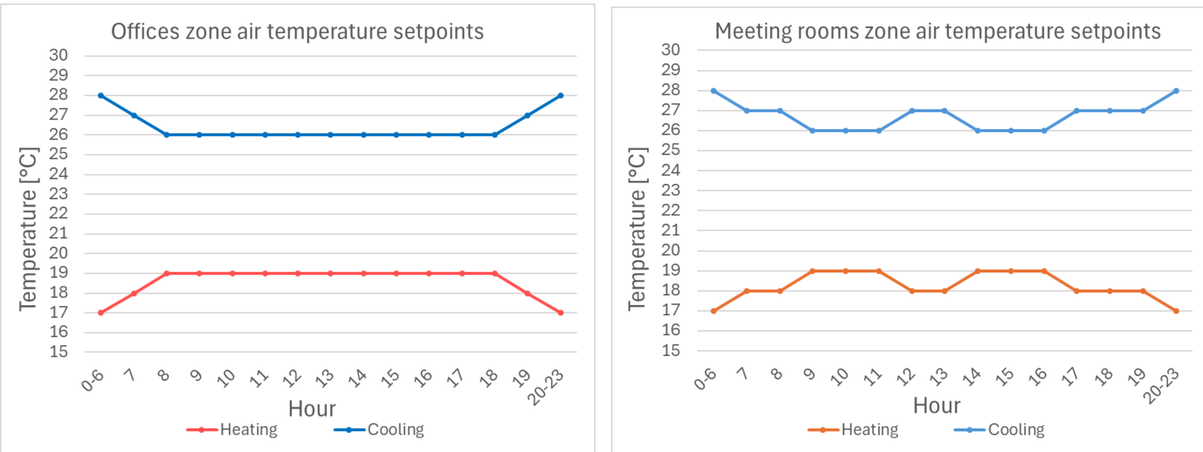

Figure C.1: Zone mean air temperature contractual setpoints

Appendix D HVAC system

Table D.1: HVAC system schedule and settings

Ventilation setpoints

Zone	Supply flow rate	Unit	Control
Offices	25	[m3/h/pers]	
Meeting rooms	30	[m3/h/pers]	
Offices	6.94	L/s/pers	Constant flow for IAQ when occupied (based on max occupation)
	0.66	L/s/m^2	
Offices Zone 2 & 5	0.049	m3/s/zone	
	177	m3/h	
	0.82	ac/h	
Offices Zone 7 & 9	0.13	m3/s/zone	
	454	m3/h	
	0.82	ac/h	
Meeting rooms	8.33	L/s/pers	20% of max for IAQ + proportional to occupation
	4.17	L/s/m^2	
Max flow rate	0.175	m3/s/zone	
	630	m3/h	
	5.30	ac/h	
20% max flow rate	0.035	m3/s/zone	
	0.87	L/s.m^2	

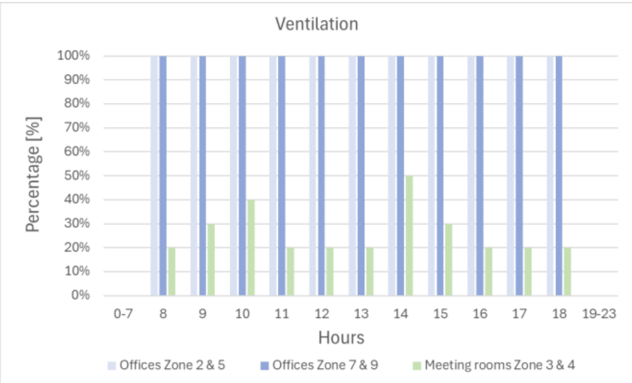

Radiant ceiling

Zone	-	Offices & meeting rooms
Heating capacity	[W/m^2]	58.70
Cooling capacity	[W/m^2]	92.95
Hot water loop temperature	[°C]	35
Chilledwater loop temperature	[°C]	13
Tube diameter	[m]	0.013
Type	-	Variable flow
Throttling range	[°C]	2
Schedule	-	Always ON

AHU

AHU type	-	Dual-flow
Monday to Friday	-	8AM-7PM
Weekends / Public holidays	-	OFF
Heating	-	Electrical heating coil
Cooling	-	Hydronic cooling coil

Heating coil

Type	-	Electric
Nominal capacity	[W]	18,000
Efficiency	-	1

Cooling coil

Type	-	Hydronic
Inlet water temperature	[°C]	6
Design water flow rate	[m3/s]	Autosize
Heat exchanger	-	Cross-flow

Fans

Type	-	Variable volume
Pressure rise	[Pa]	450
Efficiency	-	0.8

AHU heat recovery

Heat exchanger type	-	Rotary
Monday to Friday	-	8AM-7PM
Weekends / Public holidays	-	OFF
Sensible effectiveness at 75% airflow	-	0.8
Sensible effectiveness at 100% airflow	-	0.7
Latent effectiveness (heating only) at 75%	-	0.5
Latent effectiveness (heating only) at 100%	-	0.5

AHU frost control

Type	-	Minimum exhaust temperature
Treshold	[°C]	0

In this work, the ceiling maximum water mass flow rate is set at "Autosize" in DesignBuilder, which allows it to exceed the input thermal capacity and to reach a capacity of 119 W/m^2 in cooling.

The AHU cooling coil chilled water loop and the radiant ceiling hot and chilled water loops are part of the district heating and cooling network. Neither pre-ventilation nor post-ventilation is implemented, and high-performance diffusers are assumed.

Appendix E Performance indicators of all configurations

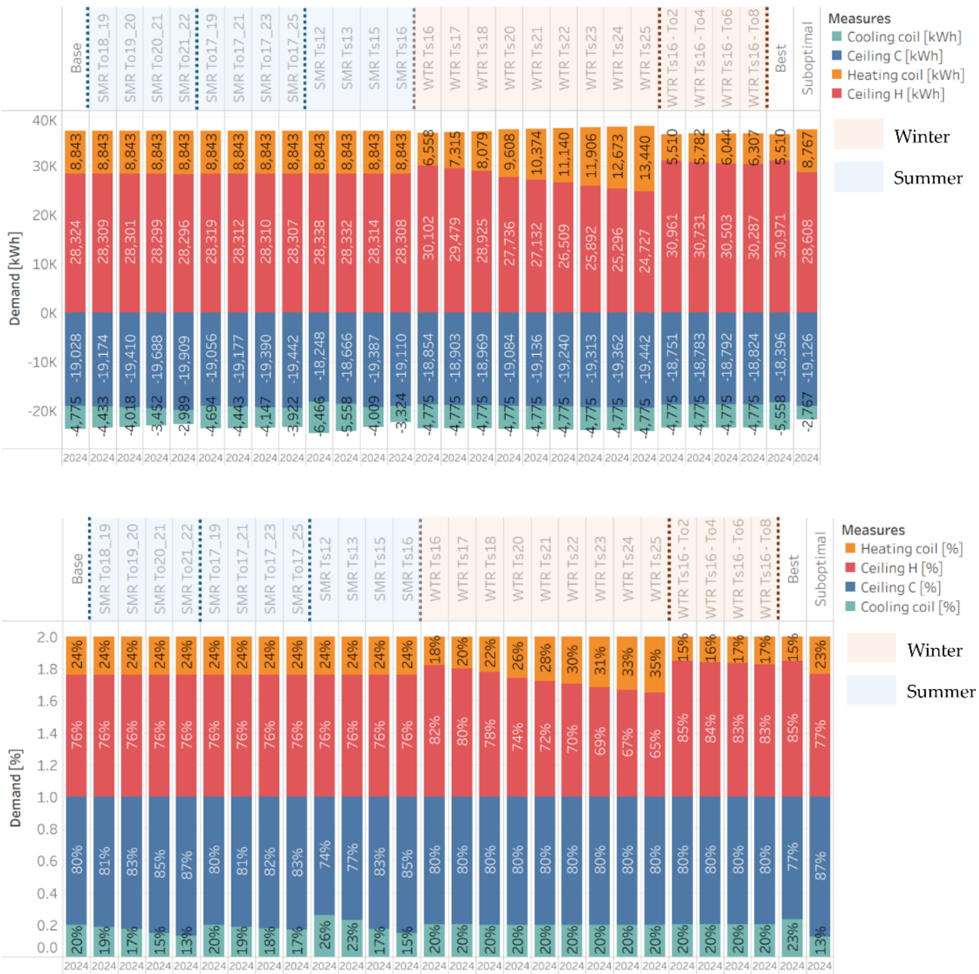

Figure E.1: Heating and cooling demand in [kWh] (top) and distribution between ceiling and AHU [%] (bottom) per year

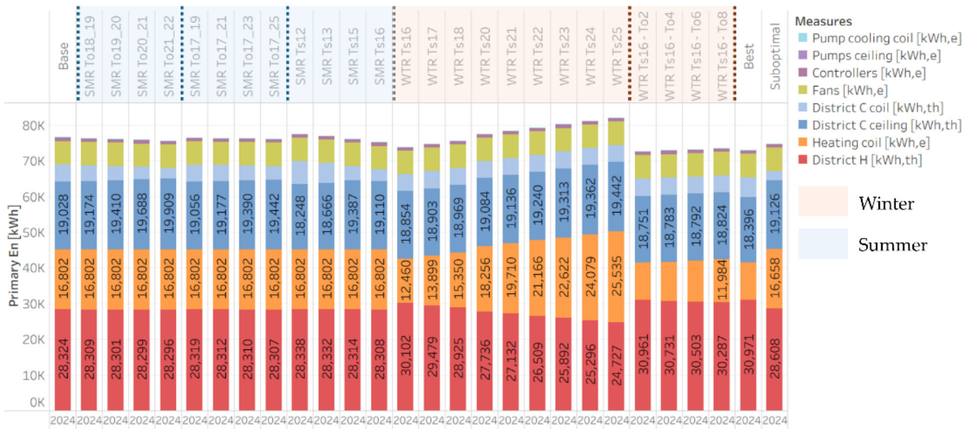

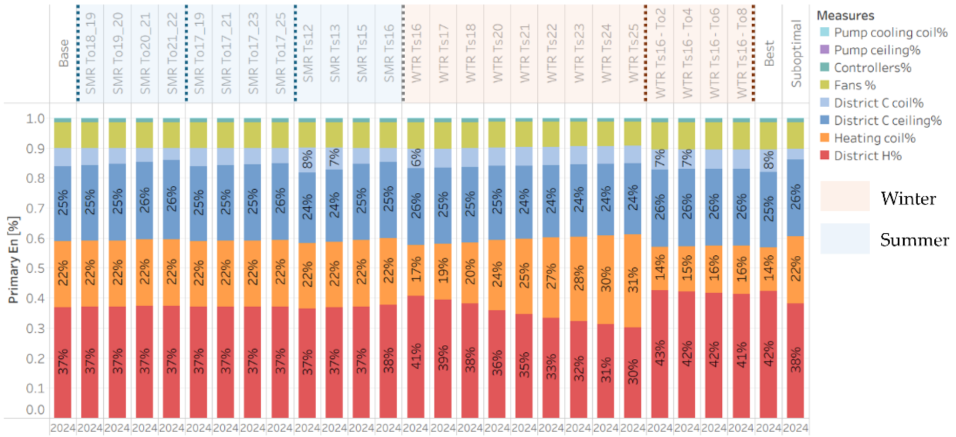

Figure E.2: Combined AHU and radiant ceiling primary energy consumption in [kWh] (top) and components breakdown [%] (bottom) over a year

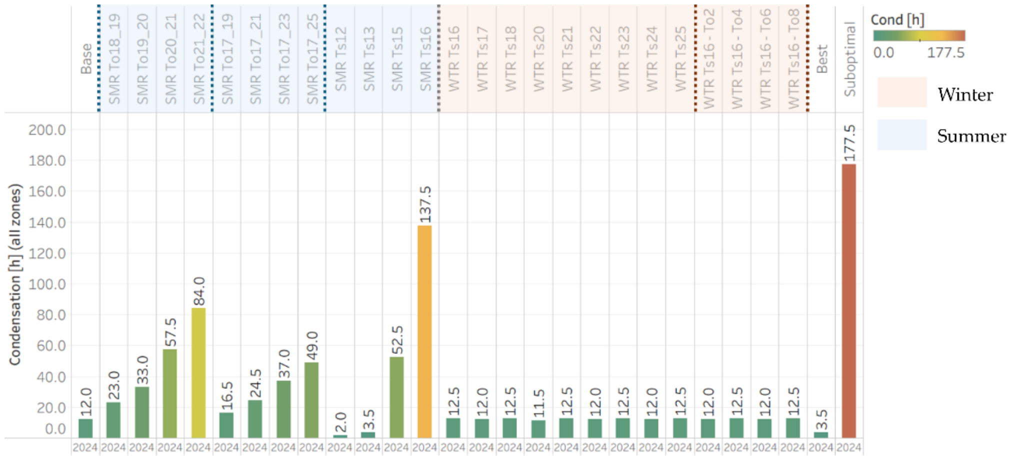

Figure E.3: : Condensation occurrences in [h] for all zones concurrently over a year

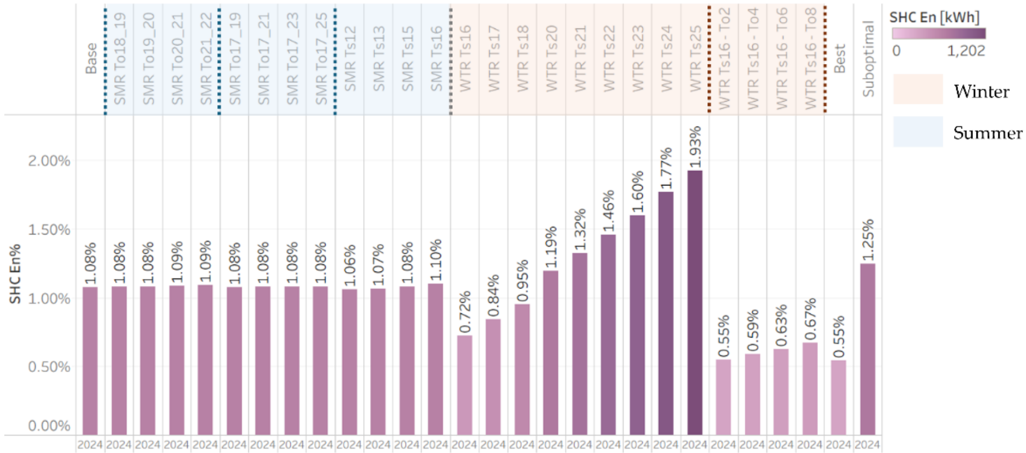

Figure E.4: Simultaneous heating and cooling wasted energy in [%total demand] over a year

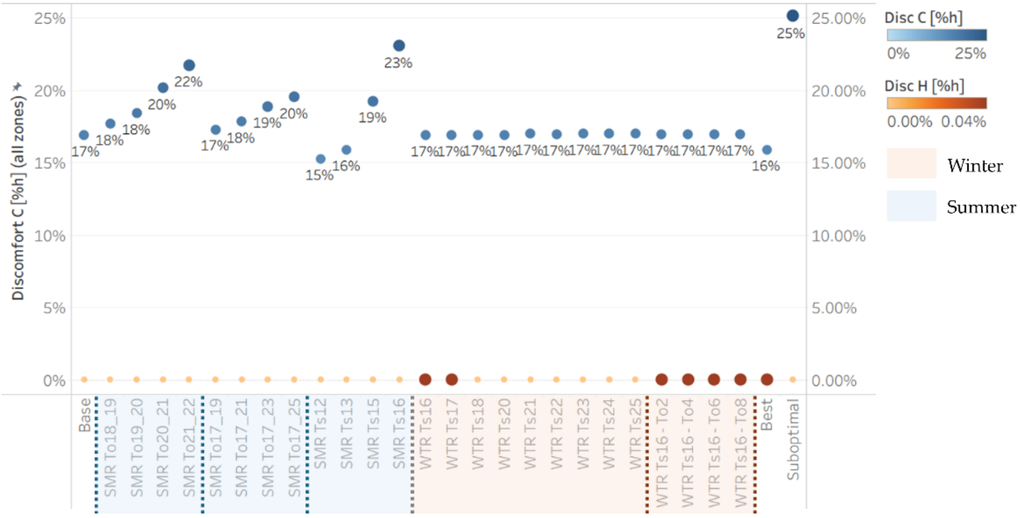

Figure E.5: Heating and cooling discomfort in [%h] over the corresponding season

Appendix F Local study of supply air control impact

Table F.1: Local study of supply air control impact on system performance

		Parameter variation	Indicator	Performance requirement	Score variation	Variation intensity	Comment
To,max heating	WTR Ts16 - To8	2	Avg. Demand H indicator	Energy efficiency	-0.014	/	CeilingH% decreased slightly, since AHU provides more heating
		2	Avg. Demand C indicator	Energy efficiency	-0.007	/	CeilingC% increased slightly probably due to the SHC increase leading to ceilingC demand increase
		2	Avg. Ceiling H% indicator	Energy efficiency	-0.017	/	Total heating demand increased a bit since AHU heats a bit more (heating slope is sharper)
		2	Avg. Ceiling C% indicator	Energy efficiency	0.001	/	Total cooling demand increased a bit and from ceiling probably due to the higher SHC
		2	Avg. Condensation indicator	Condensation prevention	-0.003	/	There is slightly more condensation, also for the oposite To,max heating variation, so this parameter is independant from condensation
		2	Avg. SHC En% indicator	Operation coordination	-0.017	/	Heating starts at a milder Tout, risk of overheating increases, hence more SHC
		2	Avg. Discomfort H% indicator	Thermal comfort	0.000	/	No impact since discomfort is already low
		2	Avg. Discomfort C% indicator	Thermal comfort	0.000	/	No impact since no impact on summer side
		2	Avg. Indicator		**-0.007**	/	**Slightly negative impact on the global score**
	WTR Ts16 - To4	-2	Avg. Demand H indicator	Energy efficiency	0.010	/	Total heating demand decreased a bit since AHU heats a bit more (heating slope is larger)
		-2	Avg. Demand C indicator	Energy efficiency	0.002	/	Total cooling demand decreased a bit, from ceiling probably due to the lower SHC
		-2	Avg. Ceiling H% indicator	Energy efficiency	0.017	/	CeilingH% increased a bit, since AHU provides less heating
		-2	Avg. Ceiling C% indicator	Energy efficiency	0.000	/	No variation since cooling not impacted by winter side
		-2	Avg. Condensation indicator	Condensation prevention	-0.003	/	There is slightly more condensation, also for the oposite To,max heating variation, so this parameter is independant from condensation
		-2	Avg. SHC En% indicator	Operation coordination	0.014	/	Heating starts at a colder Tout, risk of overheating decreases, hence less SHC
		-2	Avg. Discomfort H% indicator	Thermal comfort	0.000	/	No impact since discomfort is already low
		-2	Avg. Discomfort C% indicator	Thermal comfort	0.000	/	No impact since no impact on summer side
		-2	Avg. Indicator		**0.003**	/	**Slightly positive impact on the global score**
Ts,max heating	WTR Ts18	1	Avg. Demand H indicator	Energy efficiency	-0.124	- -	Much higher total heating demand since AHU is heating more
		1	Avg. Demand C indicator	Energy efficiency	-0.029	-	More cooling demand since more SHC
		1	Avg. Ceiling H% indicator	Energy efficiency	-0.097	- -	Much less celingH% since AHU provides more for the heating
		1	Avg. Ceiling C% indicator	Energy efficiency	0.004	/	More ceilingC% since more cooling demand from ceiling, from higher SHC
		1	Avg. Condensation indicator	Condensation prevention	-0.007	/	There is slightly more condensation, also for the oposite Ts,max heating variation, so this parameter is independant from condensation
		1	Avg. SHC En% indicator	Operation coordination	-0.079	- -	Higher supply temperature = more SHC
		1	Avg. Discomfort H% indicator	Thermal comfort	0.000	/	No impact since discomfort is already low
		1	Avg. Discomfort C% indicator	Thermal comfort	-0.003	/	Cooling discomfort increased since AHU is overheating
		1	Avg. Indicator		**-0.034**	-	**Negative impact on the global score**
	WTR Ts16	-1	Avg. Demand H indicator	Energy efficiency	0.079	+ +	Much lower total heating demand since AHU since AHU is heating less
		-1	Avg. Demand C indicator	Energy efficiency	0.022	+	Less cooling demand since less SHC
		-1	Avg. Ceiling H% indicator	Energy efficiency	0.099	+ +	Much more celingH% since AHU provides less for the heating
		-1	Avg. Ceiling C% indicator	Energy efficiency	-0.003	/	Less ceilingC% since less cooling demand, from lower SHC
		-1	Avg. Condensation indicator	Condensation prevention	-0.007	/	There is slightly more condensation, also for the oposite Ts,max heating variation, so this parameter is independant from condensation
		-1	Avg. SHC En% indicator	Operation coordination	0.087	+ +	Lower supply temperature = less SHC
		-1	Avg. Discomfort H% indicator	Thermal comfort	0.000	/	No impact since discomfort is already low
		-1	Avg. Discomfort C% indicator	Thermal comfort	0.000	/	No impact since AHU is not overheating yet
		-1	Avg. Indicator		**0.026**	+	**Positive impact on the global score**

		Parameter variation	Indicator	Performance requirement	Score variation	Variation intensity	Comment
To,cooling	SMR To21_22	1	Avg. Demand H indicator	Energy efficiency	0.001	/	No impact on CeilingH%, since change of cooling side temperature
		1	Avg. Demand C indicator	Energy efficiency	0.106	+ +	CeilingC% increased a lot since AHU starts cooling at higher Tout so contributes less
		1	Avg. Ceiling H% indicator	Energy efficiency	0.000	/	Slightly less heating demand
		1	Avg. Ceiling C% indicator	Energy efficiency	0.142	+ +	Less cooling demand, since AHU deadband is larger
		1	Avg. Condensation indicator	Condensation prevention	-0.137	- -	Much more condensation since supply air is too hot and not dehumidified enough, so condensation fluctuates a lot at least in the range of Tout between 19°C and 21°C
		1	Avg. SHC En% indicator	Operation coordination	-0.003	/	Slightly more SHC
		1	Avg. Discomfort H% indicator	Thermal comfort	0.000	/	No impact on discomfort since heating side unchanged
		1	Avg. Discomfort C% indicator	Thermal comfort	0.000	/	No impact on discomfort
		1	Avg. Indicator		**-0.023**	-	**Negative impact on the global score since condensation has the highest weight**
	SMR To19_20	-1	Avg. Demand H indicator	Energy efficiency	-0.002	/	Slightly more heating demand
		-1	Avg. Demand C indicator	Energy efficiency	-0.126	- -	More cooling demand, since AHU deadband is tighter
		-1	Avg. Ceiling H% indicator	Energy efficiency	0.000	/	No impact on CeilingH%, since change of cooling side temperature
		-1	Avg. Ceiling C% indicator	Energy efficiency	-0.170	- -	CeilingC% decreased a lot since AHU starts cooling at lower Tout so contributes more
		-1	Avg. Condensation indicator	Condensation prevention	0.193	+ +	Much less condensation since supply air is cold and dehumidified enough
		-1	Avg. SHC En% indicator	Operation coordination	0.004	/	Slightly less SHC
		-1	Avg. Discomfort H% indicator	Thermal comfort	0.000	/	No impact on discomfort since heating side unchanged
		-1	Avg. Discomfort C% indicator	Thermal comfort	0.158	+ +	Much lower cooling discomfort since cooling starts at lower Tout
		-1	Avg. Indicator		**0.055**	+ +	**Very positive impact on the global score since condensation has the highest weight**
To,cooling slope	SMR To17_23	2	Avg. Demand H indicator	Energy efficiency	0.001	/	Sligltly less cooling demand, since ceiling since AHU cooling slope is smoother (starts cooling at Tmin, cooling for higher Tout) so contributes less
		2	Avg. Demand C indicator	Energy efficiency	0.018	/	Slightly less heating demand, since less SHC, ceiling needs less to compensate for AHU overcooling
		2	Avg. Ceiling H% indicator	Energy efficiency	0.000	/	No impact on CeilingH%, since change of cooling side temperature
		2	Avg. Ceiling C% indicator	Energy efficiency	0.046	+	CeilingC% increased since AHU cooling slope is smoother (starts cooling at Tmin, cooling for higher Tout) so contributes less
		2	Avg. Condensation indicator	Condensation prevention	-0.063	- -	Much more condensation since supply air is too hot and not dehumidified enough, as seen previously for Tout between 19°C and 21°C, condensation is critical
		2	Avg. SHC En% indicator	Operation coordination	-0.001	/	Slightly more SHC
		2	Avg. Discomfort H% indicator	Thermal comfort	0.000	/	No impact on discomfort since heating side unchanged
		2	Avg. Discomfort C% indicator	Thermal comfort	-0.052	- -	Much more cooling discomfort since AHU starts cooling at higher Tout
		2	Avg. Indicator		**-0.020**	-	**Negative impact on the global score, even more since condensation has the highest weight**
	SMR To17_19	-2	Avg. Demand H indicator	Energy efficiency	-0.002	/	Slightly more heating demand, since less SHC, ceiling needs more to compensate for AHU overcooling
		-2	Avg. Demand C indicator	Energy efficiency	-0.028	-	More cooling demand, Less cooling demand, since ceiling since AHU cooling slope is sharper (starts cooling at Tmin, cooling for lower Tout) so contributes more
		-2	Avg. Ceiling H% indicator	Energy efficiency	0.000	/	No impact on CeilingH%, since change of cooling side temperature
		-2	Avg. Ceiling C% indicator	Energy efficiency	-0.036	-	CeilingC% decreased since AHU starts cooling slope is sharper (starts cooling at Tmin, cooling for lower Tout) so contributes more
		-2	Avg. Condensation indicator	Condensation prevention	0.047	+	Less condensation since supply air is colder and more dehumidified, as seen previously for Tout between 19°C and 21°C, condensation is critical
		-2	Avg. SHC En% indicator	Operation coordination	0.001	/	Slightly less SHC
		-2	Avg. Discomfort H% indicator	Thermal comfort	0.000	/	No impact on discomfort since heating side unchanged
		-2	Avg. Discomfort C% indicator	Thermal comfort	0.028	+	Less cooling discomfort since AHU starts cooling at lower Tout
		-2	Avg. Indicator		**0.013**	/	**Slightly positive impact on the global score since condensation has the highest weight**

Ts,min cooling	SMR Ts15	1	Avg. Demand H indicator	Energy efficiency	0.006	/	A bit less heating demand
		1	Avg. Demand C indicator	Energy efficiency	0.178	+ +	Much less cooling demand, since AHU is not overcooling
		1	Avg. Ceiling H% indicator	Energy efficiency	0.000	/	No impact on CeilingH%, since change of cooling side temperature
		1	Avg. Ceiling C% indicator	Energy efficiency	0.223	+ +	CeilingC% increased a lot since AHU supplies hotter air so contributes less to cooling
		1	Avg. Condensation indicator	Condensation prevention	-0.402	- -	Much more condensation since supply air is too hot and not dehumidified enough
		1	Avg. SHC En% indicator	Operation coordination	-0.006	/	A bit more SHC
		1	Avg. Discomfort H% indicator	Thermal comfort	0.000	/	No impact on heating discomfort
		1	Avg. Discomfort C% indicator	Thermal comfort	-0.238	- -	Much more discomfort hours since the supply air is too hot
		1	Avg. Indicator		**-0.121**	- -	**Very negative impact on the global score, since condensation has the highest weight**
	SMR Ts13	-1	Avg. Demand H indicator	Energy efficiency	-0.004	/	A bit more heating demand
		-1	Avg. Demand C indicator	Energy efficiency	-0.185	- -	Much more cooling demand, since AHU is not overcooling
		-1	Avg. Ceiling H% indicator	Energy efficiency	0.000	/	No impact on CeilingH%, since change of cooling side temperature
		-1	Avg. Ceiling C% indicator	Energy efficiency	-0.220	- -	CeilingC% decreased a lot since AHU supplies colder air so contributes more to cooling
		-1	Avg. Condensation indicator	Condensation prevention	0.125	+ +	Much less condensation since supply air is cold and dehumidified enough
		-1	Avg. SHC En% indicator	Operation coordination	0.005	/	A bit less SHC
		-1	Avg. Discomfort H% indicator	Thermal comfort	0.000	/	No impact on heating discomfort
		-1	Avg. Discomfort C% indicator	Thermal comfort	0.100	+ +	Much less discomfort hours since the supply air is cool enough
		-1	Avg. Indicator		**0.019**	/	**Slightly positive impact on the global score since condensation has the highest weight**

Appendix G Simultaneous heating and cooling details

For each configuration, the indicator "SHC (H or C)" returns 1 if heating rate is higher than cooling rate, and 2 otherwise, allowing to determine if the effect is overheating or overcooling. A second indicator, "SHC (ceiling or AHU)", returns 1 if ceiling rate is higher than the AHU rate (Figure G.1), and 2 otherwise (Figure G.2).

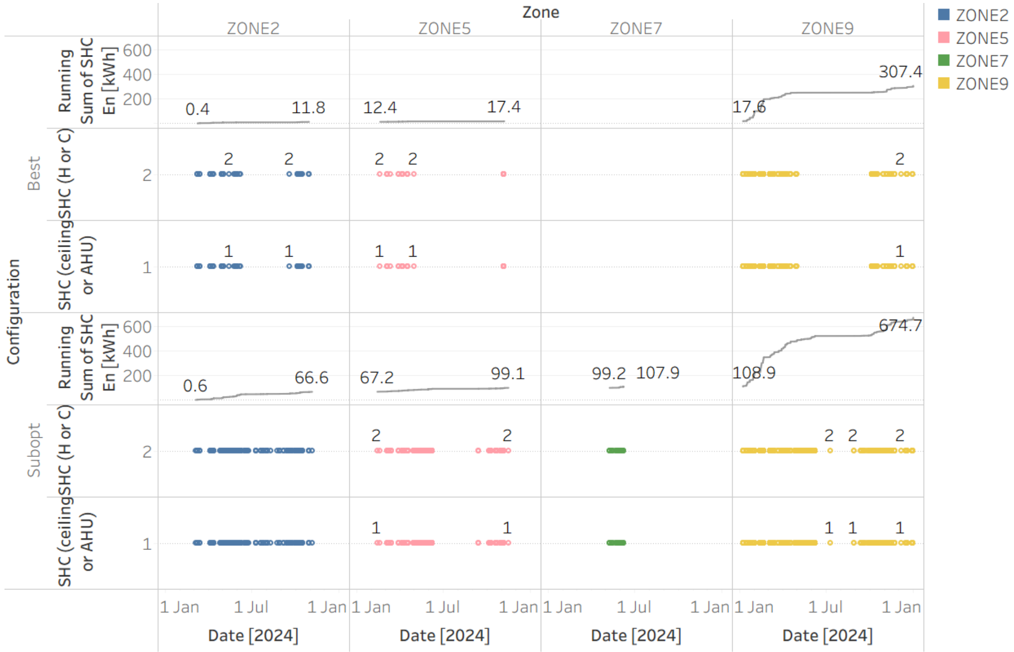

Figure G.1: Simultaneous heating and cooling detail—Ceiling overcooling

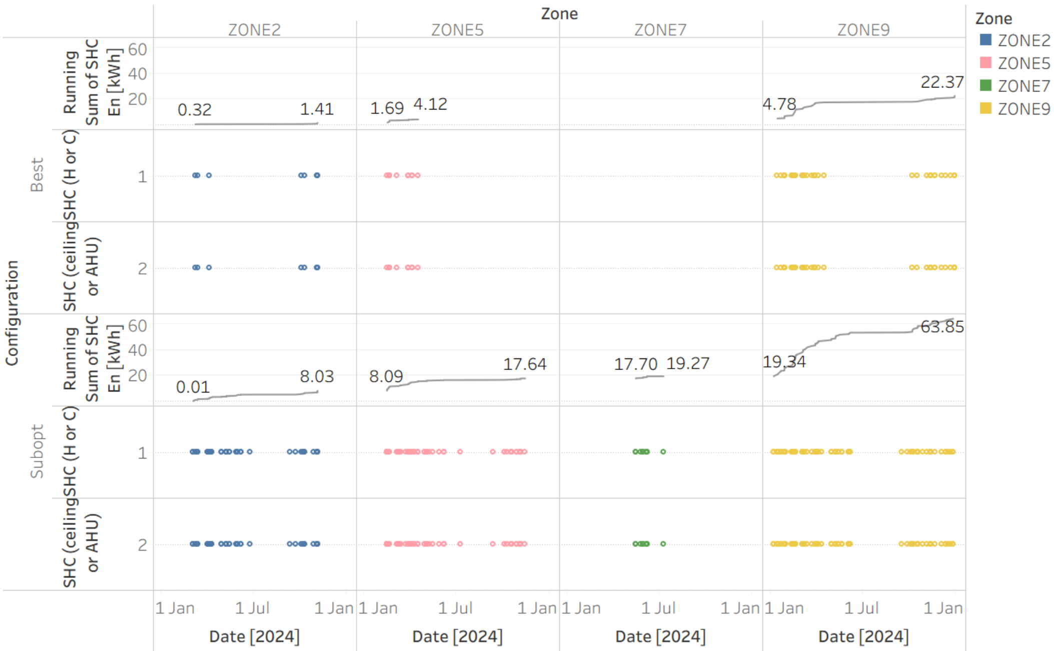

Figure G.2: Simultaneous heating and cooling detail—AHU overheating

Acknowledgements

This thesis has been made possible by the contribution of many people, to whom I wish to express my gratitude.

First and foremost, I would like to thank my advisor, Francesco Causone, for his guidance throughout this work. His high standards and thoughtful advice were essential, constantly encouraging me to deepen my thinking and always strive to do better.

My sincere thanks also go to my co-advisors. To Yacine Allab, for his invaluable guidance and for continuously challenging me to push the boundaries of my work. His availability and the trust he placed in me were a genuine source of motivation. To Vincent Lugherini, who helped me build a solid understanding of the subject, as well as for his decisive guidance in shaping the direction of my thesis.

I would also like to warmly thank all members of LHIRR, who were a tremendous source of support at every stage of this work. Their insightful advice and the richness of their shared experiences were of considerable value to this research.

Finally, I wish to express my deepest gratitude to my family and friends, whose unwavering belief in me and constant encouragement were my anchor and greatest source of strength throughout this journey.

This thesis has been far more than an academic exercise: it has been a deeply enriching and challenging experience, through which I have grown considerably in skills, initiative and resilience. In many ways, it will remain a defining milestone in both my professional and personal journey.